UNIVERSITÀ
DEGLI STUDI
FIRENZE

PhD in
Sustainable Management of Agricultural Forestry and Food Resources
Curriculum in Agriculture and Forest Engineering

CYCLE XXXVII

COORDINATOR Prof. Erminio Monteleone

Ecohydrological processes in Mediterranean forested catchments: from tree interception to runoff generation

Academic Discipline (SSD) AGRI/04-A

Doctoral Candidate
Dr. Matteo Verdone

Supervisor
Prof. Daniele Penna

Co-Supervisors
Dr. Ilja van Meerveld
Dr. Christian Massari

Coordinator
Prof. Erminio Monteleone

Academic years 2021/2024

A Giulia

Summary

Abstract

Understanding hydrological processes in forested catchments is crucial in the context of climate change, especially in vulnerable environments such as Mediterranean mountain catchments. This study aims to investigate how forest stand characteristics, seasonality in meteorological forcing, and hillslope topography influence precipitation interception and tree transpiration, as well as to characterise the effects of seasonal variability in meteorological conditions on the hydrological response of a small catchment.

The research was conducted in the Re della Pietra experimental catchment, a 2 km^2 site located in the Tuscan Apennines, Central Italy. Measurements of throughfall and sap flow were taken on a steep hillslope in the upper catchment, dominated by European beech trees (Fagus sylvatica).

Throughfall was monitored monthly from July 2020 to September 2023 using two 7x7 grids, each consisting of 49 samplers—one positioned in the lower part of the hillslope and the other in the upper part. These measurements were compared to gross precipitation. The overall throughfall-to-gross precipitation (TF/GP) ratio averaged 70 ± 3%, with higher values during the growing season than in the dormant season. The lower grid exhibited a significantly lower TF/GP ratio compared to the upper grid, reflecting differences in tree size and density, which were greater downslope. Temporal stability analysis revealed a strong persistence of the spatial throughfall patterns, particularly during the dormant season.

Sap flow velocity varied along the hillslope until mid-summer. Upslope trees experienced a rapid decline in sap flow with increasing temperatures, whereas riparian trees maintained stable sap flow rates. Midslope trees exhibited intermediate trends. Sap flow in riparian trees correlated more strongly with vapor pressure deficit (VPD) and temperature, while upslope and midslope trees' sap flow was more closely linked to soil moisture. Time lag analysis indicated a seasonal variability of the sap flow-VPD relation, with an average lag of -1.1 ± 2.7 hours (standard deviation). Higher soil moisture in the riparian zone buffered trees against temperature and water stress, resulting in elevated sap flow velocities.

Finally, the catchment hydrological response and its timing were assessed using hydrometric and electrical conductivity data. Wet and dry periods were defined based on soil moisture, and hydrographs were analyzed accordingly. The results demonstrated that seasonality significantly influences soil moisture, groundwater levels, and streamflow dynamics, with distinct differences between wet and dry periods. Stream stage and event water fractions varied across spatial scales: wet conditions produced faster streamflow responses and higher event water fractions in upper sub-catchments, while dry periods showed increased event water fractions at the catchment outlet. Time lags in peak flows highlighted complex interactions governing streamflow timing.

Further research in this and other Mediterranean catchments is necessary to validate these findings and enhance our understanding of hydrological responses to climate change in these sensitive environments.

Introduction

Forests cover roughly one-third of the Earth's surface (Bourgoin et al., 2018), making them among the most important ecosystems for delivering a wide range of hydrological services. These include water production and protection, as most of the world's accessible freshwater originates from forested catchments (Keleş, 2018). Forests ensure both the quantity and quality of water yields and provide critical protective functions such as flood mitigation, soil conservation, and landslide prevention (Larsen, 2017). The hydrological response of a catchment across different timescales is shaped by a complex interplay of biotic and abiotic factors, often acting concurrently (Zabaleta and Antigüedad, 2013). These processes dictate how water is mixed, stored, and released over varying spatial and temporal scales (Pfister et al., 2017). In forested landscapes, this complexity is heightened by the diversity of tree species, each with unique canopy structures, root systems, basal areas, and spatial distributions. Topography further influences the distribution of water resources within catchments. Understanding these processes is essential for managing both water quantity and quality during periods of rapid environmental change, particularly those driven by shifts in land use and climate (e.g., Naef et al., 2002; Negley and Eshleman, 2006), to sustain and maximize the ecosystem services forests provide.

Tree species composition and their characteristics influence the proportion of precipitation reaching the soil, either as throughfall—water passing through the canopy—or as stemflow—water running down tree trunks. Throughfall typically accounts for 70–80% of water input in forested catchments (Llorens and Domingo, 2007; Siegert et al., 2016). The redistribution of water across the soil surface, mediated by canopy cover and topography, significantly affects hydrological, biogeochemical, and ecological processes (Keim et al., 2005; Zhu et al., 2021) favouring groundwater recharge and flood lamination. Consequently, throughfall plays a pivotal role in regulating soil moisture patterns (Coenders-Gerrits et al., 2013; Molina et al., 2019; Fischer-Bedtke et al., 2023), nutrient inputs, root development (Klos et al., 2014; Liu et al., 2017), forest floor composition (Mottonen et al., 1999), pedogenesis (Baba and Okazaki, 1999), soil and groundwater chemistry (Manderscheid and Matzner, 1995; André et al., 2008), nutrient cycling (Chang and Matzner, 2000), and stream water chemistry (Beier, 1998). Thus, a comprehensive understanding of the spatio-temporal variability of throughfall and its controlling factors is crucial. Despite the abundant literature focusing on TF analysis in forested catchments, the effects of topography on TF ratios, either via differences in stand characteristics or micro-climate, have rarely been studied.

Soil water redistribution, topography, and atmospheric demand—particularly vapor pressure deficit (VPD)—also influence tree transpiration dynamics throughout the seasons. VPD is recognized as the main driver of tree transpiration: as VPD rises, transpiration increases until a physiological threshold is reached, after which trees close their stomata to prevent excessive water loss (Cochard et al., 2001). This results in a nonlinear transpiration response to VPD, with an initial increase followed by a decline once the threshold is exceeded (Bachofen et al., 2023). Topography affects soil water availability along hillslopes (Penna et al., 2015; Xiao et al., 2021), with upper slopes generally drier than lower slopes (Penna et al., 2009). Steep slopes create microclimatic gradients, with footslopes experiencing lower evaporative demand due to reduced solar radiation and cooler temperatures (Hoylman et al., 2018).

Additionally, footslope soils are typically deeper and richer in organic matter compared to those upslope (Li et al., 2022). As a result, trees on upper slopes are more susceptible to water stress than those in areas with greater soil moisture (Meusburger et al., 2022). Although many studies have focused on the relation between VPD and sap flow dynamics no studies have so far analyzed the climatic and topographic controls on the sap flow-VPD relation in Mediterranean mountain catchments.

Research into water-forest interactions at the catchment scale began nearly a century ago, with early studies conducted at American sites (Bates and Henry, 1928). Since then, forest hydrologists have undertaken a wide range of field experiments and modeling studies worldwide, seeking to unravel the roles of climatic (primarily precipitation and snowmelt), hydrological (catchment wetness), pedological, vegetational, geological, and geomorphological controls on streamflow response (Bracken and Croke, 2007; Llorens et al., 2018). Experimental catchments are fundamental to hydrological research. Long-term ecohydrological monitoring in forested catchments is essential for formulating and testing hypotheses, as well as for developing or challenging theoretical frameworks. These catchments, often maintained over decades, provide invaluable data for analyzing and predicting hydrological trends, extremes, and disturbances. Such data are especially important in sensitive environments, supporting assessments of climate-vegetation-soil interactions and informed water resource management. Experimental catchments serve as sentinels for hydrological metrics, with their value increasing over time (Penna, 2024). Improved understanding of hydrological processes and catchment properties leads to more robust models that better represent the interactions between biotic and abiotic factors (Beven, 2018). The design of new data networks, strategic field observations, and models that account for spatial and temporal heterogeneity are key to advancing hydrological science (Penna, 2024). Collecting data on fluxes, storage, and catchment properties helps reduce epistemic uncertainties (Beven, 2018). In Mediterranean catchments, particular challenges include understanding the role of antecedent soil moisture in catchment response during dry and wet periods, and how event water fractions and streamflow timing change across spatial scales. Only a few studies have been carried out on the role of antecedent moisture conditions on catchment response during dry and wet periods, and on changes in event water fractions and timing of stream response across spatial scales. Most importantly, no studies have been conducted on these aspects in Mediterranean mountain forested catchments.

To fill these gaps, this thesis aims to investigate the spatio-temporal variability of hydrological processes and their interactions from the hillslope to the small catchment scale, focusing on:

I. Examining how tree stand characteristics, seasonality, and topography influence the spatio-temporal variability of throughfall along a steep hillslope (Chapter 1);
II. Investigating the combined effects of summer drought and topography on the physiological response of beech trees on a steep hillslope (Chapter 2);
III. Gaining a mechanistic understanding of how seasonal variability in meteorological forcing affects hydrological responses at the headwater catchment scale and across different spatial scales (Chapter 3).

References

André, F., Jonard, M., Ponette, Q., 2008. Spatial and temporal patterns of throughfall chemistry within a temperate mixed oak–beech stand. Science of The Total Environment 397, 215–228. https://doi.org/10.1016/j.scitotenv.2008.02.043

Baba, M., Okazaki, M., 1999. Spatial variability of soil solution chemistry under Hinoki cypress (Chamaecyparis obtusa) in Tama Hills. Soil Science and Plant Nutrition 45, 321–336. https://doi.org/10.1080/00380768.1999.10409347

Bachofen, C., Poyatos, R., Flo, V., Martínez-Vilalta, J., Mencuccini, M., Granda, V., & Grossiord, C. (2023). Stand structure of Central European forests matters more than climate for transpiration sensitivity to VPD. Journal of Applied Ecology, 60(5), 886-897. https://doi.org/10.1111/1365-2664.14383

Beier, C., 1998. Water and element fluxes calculated in a sandy forest soil taking spatial variability into account. Forest Ecology and Management 101, 269–280. https://doi.org/10.1016/S0378-1127(97)00142-4

Beven, K. J. (2018). On hypothesis testing in hydrology: Why falsification of models is still a really good idea. WIREs Water, 5, e1278. https://doi.org/10.1002/wat2.1278

Bourgoin, C. et al., 2024. Global Forest Cover Map 2020 for EU Deforestation Regulation Support, Publications Office of the European Union. Belgium. Retrieved from https://coilink.org/20.500.12592/hyhc8v6 on 19 Apr 2025. COI: 20.500.12592/hyhc8v6.

Bracken, L. J., & Croke, J. (2007). The concept of hydrological connectivity and its contribution to understanding runoff-dominated geomorphic systems. Hydrological Processes, 21(13), 1749-1763. https://doi.org/10.1002/hyp.6313

Chang, S.-C., Matzner, E., 2000. The effect of beech stemflow on spatial patterns of soil solution chemistry and seepage fluxes in a mixed beech/oak stand. Hydrol. Process. 14, 135–144. https://doi.org/10.1002/(SICI)1099-1085(200001)14:1<135::AID-HYP915>3.0.CO;2-R

Cochard, H., Coll, L., & Le Roux, X. (2001). Unraveling the Effects of Plant Hydraulics on Stomatal Closure during Water Stress in Walnut. Plant Physiology, 128(1), 282-290. https://doi.org/10.1104/pp.010400

Coenders-Gerrits, A.M.J., Hopp, L., Savenije, H.H.G., Pfister, L., 2013. The effect of spatial throughfall patterns on soil moisture patterns at the hillslope scale. Hydrol. Earth Syst. Sci. 17, 1749–1763. https://doi.org/10.5194/hess-17-1749-2013

Fischer-Bedtke, C., Metzger, J.C., Demir, G., Wutzler, T., Hildebrandt, A., 2023. Throughfall spatial patterns translate into spatial patterns of soil moisture dynamics – empirical evidence. Hydrol. Earth Syst. Sci. 27, 2899–2918. https://doi.org/10.5194/hess-27-2899-2023

Hoylman, Z. H., Jencso, K. G., Hu, J., Martin, J. T., Holden, Z. A., Seielstad, C. A., and Rowell, E. M.: Hillslope Topography Mediates Spatial Patterns of Ecosystem Sensitivity to Climate, J. Geophys. Res.-Biogeo., 123, 353–371, https://doi.org/10.1002/2017JG004108, 2018.

Keim, R.F., Skaugset, A.E., Weiler, M., 2005. Temporal persistence of spatial patterns in throughfall. Journal of Hydrology 314, 263–274. https://doi.org/10.1016/j.jhydrol.2005.03.021

Keleş, S. (2018). An assessment of hydrological functions of forest ecosystems to support sustainable forest management. Journal of Sustainable Forestry, 38(4), 305–326. https://doi.org/10.1080/10549811.2018.1547879

Klos, P.Z., Chain-Guadarrama, A., Link, T.E., Finegan, B., Vierling, L.A., Chazdon, R., 2014. Throughfall heterogeneity in tropical forested landscapes as a focal mechanism for deep percolation. Journal of Hydrology 519, 2180–2188. https://doi.org/10.1016/j.jhydrol.2014.10.004

Larsen, M. (2016). Forested Watersheds, Water Resources, and Ecosystem Services, with Examples from the United States, Panama, and Puerto Rico. Chemistry and Water, 161-182. https://doi.org/10.1016/B978-0-12-809330-6.00004-0

Li, L., Wu, D., Wang, T., & Wang, Y. (2022). Effect of topography on spatiotemporal patterns of soil moisture in a mountainous region of Northwest China. *Geoderma Regional*, *28*, e00456. https://doi.org/10.1016/j.geodrs.2021.e00456

Liu, Y., Liu, S., Wan, S., Wang, J., Wang, H., Liu, K., 2017. Effects of experimental throughfall reduction and soil warming on fine root biomass and its decomposition in a warm temperate oak forest. Science of The Total Environment 574, 1448–1455. https://doi.org/10.1016/j.scitotenv.2016.08.116

Llorens, P., Domingo, F., 2007. Rainfall partitioning by vegetation under Mediterranean conditions. A review of studies in Europe. Journal of Hydrology 335, 37–54. https://doi.org/10.1016/j.jhydrol.2006.10.032

Llorens, P., Gallart, F., Cayuela, C., Roig-Planasdemunt, M., Casellas, E., Molina, A.J., Moreno de las Heras, M., Bertran, E., S´ anchez-Costa, E., Latron, J., 2018. What have we learnt about Mediterranean catchment hydrology? 30 years observing hydrological processes in the Vallcebre research catchments. Geographical Research Letters 44, 475–502. https://doi.org/10.18172/cig.3432.

Manderscheid, B., Matzner, E., 1995. Spatial and temporal variation of soil solution chemistry and ion fluxes through the soil in a mature Norway Spruce (Picea abies (L.) Karst.) stand. Biogeochemistry 30. https://doi.org/10.1007/BF00002726

Meusburger, K., Trotsiuk, V., Schmidt-Walter, P., Baltensweiler, A., Brun, P., Bernhard, F., Gharun, M., Habel, R., Hagedorn, F., Köchli, R., Psomas, A., Puhlmann, H., Thimonier, A., Waldner, P., Zimmermann, S., and Walthert, L.: Soil-plant interactions modulated water availability of Swiss forests during the 2015 and 2018 droughts, Glob. Change Biol., pp. 0–3, https://doi.org/10.1111/gcb.16332, 2022.

Molina, A.J., Llorens, P., Garcia-Estringana, P., Moreno De Las Heras, M., Cayuela, C., Gallart, F., Latron, J., 2019. Contributions of throughfall, forest and soil characteristics to near-surface soil water-content variability at the plot scale in a mountainous Mediterranean area. Science of The Total Environment 647, 1421–1432. https://doi.org/10.1016/j.scitotenv.2018.08.020

Möttönen, M., Järvinen, E., Hokkanen, T.J., Kuuluvainen, T., Ohtonen, R., 1999. Spatial distribution of soil ergosterol in the organic layer of a mature Scots pine (Pinus sylvestris L.)

forest. Soil Biology and Biochemistry 31, 503–516. https://doi.org/10.1016/S0038-0717(98)00122-9

Naef, F., Scherrer, S., & Weiler, M. (2002). A process based assessment of the potential to reduce flood runoff by land use change. Journal of Hydrology, 267(1-2), 74-79. https://doi.org/10.1016/S0022-1694(02)00141-5

Negley, T. L., & Eshleman, K. N. (2006). Comparison of stormflow responses of surface-mined and forested watersheds in the Appalachian Mountains, USA. Hydrological Processes, 20(16), 3467-3483. https://doi.org/10.1002/hyp.6148

Penna, D. (2024). A recipe for why and how to set up and sustain an experimental catchment. Hydrological Processes, 38(5), e15163. https://doi.org/10.1002/hyp.15163

Penna, D., Borga, M., Norbiato, D., and Dalla Fontana, G.: Hillslope scale soil moisture variability in a steep alpine terrain, J. Hydrol., 364, 311–327, https://doi.org/10.1016/j.jhydrol.2008.11.009, 2009.

Penna, D., Mantese, N., Hopp, L., Dalla Fontana, G., and Borga, M.: Spatio-temporal variability of piezometric response on two steep alpine hillslopes, Hydrol. Process., 29, 198–211, https://doi.org/10.1002/hyp.10140, 2015.

Pfister, L., Martínez-Carreras, N., Hissler, C., Klaus, J., Carrer, G. E., Stewart, M. K., & McDonnell, J. J. (2017). Bedrock geology controls on catchment storage, mixing, and release: A comparative analysis of 16 nested catchments. Hydrological Processes, 31(10), 1828-1845. https://doi.org/10.1002/hyp.11134

Siegert, C.M., Levia, D.F., Hudson, S.A., Dowtin, A.L., Zhang, F., Mitchell, M.J., 2016. Small-scale topographic variability influences tree species distribution and canopy throughfall partitioning in a temperate deciduous forest. Forest Ecology and Management 359, 109–117. https://doi.org/10.1016/j.foreco.2015.09.028

Xiao, D., Brantley, S. L., and Li, L.: Vertical Connectivity Regulates Water Transit Time and Chemical Weathering at the Hillslope Scale, Water Resour. Res., 57, 1–21, https://doi.org/10.1029/2020WR029207, 2021.

Zabaleta, A. and Antigüedad, I.: Streamflow response of a small forested catchment on different timescales, Hydrol. Earth Syst. Sci., 17, 211–223, https://doi.org/10.5194/hess-17-211-2013, 2013.

Zhu, X., He, Z., Du, J., Chen, L., Lin, P., Tian, Q., 2021. Spatial heterogeneity of throughfall and its contributions to the variability in near-surface soil water-content in semiarid mountains of China. Forest Ecology and Management 488, 119008. https://doi.org/10.1016/j.foreco.2021.119008

1. Variability and temporal stability of throughfall along a hillslope

This chapter is taken from: Verdone, M., Van Meerveld, I., Massari, C., & Penna, D. (2025). Variability and temporal stability of throughfall along a hillslope. *Journal of Hydrology*, *647*, 132294. https://doi.org/10.1016/j.jhydrol.2024.132294

Abstract

Tree species composition, tree size, and microclimate can vary along hillslopes in forest ecosystems. This will affect the amount of throughfall (TF) that reaches the ground. However, few studies have focused on the effects of topography on the spatio-temporal variability of throughfall. We, therefore, measured throughfall on a steep roughly 110 m long hillslope covered by European beech trees (Fagus sylvatica) in the Re della Pietra experimental catchment, Tuscany Apennines, Central Italy. Although the trees all have a similar age, the basal area, Plant Area Index (PAI), and canopy cover are higher on the lower part of the hillslope than the upper part of the hillslope. We installed 49 throughfall collectors in two 144-m^2 square grids: one on the lower hillslope and one on the upper hillslope. In addition, we installed 29 collectors on a transect connecting the lower and upper grid. Throughfall was measured from all collectors at an approximately monthly interval and compared with gross precipitation (GP) measured in a nearby open area. The overall TF/GP ratio for the 61 manual measurements during the July 2020 to September 2023 study period was 70 ± 3 %. It was higher for the growing season (71 ± 4 %) characterised by higher rainfall intensities than the dormant season (69 ± 3 %). TF/GP was lower for the lower grid than the upper grid (61 ± 5 vs 73 ± 6 % of GP, respectively). The differences between the measurements at the lower and upper grid were significant for almost all measurement days and reflect the differences in tree size and stand density. Temporal stability analysis indicated a high persistence of the spatial TF pattern for both grids, especially in the dormant season. The higher temporal stability for in the upper grid seems to be related to the lower variability in tree size. Although these results need to be confirmed by larger-scale studies at different hillslopes, they suggest that topographic differences in stand characteristics should be taken into account when determining the water balance for forested catchments.

1.1. Introduction

Throughfall (TF), i.e., the part of the gross precipitation (GP) that passes through the tree canopy and reaches the soil, can account for up to 70–80 % of GP (Llorens and Domingo, 2007, Siegert et al., 2016). The amount of TF or the ratio of TF over GP (TF ratio) depends on precipitation characteristics, such as the amount, intensity, and duration of GP (Carlyle-Moses et al., 2004, Levia and Frost, 2006, Staelens et al., 2008). TF amounts typically increase as a function of GP amount and GP intensity, but long events do not necessarily lead to less TF than shorter ones (Llorens et al., 1997, Blume et al., 2022). Wind speed and wind direction can negatively or positively affect TF

amounts, depending on tree species and geographical location or climate (Andre et al., 2008; Staelens et al., 2008, Šraj et al., 2008, Van Stan et al., 2014, Zabret et al., 2018). The amount of throughfall also depends on tree crown parameters, such as tree density, Leaf Area Index (LAI), and canopy cover (Crockford and Richardson, 2000, Llorens and Gallart, 2000, Park and Cameron, 2008, André et al., 2011, Siegert et al., 2016; Levia et al., 2019, Siegert et al., 2019). Llorens and Domingo (2007), for example, found a negative relation between LAI and the TF ratio for 13 studies in the north-eastern Mediterranean basin. However, other stand characteristics were better correlated to the TF ratio than LAI. Stand density also affects the amount of TF. For example, André et al. (2011) observed in the Belgian Ardennes (temperate climate) that TF amounts were slightly lower in denser mixed beech and oak forests than low density mixed beech and oak forests due to the higher degree of overlap of tree crowns in the denser forest. They also noticed that during the growing season (leaf-on period), TF volumes in the low-density forest were higher under crown extremities than near the stems. Other studies revealed that TF amounts during the growing seasons significantly decreased with increasing canopy cover above the sampling locations, although it was more closely correlated with branch cover (Staelens et al., 2006). However, Llorens and Gallart (2000) showed that canopy cover measured at the point scale was only weakly and non-linearly related to the measured TF amounts, but the relation became stronger when the point scale observations were grouped to the plot scale. Studies on regenerating forests in the tropics highlighted the relation between TF ratios and tree basal area (e.g., Keller et al., 2023), or the ratio of small to large trees (Zimmermann et al., 2013).

The spatial pattern of the redistribution of water by the canopy can persist over time and affect hydrological, biogeochemical, and ecological processes (Keim et al., 2005, Zhu et al., 2021). The spatial pattern in TF has a critical influence on soil moisture patterns (Coenders-Gerrits et al., 2013, Molina et al., 2019, Fischer-Bedtke et al., 2023), root growth (Ford and Deans, 1978, Klos et al., 2014, Liu et al., 2017), the composition of the forest floor (Möttönen et al., 1999), nutrient inputs to the soil, nutrient cycling (Chang and Matzner, 2000), soil-and groundwater chemistry (Manderscheid and Matzner, 1995, André et al., 2008), stream water chemistry (Beier, 1998), and pedogenesis (Baba and Okazaki, 1999). Consequently, understanding the spatio-temporal variability of TF and the factors that affect it is important.

A widely adopted technique to investigate the persistence of TF patterns over time (i.e., the temporal stability of the spatial patterns of TF) is the Index of Temporal Stability (ITS) (Vachaud et al., 1985). By adopting this approach, Keim et al. (2005) found for a deciduous forest in the Pacific Northwest (USA) that persistence of TF patterns was stronger for the growing season than the dormant season. In particular, the dormant season results were affected by extreme values (i.e., the samplers were empty or full of water), while during the growing season more TF collectors were completely dry than full (Keim et al., 2005). Another study in 2006 found that the spatial pattern in TF below a single dominant beech tree was also more persistent during the growing season than in the dormant season (Staelens et al., 2006). Moreover, as the length of the sampling period increased, the spatial variability in TF decreased and the temporal stability of the TF pattern increased (Staelens et al., 2006).

Almost all of these TF studies were conducted at the plot scale; they either measured TF for one plot (e.g., Murakami 2007) or compared TF measurements for different forest plots (e.g., Blume et al., 2022, Keller et al., 2023). However, lateral water flow at the

hillslope scale can affect soil water availability, tree growth, and stand characteristics (Fabiani et al. 2023; Elliott et al., 2015). Topography also affects the microclimate (Hawthorne and Miniat, 2018). The air on the lower hillslopes (i.e., near valley areas) tends to be cooler and more humid (Jencso et al., 2009, Penna et al., 2009). Radiation and windspeeds tend to be lower there as well (Hoylman et al., 2018). One could thus expect that TF ratios vary across hillslopes, even if the entire hillslope is covered with the same tree species. However, the effects of topography on TF ratios, either via differences in stand characteristics or micro-climate, have rarely been studied.

One exception is the study conducted by Siegert et al. (2016) who measured TF for four different plots, including a north-facing slope, a flat central area, a west-facing slope, and a south-facing slope in a 12-ha forested catchment in Maryland, USA. They found that TF variability was influenced by slope and aspect, which directly impacted the microclimate, growing conditions, and competition for water and nutrients. The topography-induced variations in TF were not visible for single events but became noticeable when the data were aggregated at the seasonal or annual scales (Siegert et al., 2016). However, their plots were covered by different tree species, which made it harder to infer the effect of topography via the effects of tree cover and microclimate on TF ratios.

Therefore, in this study, we use three years of TF data collected on a steep hillslope covered by European beech trees (Fagus sylvatica) in a densely forested catchment in central Italy to assess the spatial and temporal variability in TF across a steep hillslope. In particular, we address the following three research questions:

I. How do tree stand characteristics vary along a hillslope?
II. How do tree stand characteristics affect the amount and spatial variability of TF at the hillslope scale?
III. How does seasonality affect the temporal variability and stability of TF across the hillslope?

1.2. Materials and methods

1.2.1. Study area

The study hillslope is located in the Lecciona catchment (coordinates of the outlet: 43.878 N, 11.622 E), a 31-ha subcatchment of the Re della Pietra experimental catchment (Fig. 1), located in the Tuscan Apennines in central Italy. The main aspect of the study hillslope is North, the average slope is 30°. The elevation ranges between 910 and 960 m a.s.l.. The catchment and the study hillslope are densely vegetated by European beech (Fagus sylvatica), with few inclusions of oak trees (Quercus sp.). The understory is sparse (Fig. 1c). The last thinning in the Lecciona subcatchment took place in 1990. Although the entire slope is covered by evenly aged beech trees, the diameter of the trees decreases from the bottom to the top of the hillslope (see section 3.1). Soil depth varies from 1.5 m at bottom of the hillslope to 0.8 m at the ridge, as assessed by knocking pole measurements. Soils are Humic Dystrudepts (USDA, 1999), with mainly a sandy loam texture (Fabiani et al. 2023) and a high gravel and rock content. The geology consists of fractured sandstone.

The long-term mean annual precipitation and temperature (1992–2022) measured at a weather station located at 1005 m a.s.l., ~12 km south from the catchment, are

roughly 1300 mm and 10.5 °C, respectively. Typical for the Mediterranean region, precipitation is unevenly distributed over the year, with the highest rainfall amounts in autumn (the wettest month is November, with on average 185 mm of precipitation) and lowest in summer (the driest month is July, with 40 mm of precipitation on average). Precipitation intensity is higher during the period from May to October than between October and May (average intensity: 3.6 mm/h vs 2.1 mm/h for events with > 1 mm of total precipitation). Snowfall events are rare but can occur, particularly in December and January.

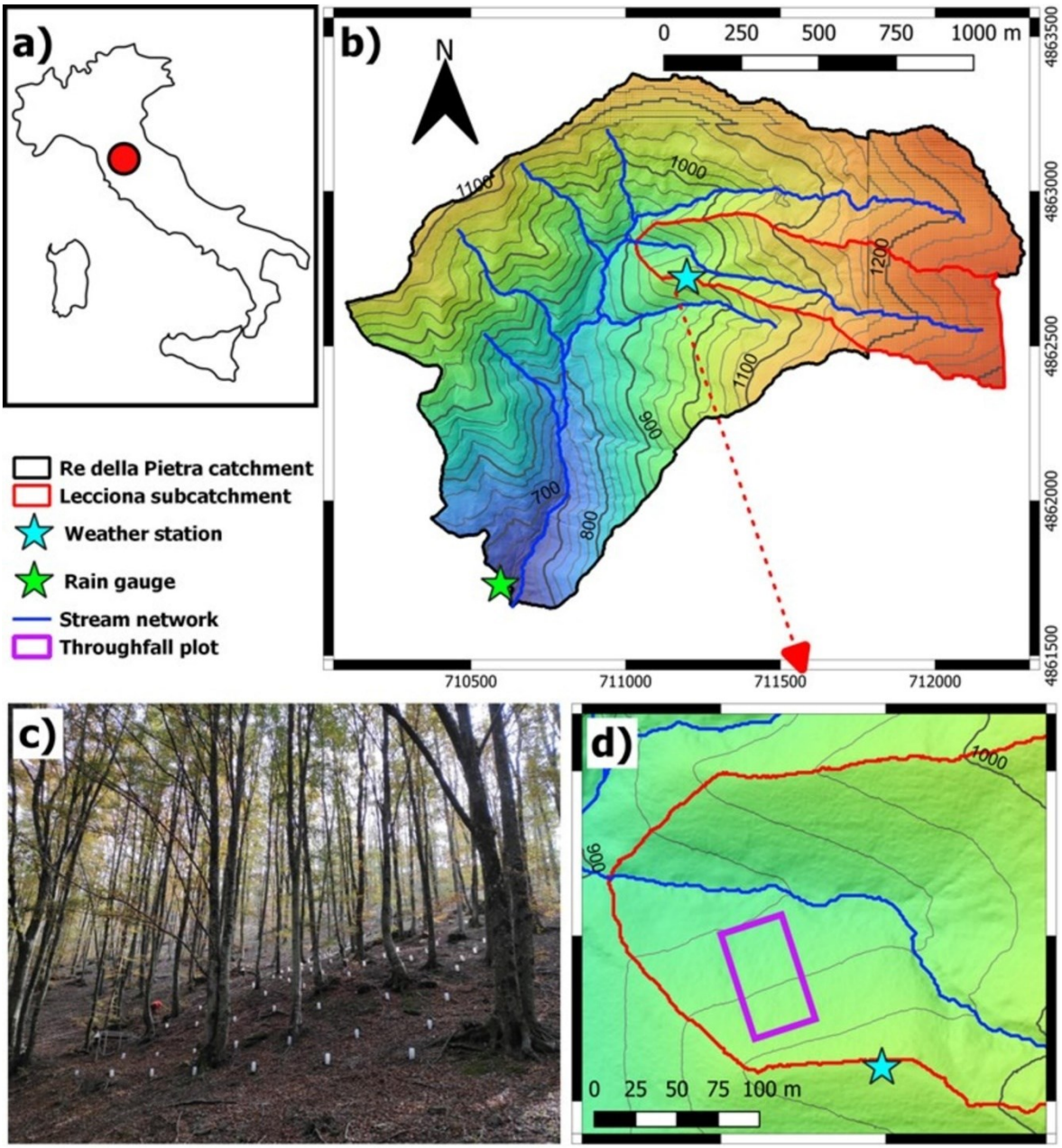

Fig. 1. Panels a) and b): Re della Pietra catchment and its location in Italy. c) Picture of the TF plot. d) Map of the lower zone of the Lecciona subcatchment and position of the experimental hillslope.

1.2.2. Field measurements

1.2.2.1. Precipitation measurements

The main meteorological parameters were measured at a weather station located in an open area at 990 m a.s.l., above the experimental hillslope (Fig. 1b and d). Gross precipitation (GP) was measured at a five-min resolution with a tipping bucket rain gauge (Davis Instruments) that was dynamically calibrated (Marsalek, 1981, Sypka, 2019) also considering the possible effect of wind undercatch (Rinehart, 1983, Hosking et al., 1985). The tipping bucket experienced some malfunctioning between 29 October and 23 November 2021. Precipitation data from the precipitation station at the Re della Pietra outlet (at 635 m a.s.l.; Fig. 1b) were used for that period.

1.2.2.2. Throughfall measurements

The TF measurements (Fig. 2) were designed to assess possible differences in TF along a hillslope. In total we used 126 samplers, located in two main plots (upper and lower grids, 196 m2 each) located to the left and the right of a linear transect along the line of the maximum slope of the experimental hillslope. The lower boundary of the lower grid was located roughly 25 m from the Lecciona stream, while the upper boundary of the upper grid was located approximately 80 m from the ridge. At each of the two grids, we installed 49 samplers at a 2 m distance (measured on the ground). The experimental design aimed to maximize the TF measurement area along the hillslope and the ratio between the number of samplers and the plot area to assess the possible variability in TF along the hillslope. The sampler density (2.9 m^2 for each grid sampler) is comparable with that used by Keim et al. (2005) (3.2 m^2 per sampler in a deciduous tree stand) and one to two orders of magnitude higher than in the studies of Fischer-Bedtke et al. (2023) and Siegert et al. (2016) (one sampler per 28 m^2 and 250 m^2, respectively). TF measurements were also taken every 1 m along a 30 m linear transect connecting the two grids.

The samplers consisted of high-density polyethylene (HDPE) cylindrical jars with a 60 cm2 opening (total collection area for all samplers: 7560 cm^2). Each sampler was emptied approximately every three weeks between August 2020 to September 2023, leading to 61 measurement days. To minimize the risk of evaporation from the samplers, the collectors were emptied directly (i.e., within 2 days) after each major rain event in summer (≥5 mm/day) based on data recorded by the weather station operated by the Regional Hydrological Service (Macchioli Grande et al., 2024), located 12 km from the catchment at 1005 m a.s.l.. On each measurement day, all samplers were emptied and the total volume of water in each sampler was recorded.

In addition to the manual TF measurements, five TF gutters were installed on the hillslope in November 2021. Each 200 cm-long and 17 cm wide gutter (3400 cm^2) was connected to a tipping bucket rain gauge that was dynamically calibrated for rainfall intensity taking into account the much larger collection area than for the rain gauge. A fine mesh protected the gauges from litter accumulation. In addition, the water inlet hole of the rain gauge was slightly enlarged to avoid clogging. All TF gutter gauges were connected to the same data logger and volumes were recorded every five minutes. The

total surface area of all gutters was 28000 cm^2, almost 3.7 time larger than that of all 126 manual samplers.

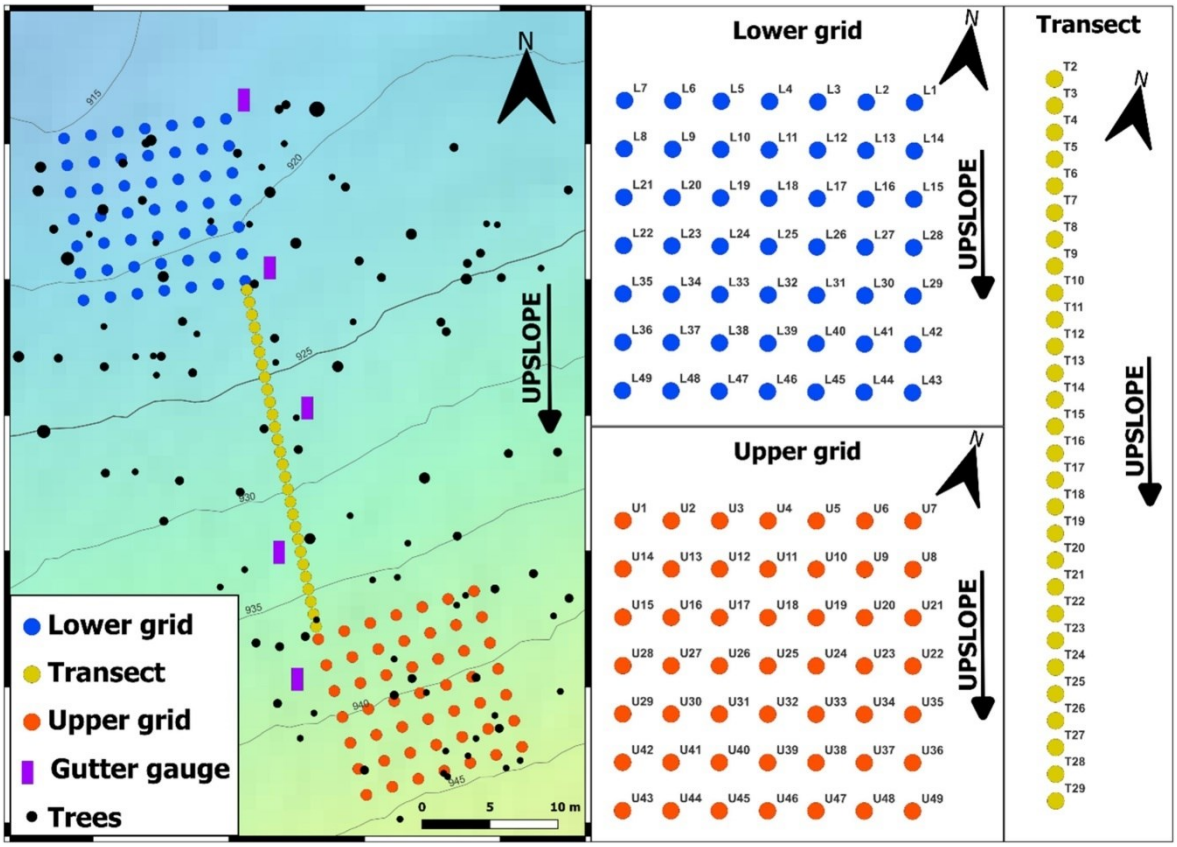

Fig. 2. Left: map of the experimental hillslope. Right: the relative position and ID of the samplers in each grid and on the transect.

1.2.2.3. Forest survey and canopy cover

In March 2022, we conducted a forest survey on the study hillslope. We marked the position of the 138 trees on the study hillslope and measured their diameter at breast height (DBH) using a calliper. We measured the height of 30 representative trees, proportionally distributed over all diameter classes, using a hypsometer. Moreover, we determined the age of twelve of the 30 representative trees (equally distributed across the diameter classes) by counting growth rings from wood cores extracted with a Pressler borer.

The Leaf Area index (LAI) was determined four times during the study period: i) 11 April 2022, before the bud break (which occurred in the second half of April 2022), ii) 19 May 2022 after the bud break, iii) 6 September 2022 (at maximum crown expansion), and iv) 6 April 2023, again before the bud break. We determined the Plant Area Index (PAI) indirectly using a simplified Norman-Jarvis model (Norman and Jarvis 1975) that accounts for the relationship between PAI and photosynthetically active radiation (PAR), assuming a spherical distribution angle for leaves (Campbell, 1986). We estimated PAR above the canopy by measuring it in an open area close to the TF plot using a ceptometer (AccuPAR LP-80, Meter Group Inc., Pullman, Washington). Below canopy measurements were taken directly afterwards above each sampler and each gutter gauge. All measurements were taken within 30 min, so that the above canopy

PAR value could be considered representative for all sampling points. The ceptometer was calibrated before each campaign using the procedure suggested by the manufacturer. To obtain the LAI from the ceptometer derived PAI values, we subtracted the Wood Area Index as proposed by Bréda (2003). The Wood Area Index, was measured by the ceptometer during the leaf-less periods (Dufrêne and Bréda 1995). However, we compared the spatial patterns of PAI (instead of LAI) and TF because both wood and leaves intercept water.
Forest canopy cover is the proportion of the forest floor covered by the vertical projection of the tree crowns (Jennings et al., 1999). Forest canopy cover was determined from non-hemispherical photographs taken above each collector and gutter (CMOS size: 1/2.8'') (Whelan and Anderson, 1996, Llorens and Gallart, 2000) on three dates: i) 12 April 2022, before the bud break, ii) 5 May 2022, after the bud break, and iii) 7 September 2022, at the time of maximum crown expansion. Each photo, appropriately cropped to avoid overlap of the canopy above two adjacent samplers, was analysed using a MATLAB-based application to distinguish the proportion of sky (gap fraction) from the canopy cover via colour difference (Llorens and Gallart, 2000).

1.2.3. Data analysis

1.2.3.1. Throughfall amounts and ratios

Samplers
For all measurement days (Table s1), the volume (in liters) of TF in each sampler was converted to a TF amount (in mm) by dividing the volume by the area of the sampler's orifice. The TF ratio was calculated for each sampler by dividing the TF amount by the total GP between the measurement date and the previous one.
We determined the average and standard error of the TF amount and the TF ratio (TF/GP) for each measurement date for the entire hillslope, the two grids, and the transect. To determine the overall TF ratio for the entire 3-year period, we weighted the average TF ratios for the individual measurement dates by the amount of GP. Again, this was done for the entire hillslope (all collectors), and for the two grids and the transect separately. To calculate the average TF ratio, we had to remove some outliers (see Table s1). Despite our efforts to minimize the possible effects of evaporation during the summer months, on one occasion (August 2023; GP: 18.4 mm), 23 days passed between the first rainfall event and the TF measurements. Therefore, these TF data were excluded from the analyses and the calculation of the average TF ratio. We also excluded eight measurements that were clearly affected by snow and ice on the hillslope and two other measurement periods during the growing season for which the hillslope average TF ratio was > 1 (GP of 176 and 14 mm), likely because of rainfall undercatch. Values of TF ratios > 1 are common (e.g., Valente et al., 1997, Crockford and Richardson, 2000, Rodrigo and Àvila, 2001) and are generally caused by either an overestimation of TF due to, for instance, samplers located below dripping points (Pook et al., 1991, Katayama et al., 2023) or an underestimation of GP. GP could be underestimated due to clogging of the tipping bucket rain gauge by ice and snow in winter (Savina et al. 2012) and high wind speeds during high-intensity rainstorms in summer. Furthermore, the measurements at sampler number eight of the transect (T8) were affected by direct dripping from the curved trunk. As a result, the sampler was

always full (equivalent to 435 mm), which made it impossible to quantify TF for this sampler correctly. For this reason, data from this sampler were discarded from all analyses as well.

We used field observations of leaf break (typically around mid-April) and leaf fall (typically in early October) to divide the measurement period into the growing season (37 measurement dates) and the dormant season (24 measurements). Again, we calculated the average TF ratio for each season by weighting the TF ratios for the individual measurements by the amount of GP for the entire hillslope (all gauges), and for the two grids and the transect separately. The Mann-Whitney test was used to determine the statistical significance of the differences in TF ratios for the two seasons.

We used the Kruskal-Wallis test (Kruskal and Allen Wallis 1952) to determine the statistical significance of the differences in TF ratios for the two grids and the transect. We used a non-parametric test to ensure that differences among the two grids and the transect were not related to outliers caused by stochastic errors in TF measurements or deterministic errors due to water redistribution (e.g., sampler T8, see discussion above about outlier removal). We, furthermore, used a jackknife procedure to corroborate the results of the Kruskal-Wallis test on the differences in TF amounts between the lower and the upper grid. We focused our attention on the differences in TF between the two grids for this analysis because the different measurement design for the transect makes it difficult to compare the results with the grids. For each measurement day, we calculated the mean TF for the upper and lower grid. Then, we randomly removed one or more samplers from each grid and recalculated the mean TF and plotted the mean TF as a function of the number of samplers removed. This procedure was repeated 10,000 times, leading to what is called a “trumpet plot” that coincides with the mean value of TF when all gauges are included (the mouthpiece of the trumpet), and multiple endings (the bell of the trumpet) when many samplers are removed. In addition, we determined for each of the 10,000 times that a certain number of samplers were removed if the mean TF for the upper grid was higher than for the lower grid. We then plotted this fraction as a function of the number of samplers that were removed. Both analyses were done for all measurement periods.

Gutter data

For the continuous data from the gutters, we divided the precipitation time series into events. Events were defined as periods with more than 1 mm of precipitation separated by at least two hours of no precipitation. Based on our field observations, this period is sufficient for the leaves to dry between two events and dripping to stop. For each event, we calculated the GP amount, event duration, mean, and maximum intensity (from the weather station in the open area), and the corresponding TF amount in each gutter gauge, as well as the TF ratio by dividing the TF amount by the amount of GP.

1.2.3.2. Temporal stability analysis

To investigate the temporal stability of TF, we used two different techniques. To explore the spatial correlation in TF, we compared the TF amount in each sampler with that of all other samplers. More specifically, correlograms were used to determine the correlation between the TF amount in a given sampler and that in all other samplers on the grid for either the full time period, the growing season, or the dormant season. This

was done to assess if the TF amount was related to the distance among samplers and if it varied seasonally.
We, furthermore, assessed the temporal stability of the TF spatial patterns using the temporal stability analysis approach (Vachaud et al., 1985, He et al., 2019). We calculated the Mean Relative Difference (MRD) of TF for each sampler (Eq. (1) and the corresponding Standard Deviation of the Relative Difference (SDRD) (Vachaud et al., 1985) (Eq. (2):

$$MRD_i = \frac{1}{m} \times \sum_{j=1}^{m} \frac{S_{ij} - \bar{S}_j}{\bar{S}_j} \quad (1)$$

And

$$SDRD_i = \sqrt{\sum_{j=1}^{m} \frac{\left(\frac{S_{ij} - \bar{S}_j}{\bar{S}_j} - MRD_i\right)^2}{m-1}} \quad (2)$$

where S_{ij} is the measured amount of TF at the i^{th} measurement location during the j^{th} measurement period, $\bar{S}_j$ is the average TF amount for all sampler locations for the j^{th} measurement period, and *m* is the number of measurement periods. The mean relative difference (MRDi) at location *i* represents the systematic bias in TF at location *i* relative to the spatial average. $SDRD_i$ represents the persistance of the location in representing the TF spatial average. To take both the MRD and SDRD metrics into account, we used the Index of Temporal Stability (ITS) that combines the effect of both the MRD and SDRD (Penna et al., 2013, Rodrigues et al., 2022):

$$ITS_i = \sqrt{{MRD_i}^2 + {SDRD_i}^2} \quad (3)$$

The lower the value of ITS, the the better it represents the mean TF for all measurement periods. This procedure was applied for the entire hillslope and for the two grids and the transect, separately.

1.3. Results

1.3.1. Forest stand characteristics

The survey revealed that trees on the lower part of the hillslope had a larger DBH (Fig. 3) and a more expanded crown compared to trees on the upper part of the hillslope (Table 1). However, tree height (mean height: 19.2 m ± standard deviation: 2.3 m) for the 30 representative trees across the hillslope was not related to hillslope position, nor the basal area. The age of the trees (52 ± 6 years) did not vary systematically across the hillslope either.

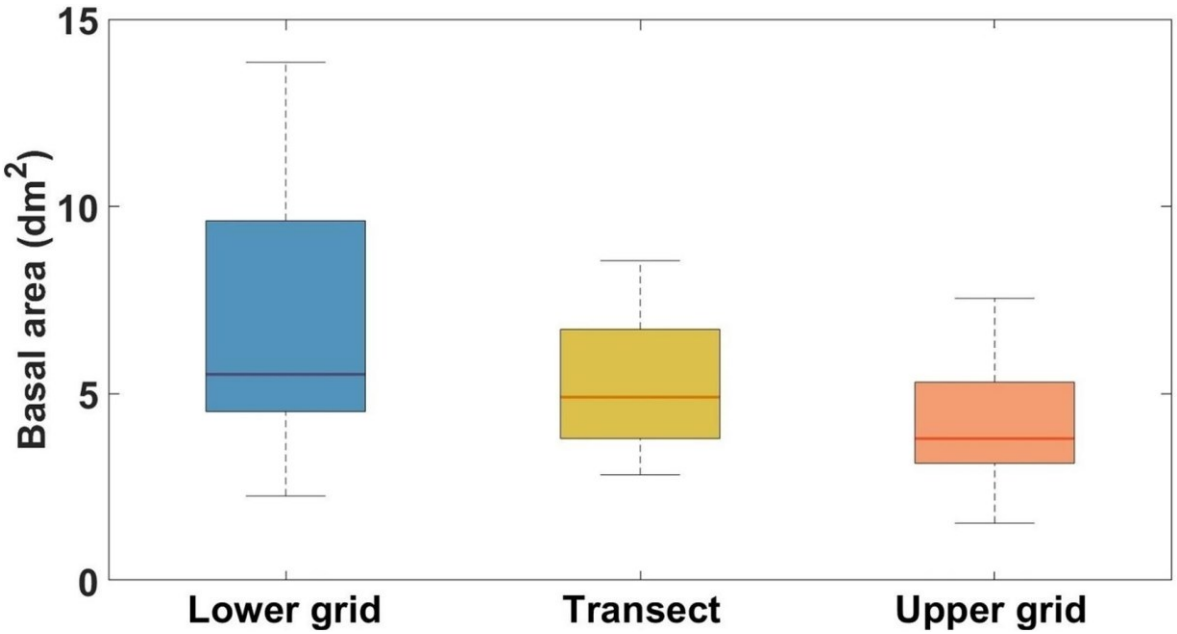

Fig. 3. Box-plot of the basal area of all trees in each grid and on the transect. The bottom and top of each box represent the 25th and 75th percentiles, respectively, the line in the box is the median, and the whiskers extend to +/–2.7 times the standard deviation.

Table 1. Characteristics of the forest stand on the study hillslope. SD: standard deviation.

	Lower grid	Transect	Upper grid
Number of trees (–)	19	8	23
Mean DBH ± SD (cm)	29 ± 8	26 ± 5	22 ± 4
Max diameter (cm)	48	39	31
Tree height ± SD (m)	19 ± 2	19 ± 5	21 ± 4
Total basal area (dm^2/m^2)	0.012	0.011	0.009

The PAI values varied between 1.9 in April (mean value for April 2022 and 2023) and 6.3 in September 2022 for the lower grid, between 1.5 and 6.3 for the transect, and between 1.6 and 5.9 for the upper grid. PAI values were statistically different among the three plots in April 2022 ($p < 0.01$) and almost statistically significant different in April 2023 ($p = 0.051$) (Fig. 4). In April 2022, PAI was similar in the lower grid and the transect (mean 1.61 and 1.58, respectively) and higher for the upper grid (2.04). The pattern was different in April 2023 (mean 1.77, 1.34 and 1.58 for the lower grid, the transect, and the upper grid, respectively). At the beginning of the growing season (May 2022), PAI became higher in the lower grid than in the upper grid and remained so during the growing season (September 2022) (Fig. 4).

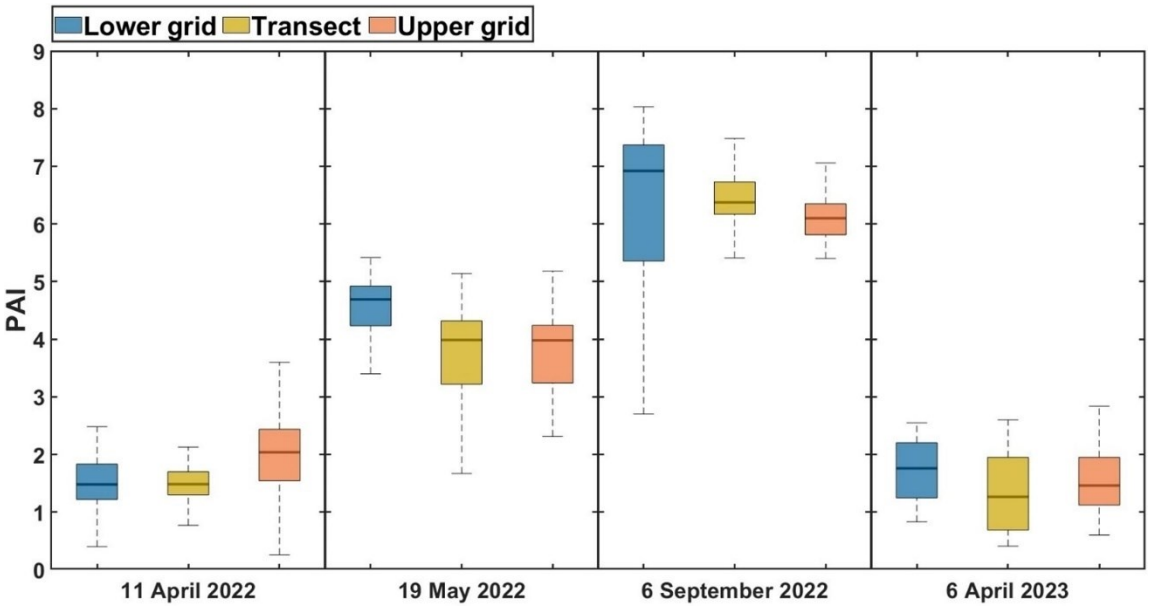

Fig. 4. Box-plot of ground-based measurements of the plant area index (PAI) for four different measurement dates. PAI was statistically different (Kruskal-Wallis test) for the three plots for all measurement dates: $p < 0.01$ for April, May and September 2022, and $p < 0.05$ for April 2023.

Canopy cover varied similarly with hillslope position, especially for the surveys conducted in April (dormant season) and in May 2023 (beginning of the growing season). Canopy cover increased from the top of the hillslope to the bottom (Fig. 5). Interestingly, the top-to-bottom trend observed for the median canopy cover values on May 5th 2022 was accompanied by an increasing variability in canopy cover towards the bottom.

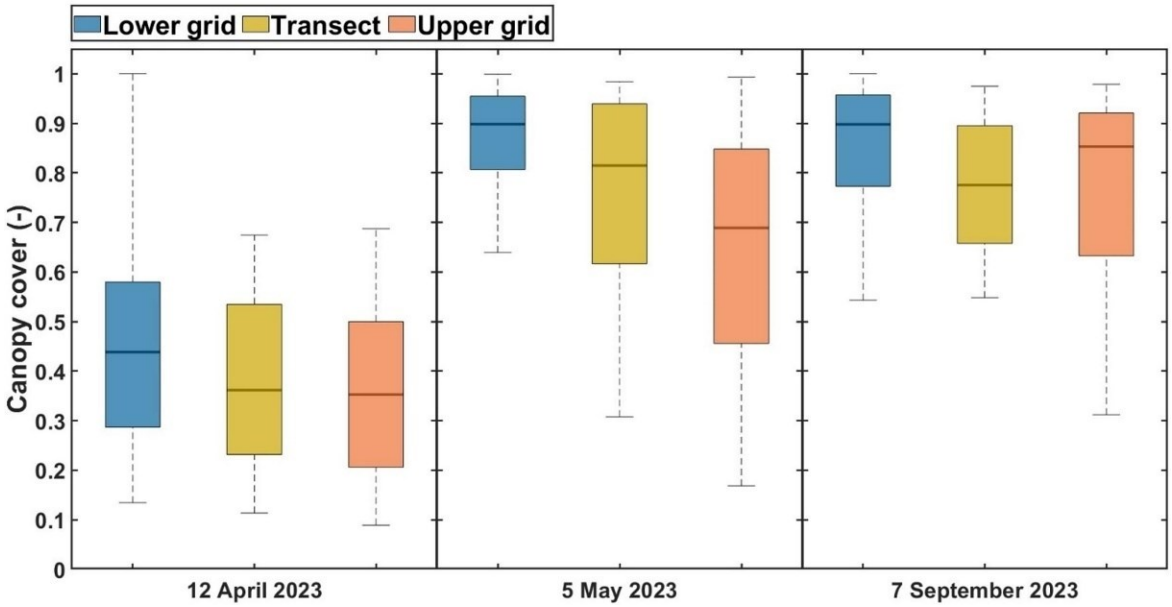

Fig. 5. Box-plot of canopy cover on three different dates. Values of canopy cover for the three plots were statistically different (Kruskal-Wallis test) only in May 2023 ($p < 0.01$).

1.3.2. Average throughfall for the study hillslope and seasonal variation

Overall, 2755 mm of GP and 1932 mm of TF were recorded over the study period (but see Section 2.3.1 and Table s1 for the events that were excluded). The overall TF ratio was 70 % (± a standard error of 3 %; Table 3). If the two measurement periods with TF > GP and the eight measurements affected by snow and ice would have been included, the overall TF ratio would have been 76 ± 7 %. If sampler T8 with very high TF amounts was included (assuming that the sampler had just filled), the mean TF ratio would have been 79 ± 7 %. The automatic gutter gauges (Table 3) recorded on average 1280 mm of TF for the period November 2021-September 2023 during which there was 1748 mm of GP, leading to an overall TF ratio was 75 ± 4 %.
As expected for a Mediterranean climate, GP varied seasonally over the study period, due to the higher precipitation in winter, spring, and fall, and less frequent and smaller but more intense events in summer (Fig. 6). The overall TF ratio was 71 ± 4 % for the growing season and 69 ± 3 % for the dormant season. The variability was higher for the growing season than the dormant season (standard deviations of 19 % and 28 % respectively). A different seasonal variation was observed for the gutters: 71 ± 3 % for the growing season and 79 ± 4 % for the dormant season.

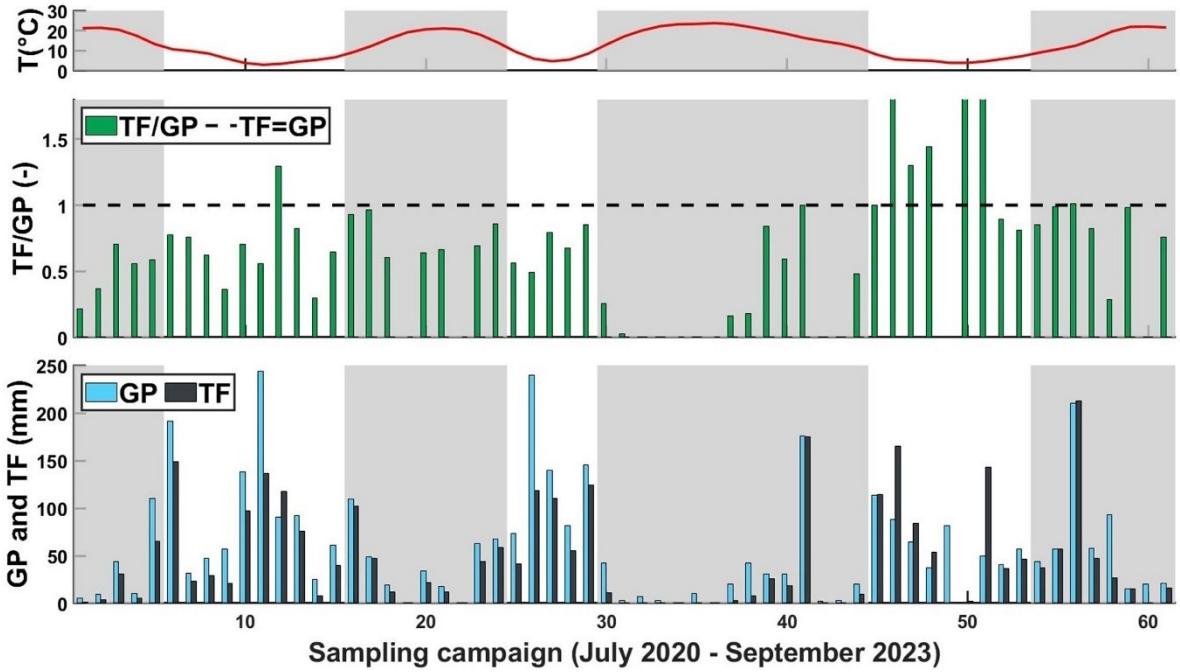

Fig. 6. Air temperature, TF ratio, and the total amount of TF and GP for each measurement period during the study period. The numbers on the x-axis indicate the measurement campaigns. Gray background shading indicates the growing season (and the white background the dormant season).

1.3.3. Differences in throughfall for the two grids and the transect

The average TF amount for the dormant season was lower in the lower grid and higher for the transect and the upper grid (Table 2). During the growing season, the same patterns of an increasing average TF amount in the upslope direction was observed (upper > transect > lower) but the mean values were more similar (Table 3, Fig. 7), though still statistically significantly different. The average TF amount was higher for the upper grid than the lower grid for 23 of the 25 individual measurement dates (92 %)

in the dormant season and for 32 of the 33 measurement dates (97 %) in the growing season (Table S1). The exceptions were the 9th, 31st, and 58th measurement dates. On the 9th measurement date, TF was the same in the two grids, whereas on the 31st and 58th measurement dates TF was slightly higher in the lower grid (mean TF 3.5 ± 0.4 mm vs 3.3 ± 03 mm and 26.5 ± 1.5 mm vs 24.5 ± 0.8 mm, respectively).

Free TF proportion difference (calculated as differences between canopy cover) between growing period and dormant period was 38% for upper grid and 31% for lower grid.

For 47 of the 55 measurement periods for which TF was higher in the upper grid than the lower grid, the difference between the two grids was statistically significant ($p < 0.05$). The data from the five gutters did not reveal a clear pattern with topographic position (data not shown).

Table 2. Plot average total throughfall (TF), coefficient of variation (CV) for TF, TF ratio, LAI, and canopy cover for the upper and the lower grid (±the standard deviation (SD) or standard error (SE)), as well as rainfall characteristics for the two seasons.

		Dormant season	Growing season
Total TF±SE (mm)	**Upper grid**	1197 ± 12	817 ± 10
	Lower grid	988 ± 10	708 ± 9
CV (–)	**Upper grid**	0.70	1.13
	Lower grid	0.72	1.15
TF Ratio	**Upper grid**	0.74	0.71
	Lower grid	0.61	0.62
LAI±SD (–)	**Upper grid**	1.8 ± 0.7	6.0 ± 0.7
	Lower grid	1.6 ± 0.6	6.2 ± 1.1
Canopy cover±SD (–)	**Upper grid**	0.37 ± 0.16	0.75 ± 0.22
	Lower grid	0.54 ± 0.19	0.85 ± 0.13
Mean GP event amount±SD (mm)	**Entire plot**	5.0 ± 7.3	4.5 ± 8.8
Mean GP intensity±SD (mm/h)	**Entire plot**	3.6 ± 3.2	2.1 ± 1.1
Max GP intensity±SD (mm/h)	**Entire plot**	9.1 ± 13.7	3.1 ± 3.8
GP event duration±SD (h)	**Entire plot**	2.2 ± 2.5	4.0 ± 5.8

Table 3. Total gross precipitation (GP) and total throughfall (TF) in mm and the mean TF ratio (TF/GP) for the entire study period and the dormant and growing seasons, for the manual samplers and the gutter gauges (±the standard error SE). For comparison, the mean (±standard deviation SD) and median values of the TF ratios for all events are given as well. The data period for the manual samplers is from August 2020 to September 2023, and for the gutter gauges from November 2021 to September 2023.

	Dormant	**Growing**	**Total**
Manual samplers			
Total GP (mm)	1621	1145	2766
Total TF±SE (mm)	1119±30	813±33	1932±66
TF ratio (TF/GP)±SE (−)	0.69±0.03	0.71±0.04	0.70±0.03
Mean TF/GP (±SD) (−)	0.69±0.19	0.61±0.28	0.64±0.24
Median TF/GP (−)	0.73	0.66	0.70
Gutter gauges			
Total GP (mm)	805	908	1713
Total TF±SE (mm)	636±25	654±22	1290±46
TF ratio (TF/GP)±SE (−)	0.79±0.04	0.71±0.03	0.75±0.04
Mean TF/GP (±SD) (−)	0.65±0.26	0.55±0.23	0.61±0.25
Median TF/GP (−)	0.74	0.60	0.66

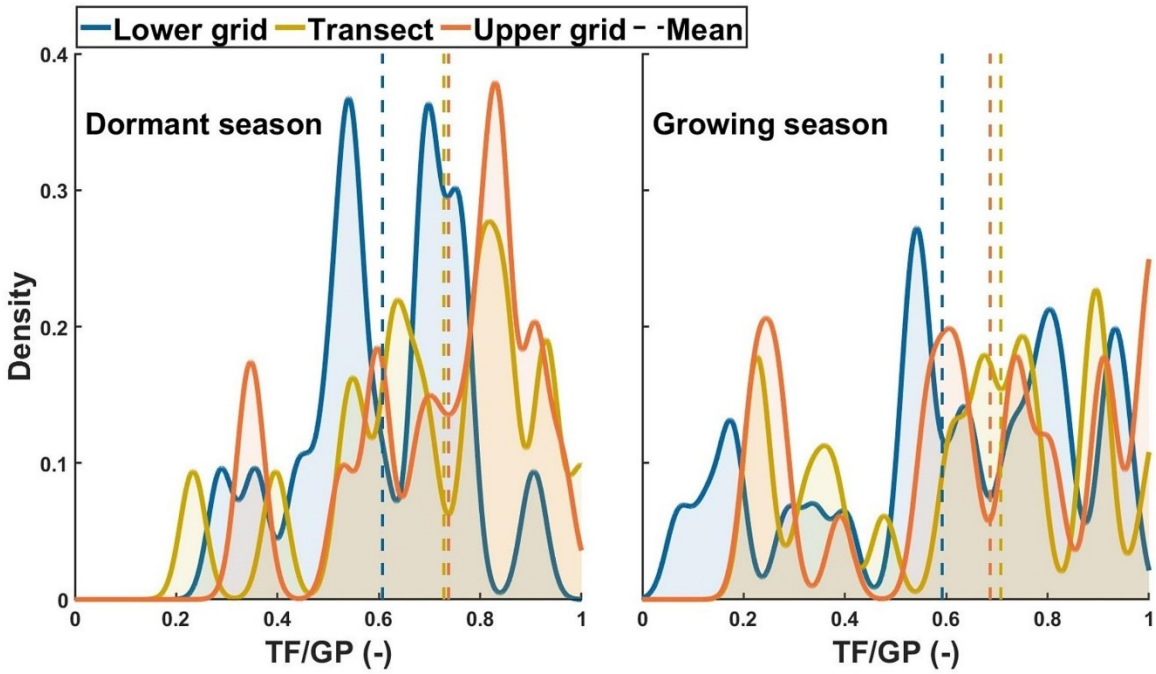

Fig. 7. Relative frequency of the TF ratios for all samplers for all dates for the two grids and transect for the growing season (left) and the dormant season (right). The vertical lines mark the mean TF ratio. TF ratios were lower for the lower grid and higher in the upper grid and the transect. Differences in the TF ratio were statistically significant (based on the Kruskal-Wallis test) between the lower grid and the

upper grid or transect but not between the transect and the upper grid ($p > 0.5$). Measurements with TF higher than GP were excluded (see Section 1.2.3.1).

The jack-knifing procedure confirmed the higher TF ratios for the upper grid than the lower grid. TF was higher in the upper grid for almost all measurement campaigns (top row of Fig. 8 is very often white) and the difference persisted even if over half of the gauges were removed from the calculation of the mean TF ratios. This was the case for both seasons (Fig. 8). Fig. 9 shows the trumpet plots for four selected measurement periods. For most cases, the two trumpets partially overlapped but were distinctly different from each other, with TF being higher in the upper grid than the lower grid (Fig. 9b, c). For the measurements on December 4th, 2020, mean TF was very similar for both grids (Fig. 8a). The final portion of the trumpet for the upper grid was skewed downward due to the larger number of measurements below the mean. The opposite trend was found for the lower grid. For the 58th measurement date, there was a large amount of TF in the lower grid, and the trumpet representing the lower grid was strongly skewed upward (Fig. 9d).
Although the differences in the average TF ratios for the grids seem to be related to PAI and canopy cover (Table 2), there was no consistent statistically significant relation between the average TF ratio (weighted by the GP) for each gauge and PAI, canopy cover, or distance to the closest tree stem, neither for the entire period nor the growing or dormant seasons (Table S2).

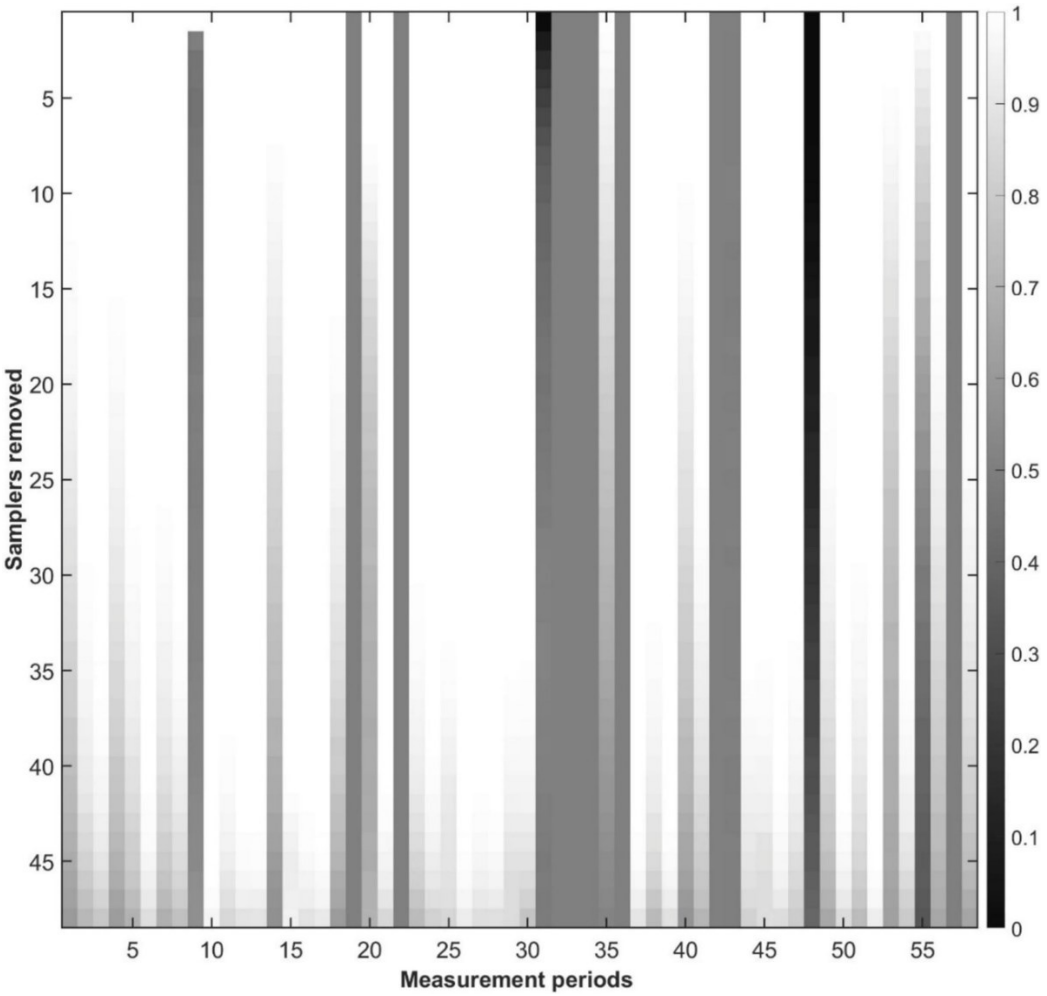

Fig. 8. Jackknife plot showing the fraction of the 10,000 times that the mean TF was higher in the upper grid than the lower grid after we progressively and randomly removed one (or more) samplers from each

grid and recalculated the mean values. The more the colour for a measurement period (on the x-axis) tends towards white, the more frequently the TF was higher for the upper grid than the lower grid, regardless of the number of samplers removed.

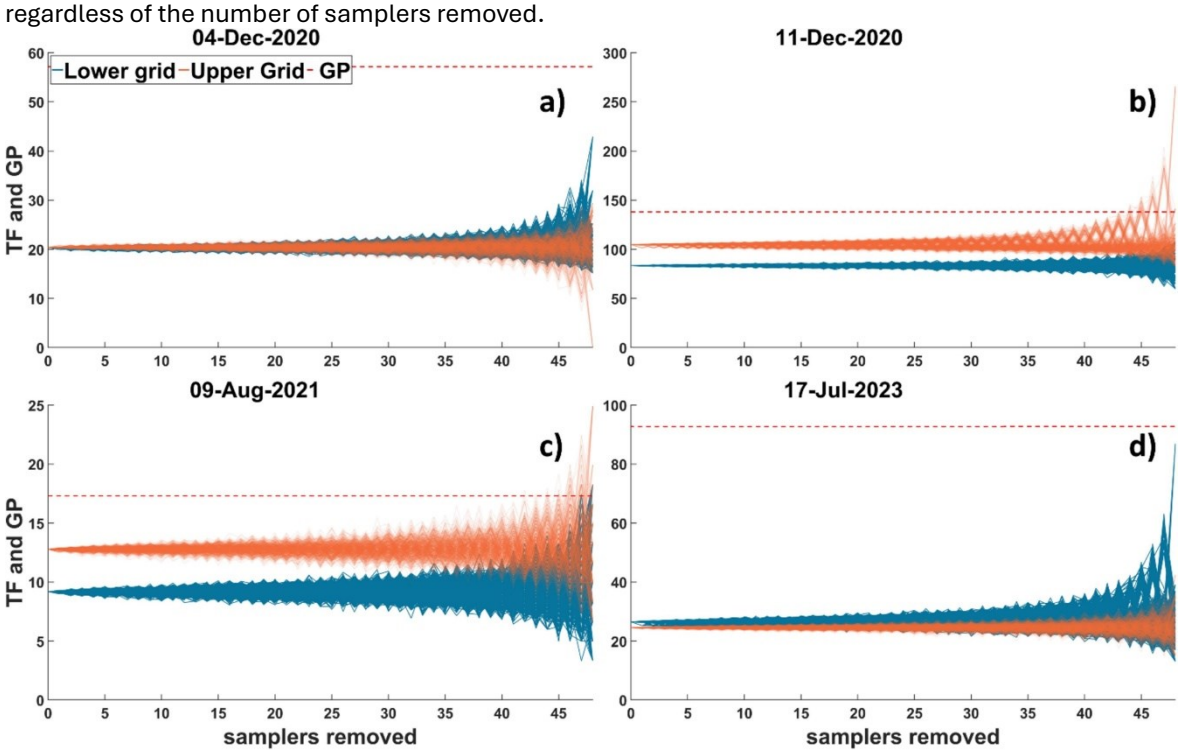

Fig. 9. Trumpet-plot for four selected measurement periods (the date reported in each panel refers to the measurement day). Each group of lines (10,000 line for each grid) was constructed by progressively and randomly removing one or more samplers and recalculating the mean TF. The shape of the trumpet bell depends on the TF distribution within each grid. Large bells reflect a high sensitivity to the selection of samplers and thus indicate a large TF variability for a given measurement period. Bell asymmetry is related to values above (bell skewed upward) or below (bell skewed downward) the mean TF for a given measurement period. The red horizonal line indicates the GP for that period.

1.3.4. Throughfall spatial variability and temporal stability within the two grids

The spatial variation in TF ratios in the two grids and the transect was high in both the growing season and the dormant season, but most pronounced in the growing season (Fig. 7). The correlations between the measured TF amounts were lower for the dormant season (mean r = 0.91 and 0.83 for the upper and the lower grid, respectively) than the growing season (mean r = 0.94 and 0.96 for the upper and the lower grid, respectively). All correlations between samplers were significant ($p < 0.01$). The correlations between the amount of TF in the different gauges was not related to the distance between samplers, as revealed by the lack of a color gradient in the correlogram when moving from the closest samplers to the distant samplers (Fig. 10). The correlograms indicate that the amount of TF in sampler number 38 in the upper grid was consistently poorly related to the amount of TF in the other samplers. This was also the case for sampler number 16 in the upper grid during the growing season (Fig. 10a, b). In the lower grid, sampler number 40 was an outlier, especially during the dormant season (Fig. 10c).

The ITS values from the temporal stability analysis (Table 4, Fig S1) are very low, indicating a high persistence of TF patterns over time. For both grids, ITS was lower in the dormant season than in the growing season. In the growing season, there were

more samplers with values above the 90th percentile, characterized by high instability. However, no relation was found between “unstable” samplers and PAI, canopy cover, or distance to the closest stem. The unstable samplers were different between the dormant and the growing season for both the lower and the upper grid.

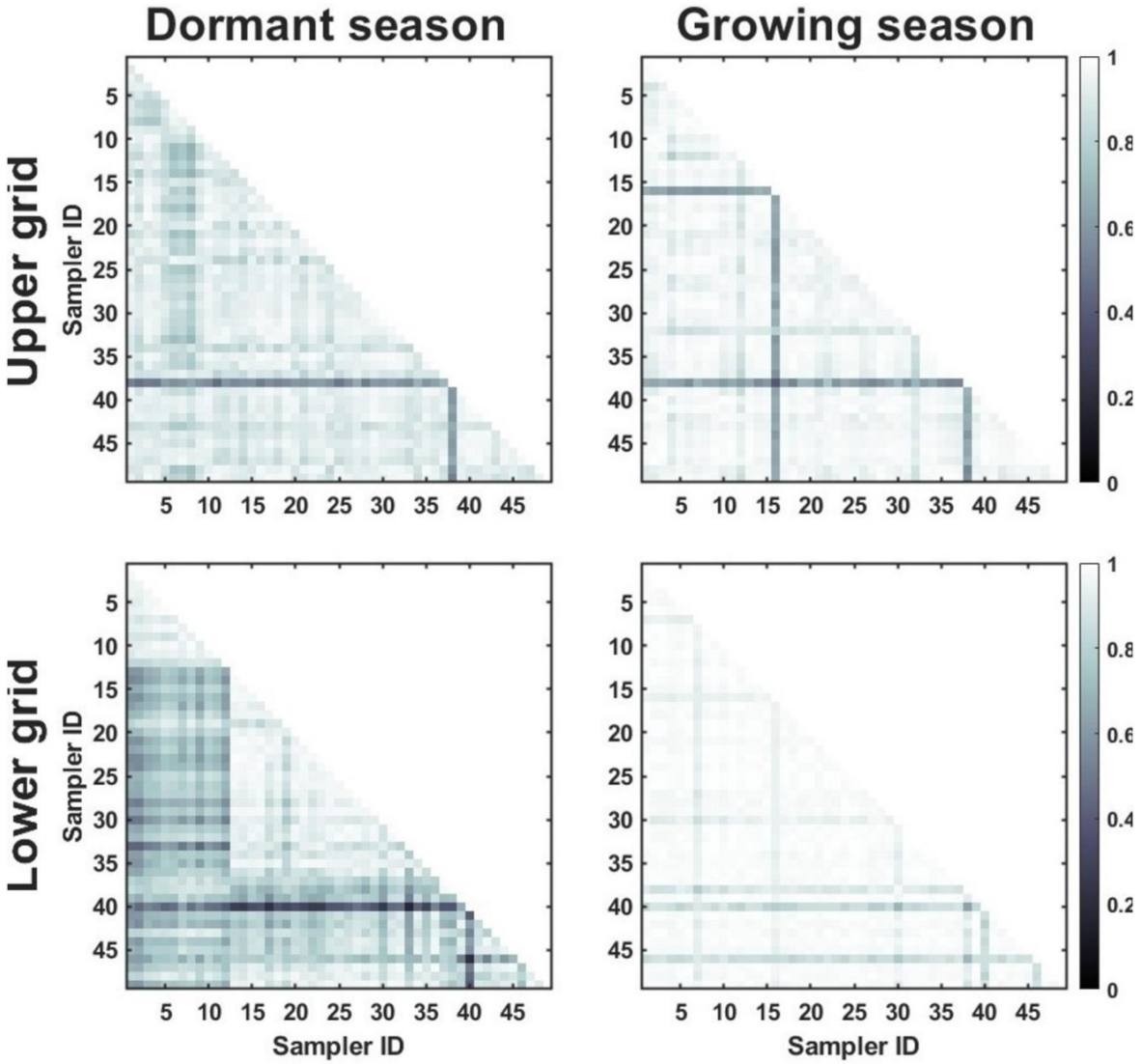

Fig. 10. Correlograms of TF for samplers in the lower and upper grid for the dormant (left column) and growing (right column) season. All correlations are highly significant ($p < 0.01$).

Table 4. Mean and median values of the ITS of TF for the dormant and growing seasons. Median values are lower than the mean values, indicating a positive asymmetry resulting from the high temporal variability (higher values of ITS) for a few samplers in each subplot.

	Lower grid		**Transect**		**Upper grid**	
	Dormant	**Growing**	**Dormant**	**Growing**	**Dormant**	**Growing**
Mean ITS ± SD	0.25 ± 0.13	0.80 ±1.44	0.41±0.22	1.65±1.79	0.24±0.39	0.47±1.51
75th percentile of ITS	0.29	0.53	0.24	0.49	0.26	0.50
Median ITS	0.21	0.55	0.20	0.42	0.18	0.42

1.4. Discussion

1.4.1. Variation in forest characteristics along a hillslope

Even though the trees along the hillslope had approximately the same age, DBH and basal area were larger in the lower grid than the upper grid, while tree density (number of trees per grid) was smaller in the lower grid than in the upper grid (Table 1, Fig. 3). Lateral redistribution of water along the hillslope causes the bottom parts of hillslopes to be wetter. This can lead to higher transpiration rates during the dry season, and higher overall primary productivity compared to the drier upper part of the hillslope (Tromp-van Meerveld and McDonnell, 2006, Penna et al., 2009) Indeed, Fabiani et al. (2023) found that the thick litter layer and high soil moisture in the lower part of the hillslope led to a different transpiration response to vapour pressure deficit (VPD) during summer. Trees at the base of the hillslopes maintained a high sap velocity even when daily mean VPD values were the highest of the season, while transpiration of trees in the upper part decreased progressively from August to September (Fabiani et al. 2023). Trees in the upper hillslope were more affected by water stress (cf. Oberhuber and Kofler, 2000), which could explain their smaller basal area. In addition to soil water availability, aspect can also affect tree growth (Siegert et al., 2016) and the microclimate can be different (see also section 4.3). Our field observations did not highlight any evidence of bad phytosanitary conditions (e.g., disease or fungal infections) of trees growing in different parts of the Lecciona hillslope, and therefore we do not think that this caused the variation in stand characteristics. Instead, we think that the observed variation in tree stand and canopy characteristics along a hillslope can be expected for other hillslopes as well. As these differences affect the average TF ratio, we recommend that future studies on TF (and other ecohydrological studies) take this systematic variability in tree characteristics into account. This could be based on remote sensing techniques such as laser scanners, drone photogrammetry, and satellite products (Manfreda et al., 2018).

The different tree sizes resulted partly in a different PAI and canopy cover fraction (cf. Landsberg and Waring, 1997, Binkley et al., 2013a). Seasonal variations in PAI were different between the upper and lower grid (Fig. 4) but there was not a clear pattern in PAI as a function of the hillslope position (Fig. 4). We hypothesize that PAI in the growing season (corresponding to LAI + WAI) was not strictly linked to PAI in the dormant season (corresponding to WAI) because only small (and living) branches put on leaves while primary stems do not. So, we can have two sites with equal WAI but different PAI if, for example the first site is characterized by higher number of small branches than the second. Vice versa, for young shoots, PAI was much greater than WAI in the growing season. Differences between observations conducted in April 2022 and April 2023 can be explained by different proportions of sky recorded by the WAI along the hillslope due to small differences in the ceptometer orientation. However, the values of PAI for the dormant season were in good agreement with other studies (e.g., 1.52 for a mixed stand of European beech and Irish oak by Dufrêne and Bréda 1995) and PAI values for the growing season are consistent with those reported by Černý et al. (2020) for a European beech forest in Czech Republic.
Similar to PAI, the canopy cover was higher for the lower grid than the upper grid (Fig. 5). The higher variability in the dormant season for the lower grid was probably caused by the fact that some samplers were located in canopy gaps (canopy cover = 0) and some samplers were located near tree stems (canopy cover = 1). During the growing season, this difference was obliterated by the leaves that filled the gaps. The lack of any relation between PAI and canopy cover (Table S2) for the individual samplers was expected because canopy cover is affected only by the absence or presence of aerial biomass, while LAI (and also PAI) is affected by aerial biomass layers (Jennings et al., 1999), resulting in locations with equal canopy cover but different values of PAI.

1.4.2. Overall throughfall ratios

The overall TF ratios for the hillslope based on the manual samplers (70 ± 3 %) and the gutter gauges (75 ± 4 %) are in good agreement with those reported by previous studies for beech forests (Staelens et al., 2006, Frischbier and Wagner, 2015; Blume et al., 2022). The higher TF ratio in the growing season for the gutter gauges can be related to different rainfall event characteristics (Table 2), rather than the effect of leaves in intercepting the water inputs (cf. Blume et al., 2022). Despite the different climatic conditions, the different TF ratios for the growing season and the dormant season for the gutters (Table 3) are consistent with previous results by Blume et al., (2022), who measured TF using automatic samplers in a beech stand in Germany. Overall, the TF ratio for the manual samplers is similar between the growing and the dormant season as differences in rainfall characteristics and in particular the period-based (rather than event-based) measurements could have masked any seasonal TF differences (Table 3). The different TF ratios between the gutter gauges and the manual samplers can be explained by the different sampling design, the different study periods, and possibly a small amount of evaporation for some measurements in summer. On the other hand, the small number of gutter gauges was not able to capture the spatial variability of TF (that the manual samplers in the grids did show). Thus, measurements at a fortnight or monthly temporal scale can make it difficult to assess the role of the events characteristics (rainfall amount and intensity) on TF spatial distribution. However, such

measurements have the advantage that they can show the spatial differences in TF between two or more regions or sites.

1.4.3. Topographic variations in throughfall ratios

TF was higher in the upper grid than in the lower grid (difference of 224 mm over the three dormant seasons and 122 mm over the three and a half growing seasons) and this difference was confirmed by the jackknife procedure (Fig. 7). This difference can be explained by the differences in stand characteristics, in particular the smaller trees size, lower canopy cover, and lower PAI for the upper grid than the lower grid (Fig. 9; Table 3). This finding agrees with the results by André et al., (2011), who measured systematically higher TF amounts in a low-density mixed stand of beech and oak trees than in a denser stand. The findings also agree with studies that found that the TF ratio increased after damaging storms changed the canopy cover and lowered the LAI (Zhang et al., 2019, Scatena et al., 1996, Heartsill-Scalley et al., 2007), as well as the marked sensitivity of a TF model to canopy cover for the highly variable canopy cover in a hardwood forest (Bryant et al., 2005).

However, our results do not agree with those of Llorens and Gallart (2000), who did not find a decrease in TF ratios with increasing tree density or basal area. This can be explained by the different spatial scales considered for TF observations and the differences in stand characteristics. In agreement with Llorens and Domingo (2007), we observed a weak negative trend between the TF amount and PAI for the two grids (Table 3), but when comparing PAI and TF ratios for the individual samplers there was no clear relation (Table. S2). This highlights the importance of other tree characteristics, such as branch orientation for the very local variation in TF (Park and Cameron, 2008). Siegert et al. (2016) found for four experimental plots with different slope, orientation, and forest composition a positive relation between plant area index (PAI) and the TF ratio for the growing season, and a weak negative relation for the dormant season suggesting the important effects of season, individual species characteristics, such as leaf and branch orientation (Park and Cameron, 2008), and leaf texture (Holder, 2007) on the TF ratio. Furthermore, it must be noted that the measurement area of the ceptometer we used was larger than the area above each sampler. This would also lead to a weak relation between plot-scale PAI and TF but no relation between PAI and TF for the individual samplers. The lack of a relation between TF and canopy cover, and TF and distance to stem for each sampler disagrees with the observations by Jochheim et al. (2022), who found that TF was lower near the stem than further away in summer and higher in winter. The absence of relation between TF samplers and distance to the closest stem confirms previous findings from studies conducted in other climates (Ford and Deans, 1978, Loescher et al., 2002, Staelens et al., 2006, Nanko et al., 2011). Perhaps the use of a regular grid affected our ability to study the spatial correlation between TF samplers. Indeed, there was no spatial correlation because the 2 m minimum spacing between the samplers is too large (Keim et al., 2005; Fischer-Bedtke et al., 2023).

Although the topography-induced variations of stand characteristics (Section 4.1) explained the TF differences between the two grids, the effects of microclimate need to be considered as well. Higher windspeeds near the ridges can increase evaporation and thus reduce TF. We cannot exclude that measurements in the growing season are affected by evaporation in the samplers, but we argue that this is not responsible for the difference in TF between the two grids because higher evaporation rates on the

upper part of hillslope would lead to less TF for the upper grid, not more. In other words, if evaporation affected our results, the differences between the two grids should be even larger.
The difference in TF between the two grids was statistically significant ($p < 0.05$) for the majority of the measurement periods. The analysis of the exceptions suggests that for large (GP > 15 mm) and intense rainfall events (GP > 10 mm/h) the leaves became less efficient in intercepting water and TF increased (cf. Blume et al., 2022), and differences between the plots became smaller. For small events, measurement errors and evaporation processes could affect TF values in a more pronounced way, obscuring any differences in TF.

1.4.4. Throughfall temporal stability across the hillslope

The very low values of ITS suggest a high temporal stability of the TF pattern in both grids (Fig. 10). This is in agreement with Keim et al. (2005), who showed that patterns of normalized TF persisted among rainfall events, both in the growing and the dormant season. Different from Keim et al. (2005) and Staelens et al. (2006), there was a higher temporal stability of TF for the dormant season (characterized by lower intensity events) (Fig. 10 and Table 3). In our case, the ITS values for the growing season were affected by extreme high values of TF, probably due to dripping from stems during some rainfall events (Keim et al., 2005), and it appears that this pattern was not stable. For the dormant season, there was a similar number of gauges with a lot more TF than the mean and gauges with a lot less TF than the mean. In addition, the CV of rainfall intensity was lower in the dormant season than in the growing season (0.52 and 0.89, respectively), leading to a negative effect of large GP intensity variation on TF temporal stability. This explanation is corroborated by the correlograms (Fig. 10) that showed that TF spatial variability was less pronounced in the growing season than in the dormant season.
The differences in temporal stability between the upper and the lower grid were related to differences in canopy structure and tree size (assuming no differences in rainfall characteristics). In particular, the basal area of trees in the lower part of the hillslope was more variable (Fig. 3, Table 1). However, the differences between the upper and the lower grid became less marked during the dormant seasons, indicating that tree size is not the only control on TF temporal stability.

1.5. Conclusions

The aim of this three-year study was to investigate the often-neglected relation between hillslope position and throughfall (TF). Field observations in a monospecific forest stand in the Apennine Mountains, Central Italy, revealed that there was a marked spatial variability in TF amounts and a very high persistence of TF spatial patterns, especially during the dormant season. Tree stand characteristics (tree density, tree size, and crown) varied systematically along the hillslope and this, in turn, affected the amount of TF along the hillslope. Total TF was less for the lower part of the hillslope where trees are larger but the stand is less dense than for the upper part of the hillslope. These differences in the volume of water that reaches the soil can have

important effects on water availability for root water uptake and water redistribution along the hillslope. Hillslope (or catchment) scale hydrological models should take topography-related variations in stand or canopy characteristics and their effect on TF into account. However, there was no clear relation between crown characteristics and the TF ratio for the individual gauges. At the very local variation in TF, other parameters than canopy cover, such as branch angles, affect the variation in TF. Future studies on TF variability along other steep hillslopes should include measurements of microclimatic variables (VPD, windspeed, solar radiation, temperature) in order to better capture the spatial variability in the climatic conditions. Future studies should also use an appropriate combination of manual and automatic samplers. The five gutter gauges highlighted the difference in the TF ratio between the growing and the dormant seasons but did not show the variation in TF across the hillslope. We, therefore, recommend to use both measurement techniques for studying the spatio-temporal variability in TF.

Funding and acknowledgements

This study was supported by the following research projects: “WATer mixing in the critical ZONe: observations and predictions under environmental changes – WATZON” (call PRIN 2017, code: 2017SL7ABC), funded by the Italian Ministry of University and Research (MIUR); “Unravelling interactions between WATER and carbon cycles during drought and their impact on water resources and forest and grassland ecosySTEMs in the Mediterranean climate – WATERSTEM” (call PRIN 2020, code: 20202WF53Z), funded by the Italian Ministry of University and Research (MUR); “Carbon and water cycles interactions during drought and their impact on WAter and ForEst Resources in the Mediterranean region –WAFER” funded by the Italian National Research Council (Consiglio Nazionale delle Ricerche – CNR); and “Hydrological controls on carbonate-mediated CO2 consumptions – HYDRO4C (call PRIN 2022, code: 2022PFNNRS) funded by the European Union, Next Generation EU.
The authors thank the local Forest Service (Unione Comuni Valdarno e Valdisieve) for their logistical support in managing the Re della Pietra experimental catchment. MV gives special thanks to Pilar Llorens (IDAEA-Csic, Spain) for hosting him and for her suggestions on the preliminary results. The authors also extend their thanks to Pietro Castellucci, Andrea Dani, Konstantinos Kaffas, Monica Macchini, Francesca Sofia Manca di Villahermosa, Mattia Papi, and Francesca Torre who contributed to TF data collection. The dataset is available upon request.

Authors’ contribution

M. Verdone: Writing – original draft, Visualization, Methodology, Investigation, Formal analysis, Data curation, Conceptualization. **I. van Meerveld**: Writing – review & editing, Validation, Supervision, Conceptualization. **C. Massari**: Writing – review & editing, Visualization, Supervision, Funding acquisition, Conceptualization. **D. Penna**: Writing – review & editing, Validation, Supervision, Project administration, Methodology, Investigation, Funding acquisition, Data curation, Conceptualization.

References

André, F., Jonard, M., Ponette, Q. Spatial and temporal patterns of throughfall chemistry within a temperate mixed oak-beech stand (2008) Science of the Total Environment, 397 (1-3), pp. 215-228. DOI: 10.1016/j.scitotenv.2008.02.043

André, F., Jonard, M., Jonard, F., Ponette, Q. Spatial and temporal patterns of throughfall volume in a deciduous mixed-species stand (2011) Journal of Hydrology, 400 (1-2), pp. 244-254. DOI: 10.1016/j.jhydrol.2011.01.037

Baba, M., Okazaki, M. Spatial variability of soil solution chemistry under Hinoki cypress (Chamaecyparis obtusa) in Tama Hills (1999) Soil Science and Plant Nutrition, 45 (2), pp. 321-336. DOI: 10.1080/00380768.1999.10409347

Beier, C. Water and element fluxes calculated in a sandy forest soil taking spatial variability into account (1998) Forest Ecology and Management, 101 (1-3), pp. 269-280. DOI: 10.1016/S0378-1127(97)00142-4

Binkley, D., Campoe, O.C., Gspaltl, M., Forrester, D.I. Light absorption and use efficiency in forests: Why patterns differ for trees and stands (2013) Forest Ecology and Management, 288, pp. 5-13. DOI: 10.1016/j.foreco.2011.11.002

Blume, T., Schneider, L., Güntner, A. Comparative analysis of throughfall observations in six different forest stands: Influence of seasons, rainfall- and stand characteristics (2022) Hydrological Processes, 36 (3), art. no. e14461. DOI: 10.1002/hyp.14461

Bréda, N.J.J. Ground-based measurements of leaf area index: A review of methods, instruments and current controversies (2003) Journal of Experimental Botany, 54 (392), pp. 2403-2417. Cited 1166 times. DOI: 10.1093/jxb/erg263

Bryant, M.L., Bhat, S., Jacobs, J.M. Measurements and modeling of throughfall variability for five forest communities in the southeastern US (2005) Journal of Hydrology, 312 (1-4), pp. 95-108. DOI: 10.1016/j.jhydrol.2005.02.012

Campbell, G.S.Extinction coefficients for radiation in plant canopies calculated using an ellipsoidal inclination angle distribution (1986) Agricultural and Forest Meteorology, 36 (4), pp. 317-321. DOI: 10.1016/0168-1923(86)90010-9

Carlyle-Moses, D.E., Laureano, J.S.F., Price, A.G. Throughfall and throughfall spatial variability in Madrean oak forest communities of northeastern Mexico (2004) Journal of Hydrology, 297 (1-4), pp. 124-135. DOI: 10.1016/j.jhydrol.2004.04.007

Černý, J., Haninec, P., Pokorný, R. Leaf area index estimated by direct, semi-direct, and indirect methods in European beech and sycamore maple stands (2020) Journal of Forestry Research, 31 (3), pp. 827-836. DOI: 10.1007/s11676-018-0809-0

Chang, S.-C., Matzner, E. The effect of beech stemflow on spatial patterns of soil solution chemistry and seepage fluxes in a mixed beech/oak stand (2000) Hydrological Processes, 14 (1), pp. 135-144. DOI: 10.1002/(SICI)1099-1085(200001)14:1<135::AID-HYP915>3.0.CO;2-R

Coenders-Gerrits, A.M.J., Hopp, L., Savenije, H.H.G., Pfister, L. The effect of spatial throughfall patterns on soil moisture patterns at the hillslope scale (2013) Hydrology and Earth System Sciences, 17 (5), pp. 1749-1763. DOI: 10.5194/hess-17-1749-2013

Crockford, R.H., Richardson, D.P. Partitioning of rainfall into throughfall, stemslow∠d interception effect of forest type, ground cover and climate (2000) Hydrological Processes, 14 (16-17), pp. 2903-2920. DOI: 10.1002/1099-1085(200011/12)14:16/17<2903::AID-HYP126>3.0.CO;2-6

Dufrêne, E., Bréda, N. Estimation of deciduous forest leaf area index using direct and indirect methods (1995) Oecologia, 104 (2), pp. 156-162. DOI: 10.1007/BF00328580

Elliott, K.J., Miniat, C.F., Pederson, N., Laseter, S.H. Forest tree growth response to hydroclimate variability in the southern Appalachians (2015) Global Change Biology, 21 (12), pp. 4627-4641. DOI: 10.1111/gcb.13045

Fabiani, G., Klaus, J., Penna, D. The influence of hillslope topography on beech water use: a comparative study in two different climates (2024) Hydrology and Earth System Sciences, 28 (12), pp. 2683-2703. DOI: 10.5194/hess-28-2683-2024

Fischer-Bedtke, C., Metzger, J.C., Demir, G., Wutzler, T., Hildebrandt, A. Throughfall spatial patterns translate into spatial patterns of soil moisture dynamics - empirical evidence (2023) Hydrology and Earth System Sciences, 27 (15), pp. 2899-2918. DOI: 10.5194/hess-27-2899-2023

Ford, E.D., Deans, J.D. The effects of canopy structure on stemflow, throughfall and interception loss in a young Sitka spruce plantation (1978) J. Appl. Ecol., 15 (3), pp. 905-917. Cited 190 times.

Frischbier, N., Wagner, S. Detection, quantification and modelling of small-scale lateral translocation of throughfall in tree crowns of European beech (Fagus sylvatica L.) and Norway spruce (Picea abies (L.) Karst.) (2015) Journal of Hydrology, 522, pp. 228-238. DOI: 10.1016/j.jhydrol.2014.12.034

Hawthorne, S., Miniat, C.F. Topography may mitigate drought effects on vegetation along a hillslope gradient (2018) Ecohydrology, 11 (1), art. no. e1825. DOI: 10.1002/eco.1825

He, Z.-B., Zhao, M.-M., Zhu, X., Du, J., Chen, L.-F., Lin, P.-F., Li, J. Temporal stability of soil water storage in multiple soil layers in high-elevation forests (2019) Journal of Hydrology, 569, pp. 532-545. DOI: 10.1016/j.jhydrol.2018.12.024

Heartsill-Scalley, T., Scatena, F.N., Estrada, C., McDowell, W.H., Lugo, A.E. Disturbance and long-term patterns of rainfall and throughfall nutrient fluxes in a subtropical wet forest in Puerto Rico (2007) Journal of Hydrology, 333 (2-4), pp. 472-485. DOI: 10.1016/j.jhydrol.2006.09.019

Holder, C.D. Leaf water repellency of species in Guatemala and Colorado (USA) and its significance to forest hydrology studies (2007) Journal of Hydrology, 336 (1-2), pp. 147-154. DOI: 10.1016/j.jhydrol.2006.12.018

Hosking, J.G., Stow, C.D., Bradley, S.G. Corrections for horizontal winds and wind shear in raindrop size spectrometers (1985) Journal of Atmospheric and Oceanic Technology, 2, pp. 181-189.

Hoylman, Z.H., Jencso, K.G., Hu, J., Martin, J.T., Holden, Z.A., Seielstad, C.A., Rowell, E.M. Hillslope Topography Mediates Spatial Patterns of Ecosystem Sensitivity to Climate (2018) Journal of Geophysical Research: Biogeosciences, 123 (2), pp. 353-371. DOI: 10.1002/2017JG004108

Jencso, K.G., McGlynn, B.L., Gooseff, M.N., Wondzell, S.M., Bencala, K.E., Marshall, L.A. Hydrologic connectivity between landscapes and streams: Transferring reach- and plot-scale understanding to the catchment scale(2009) Water Resources Research, 45 (4), art. no. W04428. DOI: 10.1029/2008WR007225

Jennings, S.B., Brown, N.D., Sheil, D. Assessing forest canopies and understorey illumination: Canopy closure, canopy cover and other measures (1999) Forestry, 72 (1), pp. 59-73. DOI: 10.1093/forestry/72.1.59

Jochheim, H., Lüttschwager, D., Riek, W. Stem distance as an explanatory variable for the spatial distribution and chemical conditions of stand precipitation and soil solution under beech (Fagus sylvatica L.) trees (2022) Journal of Hydrology, 608, art. no. 127629. DOI: 10.1016/j.jhydrol.2022.127629

Katayama, A., Nanko, K., Jeong, S., Kume, T., Shinohara, Y., Seitz, S. Short communication: Concentrated impacts by tree canopy drips – hotspots of soil erosion in forests (2023) Earth Surface Dynamics, 11 (6), pp. 1275-1282. DOI: 10.5194/esurf-11-1275-2023

Keim, R.F., Skaugset, A.E., Weiler, M. Temporal persistence of spatial patterns in throughfall (2005) Journal of Hydrology, 314 (1-4), pp. 263-274. DOI: 10.1016/j.jhydrol.2005.03.021

Keller, N., van Meerveld, I., Philipson, C.D., Asner, G.P., Godoong, E., Tangki, H., Ghazoul, J. Does heterogeneity in regenerating secondary forests affect mean throughfall? (2023) Journal of Hydrology, 625, art. no. 130083. DOI: 10.1016/j.jhydrol.2023.130083

Klos, P.Z., Chain-Guadarrama, A., Link, T.E., Finegan, B., Vierling, L.A., Chazdon, R. Throughfall heterogeneity in tropical forested landscapes as a focal mechanism for deep percolation (2014) Journal of Hydrology, 519 (PB), pp. 2180-2188. Cited 38 times. DOI: 10.1016/j.jhydrol.2014.10.004

Kruskal, W.H., Wallis, W.A. Use of Ranks in One-Criterion Variance Analysis (1952) Journal of the American Statistical Association, 47 (260), pp. 583-621. DOI: 10.1080/01621459.1952.10483441

Landsberg, J.J., Waring, R.H. A generalised model of forest productivity using simplified concepts of radiation-use efficiency, carbon balance and partitioning (1997) Forest Ecology and Management, 95 (3), pp. 209-228. Cited 1321 times. DOI: 10.1016/S0378-1127(97)00026-1

Levia, D.F., Jr., Frost, E.E. Variability of throughfall volume and solute inputs in wooded ecosystems (2006) Progress in Physical Geography, 30 (5), pp. 605-632. DOI: 10.1177/0309133306071145

Levia, D.F., Nanko, K., Amasaki, H., Giambelluca, T.W., Hotta, N., Iida, S., Mudd, R.G., Nullet, M.A., Sakai, N., Shinohara, Y., Sun, X., Suzuki, M., Tanaka, N., Tantasirin, C., Yamada, K. Throughfall partitioning by trees (2019) Hydrological Processes, 33 (12), pp. 1698-1708. DOI: 10.1002/hyp.13432

Liu, Y., Liu, S., Wan, S., Wang, J., Wang, H., Liu, K. Effects of experimental throughfall reduction and soil warming on fine root biomass and its decomposition in a warm temperate oak forest (2017) Science of the Total Environment, 574, pp. 1448-1455. DOI: 10.1016/j.scitotenv.2016.08.116

Llorens, P., Domingo, F. Rainfall partitioning by vegetation under Mediterranean conditions. A review of studies in Europe (2007) Journal of Hydrology, 335 (1-2), pp. 37-54. DOI: 10.1016/j.jhydrol.2006.10.032

Llorens, P., Gallart, F. A simplified method for forest water storage capacity measurement (2000) Journal of Hydrology, 240 (1-2), pp. 131-144. Cited 187 times. DOI: 10.1016/S0022-1694(00)00339-5

Llorens, P., Poch, R., Latron, J., Gallart, F. Rainfall interception by a Pinus sylvestris forest patch overgrown in a Mediterranean mountainous abandoned area I. Monitoring design and results down to the event scale (1997) Journal of Hydrology, 199 (3-4), pp. 331-345. DOI: 10.1016/S0022-1694(96)03334-3

Loescher, H.W., Powers, J.S., Oberbauer, S.F. Spatial variation of throughfall volume in an old-growth tropical wet forest, Costa Rica (2002) Journal of Tropical Ecology, 18 (3), pp. 397-407. DOI: 10.1017/S0266467402002274

Macchioli Grande, M., Kaffas, K., Verdone, M., Borga, M., Cocozza, C., Dani, A., Errico, A., Fabiani, G., Gourdol, L., Klaus, J., Manca di Villahermosa, F.S., Massari, C., Murgia, I., Pfister, L., Preti, F., Segura, C., Tailliez, C., Trucchi, P., Zuecco, G., Penna, D. Seasonal meteorological forcing controls runoff generation at multiple scales in a Mediterranean forested mountain catchment (2024) Journal of Hydrology, 639, art. no. 131642, . Cited 4 times. DOI: 10.1016/j.jhydrol.2024.131642

Manderscheid, B., Matzner, E. Spatial and temporal variation of soil solution chemistry and ion fluxes through the soil in a mature Norway Spruce (Picea abies (L.) Karst.) stand (1995) Biogeochemistry, 30 (2), pp. 99-114. DOI: 10.1007/BF00002726

Manfreda, S., McCabe, M.F., Miller, P.E., Lucas, R., Madrigal, V.P., Mallinis, G., Dor, E.B., Helman, D., Estes, L., Ciraolo, G., Müllerová, J., Tauro, F., de Lima, M.I., de Lima, J.L.M.P., Maltese, A., Frances, F., Caylor, K., Kohv, M., Perks, M., Ruiz-Pérez, G., Su, Z., Vico, G., Toth, B. On the use of unmanned aerial systems for environmental monitoring (2018) Remote Sensing, 10 (4), art. no. 641. DOI: 10.3390/rs10040641

Marsalek, J. Calibration of the tipping-bucket raingage (1981) Journal of Hydrology, 53 (3-4), pp. 343-354. DOI: 10.1016/0022-1694(81)90010-X

Molina, A.J., Llorens, P., Garcia-Estringana, P., Moreno de las Heras, M., Cayuela, C., Gallart, F., Latron, J. Contributions of throughfall, forest and soil characteristics to near-surface soil water-content variability at the plot scale in a mountainous Mediterranean area (2019) Science of the Total Environment, 647, pp. 1421-1432. DOI: 10.1016/j.scitotenv.2018.08.020

Möttönen, M., Järvinen, E., Hokkanen, T.J., Kuuluvainen, T., Ohtonen, R. Spatial distribution of soil ergosterol in the organic layer of a mature Scots pine (Pinus sylvestris L.) forest (1999) Soil Biology and Biochemistry, 31 (4), pp. 503-516. DOI: 10.1016/S0038-0717(98)00122-9

Murakami, S. Application of three canopy interception models to a young stand of Japanese cypress and interpretation in terms of interception mechanism (2007) Journal of Hydrology, 342 (3-4), pp. 305-319. DOI: 10.1016/j.jhydrol.2007.05.032

Nanko, K., Onda, Y., Ito, A., Moriwaki, H. Spatial variability of throughfall under a single tree: Experimental study of rainfall amount, raindrops, and kinetic energy (2011) Agricultural and Forest Meteorology, 151 (9), pp. 1173-1182. Cited 95 times. DOI: 10.1016/j.agrformet.2011.04.006

Norman, J.M. Jarvis, P.G. Photosynthesis in Sitka Spruce (Picea sitchensis (Bong.) Carr.). III. Measurements of Canopy Structure and Interception of Radiation (1974). The Journal of Applied Ecology 11, 375. 10.2307/2402028.

Oberhuber, W., Kofler, W. Topographic influences on radial growth of Scots pine (Pinus sylvestris L.) at small spatial scales (2000) Principal Component Analysis. Plant Ecology, 46, pp. 229-238.

Park, A., Cameron, J.L. The influence of canopy traits on throughfall and stemflow in five tropical trees growing in a Panamanian plantation (2008) Forest Ecology and Management, 255 (5-6), pp. 1915-1925. DOI: 10.1016/j.foreco.2007.12.025

Penna, D., Borga, M., Norbiato, D., Dalla Fontana, G. Hillslope scale soil moisture variability in a steep alpine terrain (2009) Journal of Hydrology, 364 (3-4), pp. 311-327. Cited 199 times. DOI: 10.1016/j.jhydrol.2008.11.009

Penna, D., Brocca, L., Borga, M., Dalla Fontana, G. Soil moisture temporal stability at different depths on two alpine hillslopes during wet and dry periods (2013) Journal of Hydrology, 477, pp. 55-71. DOI: 10.1016/j.jhydrol.2012.10.052

Pook, E.W., Moore, P.H.R., Hall, T. Rainfall interception by trees of Pinus radiata, and Eucalyptus viminalis, in a 1300 mm rainfall area of southeastern New South Wales: I. Gross losses and their variability (1991) Hydrological Processes, 5 (2), pp. 127-141. DOI: 10.1002/hyp.3360050202

Rinehart, R.E. Out-of-level instruments: errors in hydrometeor spectra and precipitation measurements. (1983) Journal of Climate & Applied Meteorology, 22 (8), pp. 1404-1410. DOI: 10.1175/1520-0450(1983)022<1404:OOLIEI>2.0.CO;2

Rodrigo, A., Àvila, A. Influence of sampling size in the estimation of mean throughfall in two Mediterranean holm oak forests (2001) Journal of Hydrology, 243 (3-4), pp. 216-227. DOI: 10.1016/S0022-1694(00)00412-1

Rodrigues, A.F., Terra, M.C.N.S., Mantovani, V.A., Cordeiro, N.G., Ribeiro, J.P.C., Guo, L., Nehren, U., Mello, J.M., Mello, C.R. Throughfall spatial variability in a neotropical forest: Have we correctly accounted for time stability? (2022) Journal of Hydrology, 608, art. no. 127632. DOI: 10.1016/j.jhydrol.2022.127632

Savina, M., Schäppi, B., Molnar, P., Burlando, P., Sevruk, B. Comparison of a tipping-bucket and electronic weighing precipitation gage for snowfall (2012) Atmospheric Research, 103, pp. 45-51. DOI: 10.1016/j.atmosres.2011.06.010

Scatena, F.N., Moya, S., Estrada, C., Chinea, J.D. The first five years in the reorganization of aboveground biomass and nutrient use following Hurricane Hugo in the Bisley Experimental Watersheds, Luquillo Experimental Forest, Puerto Rico (1996) Biotropica, 28 (4 A), pp. 424-440. DOI: 10.2307/2389086

Siegert, C.M., Levia, D.F., Hudson, S.A., Dowtin, A.L., Zhang, F., Mitchell, M.J. Small-scale topographic variability influences tree species distribution and canopy throughfall partitioning in a temperate deciduous forest (2016) Forest Ecology and Management, 359, pp. 109-117. DOI: 10.1016/j.foreco.2015.09.028

Siegert, C.M., Drotar, N.A., Alexander, H.D. Spatial and temporal variability of throughfall among oak and co-occurring non-oak tree species in an upland hardwood forest (2019) Geosciences (Switzerland), 9 (10), art. no. 405. DOI: 10.3390/geosciences9100405

Šraj, M., Brilly, M., Mikoš, M. Rainfall interception by two deciduous Mediterranean forests of contrasting stature in Slovenia (2008) Agricultural and Forest Meteorology, 148 (1), pp. 121-134. DOI: 10.1016/j.agrformet.2007.09.007

Staelens, J., De Schrijver, A., Verheyen, K., Verhoest, N.E.C. Spatial variability and temporal stability of throughfall water under a dominant beech (Fagus sylvatica L.) tree in relationship to canopy cover (2006) Journal of Hydrology, 330 (3-4), pp. 651-662. DOI: 10.1016/j.jhydrol.2006.04.032

Staelens, J., De Schrijver, A., Verheyen, K., Verhoest, N.E.C. Rainfall partitioning into throughfall, stemflow, and interception within a single beech (Fagus sylvatica L.) canopy: Influence of foliation, rain event characteristics, and meteorology (2008) Hydrological Processes, 22 (1), pp. 33-45. DOI: 10.1002/hyp.6610

Sypka, P. Dynamic real-time volumetric correction for tipping-bucket rain gauges (2019) Agricultural and Forest Meteorology, 271, pp. 158-167. DOI: 10.1016/j.agrformet.2019.02.044

Tromp-van Meerveld, H.J., McDonnell, J.J. On the interrelations between topography, soil depth, soil moisture, transpiration rates and species distribution at the hillslope scale (2006) Advances in Water Resources, 29 (2), pp. 293-310. DOI: 10.1016/j.advwatres.2005.02.016

Vachaud, G., Passerat De Silans, A., Balabanis, P., Vauclin, M. Temporal stability of spatially measured soil water probability density function. (1985) Soil Science Society of America Journal, 49 (4), pp. 822-828. DOI: 10.2136/sssaj1985.03615995004900040006x

Valante, F., David, J.S., Gash, J.H.C. Modelling interception loss for two sparse eucalypt and pine forests in central Portugal using reformulated Rutter and Gash analytical models (1997) Journal of Hydrology, 190 (1-2), pp. 141-162. DOI: 10.1016/S0022-1694(96)03066-1

Van Stan, J.T., II, Van Stan, J.H., Levia, D.F., Jr. Meteorological influences on stemflow generation across diameter size classes of two morphologically distinct deciduous species (2014) International Journal of Biometeorology, 58 (10), pp. 2059-2069. DOI: 10.1007/s00484-014-0807-7

Whelan, M.J., Anderson, J.M. Modelling spatial patterns of throughfall and interception loss in a Norway spruce (Picea abies) plantation at the plot scale (1996) Journal of Hydrology, 186 (1-4), pp. 335-354. DOI: 10.1016/S0022-1694(96)03020-X

Zabret, K., Rakovec, J., Šraj, M. Influence of meteorological variables on rainfall partitioning for deciduous and coniferous tree species in urban area (2018) Journal of Hydrology, 558, pp. 29-41. DOI: 10.1016/j.jhydrol.2018.01.025

Zhang, J., Bruijnzeel, L.A., van Meerveld, H.J.I., Ghimire, C.P., Tripoli, R., Pasa, A., Herbohn, J. Typhoon-induced changes in rainfall interception loss from a tropical multi-species 'reforest' (2019) Journal of Hydrology, 568, pp. 658-675. DOI: 10.1016/j.jhydrol.2018.11.024

Zhu, X., He, Z., Du, J., Chen, L., Lin, P., Tian, Q. Spatial heterogeneity of throughfall and its contributions to the variability in near-surface soil water-content in semiarid mountains of China (2021) Forest Ecology and Management, 488, art. no. 119008. DOI: 10.1016/j.foreco.2021.119008

Zimmermann, B., Zimmermann, A., Scheckenbach, H.L., Schmid, T., Hall, J.S., Van Breugel, M. Changes in rainfall interception along a secondary forest succession gradient in lowland Panama (2013) Hydrology and Earth System Sciences, 17 (11), pp. 4659-4670. DOI: 10.5194/hess-17-4659-2013

Supplementary material 1

Table S1. Gross precipitation (GP) and total throughfall (TF) amount for each sampling period (all in mm). Gray cells indicate the growing period. The measurements excluded from the analysis due to GP underestimation are marked with "*".

Period number	Sampling date	GP	TF tot.	TF upper grid	TF transect	TF lower grid
1	30/07/2020	5	1	1	1	1
2	05/08/2020	9	3	4	4	3
3	02/09/2020	44	31	33	32	29
4	22/09/2020	10	6	6	6	5
5	01/10/2020	111	65	68	68	60
6	19/10/2020	192	149	161	156	133
7	28/10/2020	31	24	25	25	22
8	17/11/2020	47	29	32	30	26
9	04/12/2020	57	21	20	23	20
10	11/12/2020	138	97	105	106	83
11	19/01/2021	244	137	145	137	129
12*	02/02/2021	90	117	127	122	105
13	04/03/2021	92	76	83	85	63
14	09/04/2021	25	8	9	6	7
15	23/04/2021	61	39	44	43	33
16	14/05/2021	109	102	110	109	90
17	28/05/2021	49	47	51	51	41
18	11/06/2021	19	12	12	13	11
19	23/06/2021	0	0	0	0	0
20	27/07/2021	34	22	22	25	21
21	09/08/2021	17	12	13	13	9
22	25/08/2021	0	0	0	0	0
23	21/09/2021	63	44	46	47	40
24	06/10/2021	68	58	61	60	54
25	20/10/2021	73	41	44	45	36
26	15/12/2021	239	119	126	127	106
27	10/02/2022	140	111	118	117	99
28	29/03/2022	82	55	67	55	45
20	29/04/2022	145	124	132	134	110
30	19/05/2022	43	11	12	15	8
31	31/05/2022	3	0	0	0	0
32	16/06/2022	7	0	0	0	0
33	30/06/2022	3	0	0	0	0
34	06/07/2022	0	0	0	0	0
35	14/07/2022	10	0	0	0	0
36	26/07/2022	0	0	0	0	0
37	03/08/2022	20	3	4	5	1
38	18/08/2022	43	8	9	9	5
39	24/08/2022	31	26	28	28	23

40	07/09/2022	31	19	18	21	17
41	05/10/2022	176	175	179	196	160
41	10/10/2022	2	0	0	0	0
43	12/10/2022	3	0	0	0	0
44	14/11/2022	20	10	11	9	8
45	24/11/2022	114	114	121	122	103
46*	13/12/2022	88	165	132	123	210
47*	21/12/2022	65	84	92	89	73
48*	11/01/2023	37	54	57	57	49
49*	16/02/2023	81	-	-	-	-
50*	21/02/2023	0	2	2	2	2
51*	09/03/2023	50	146	151	152	137
52	29/03/2023	41	40	39	53	31
53	18/04/2023	57	49	48	61	43
54	27/04/2023	44	40	41	50	34
55	05/05/2023	57	60	57	70	55
56	22/05/2023	210	214	219	233	197
57	06/06/2023	58	50	47	63	46
58	17/07/2023	93	29	25	42	27
50*	26/07/2023	15	18	15	29	14
60*	23/08/2023	18	0	0	0	0
61	01/09/2023	21	16	16	17	15

Table S2. Spearman rank correlation between the overall TF ratio for each sampler and distance to the closest tree stem, Plant Area Index (PAI), or canopy cover for the entire study period, the growing, dormant season, as well as the range in Spearman rank correlation values for the TF ratios for the individual measurement dates (min-max).

CLOSEST STEM DISTANCE	**Lower grid**	**Upper grid**
Entire study period	-0.01	0.03
Growing season	0.06	-0.04
Dormant season	-0.16	0.08
Range for individual measurement dates	-0.29 – 0.27	-0.31 – 0.28
PAI		
Growing season	0.05	-0.10
Dormant season	0.05	-0.20
Range for individual measurement dates	-0.24 – 0.42	-0.29 – 0.42
CANOPY COVER		
Growing season	0.10	-0.12
Dormant season	-0.05	-0.07
Range for individual measurement dates	-0.31 – 0.20	-0.26 – 0.36

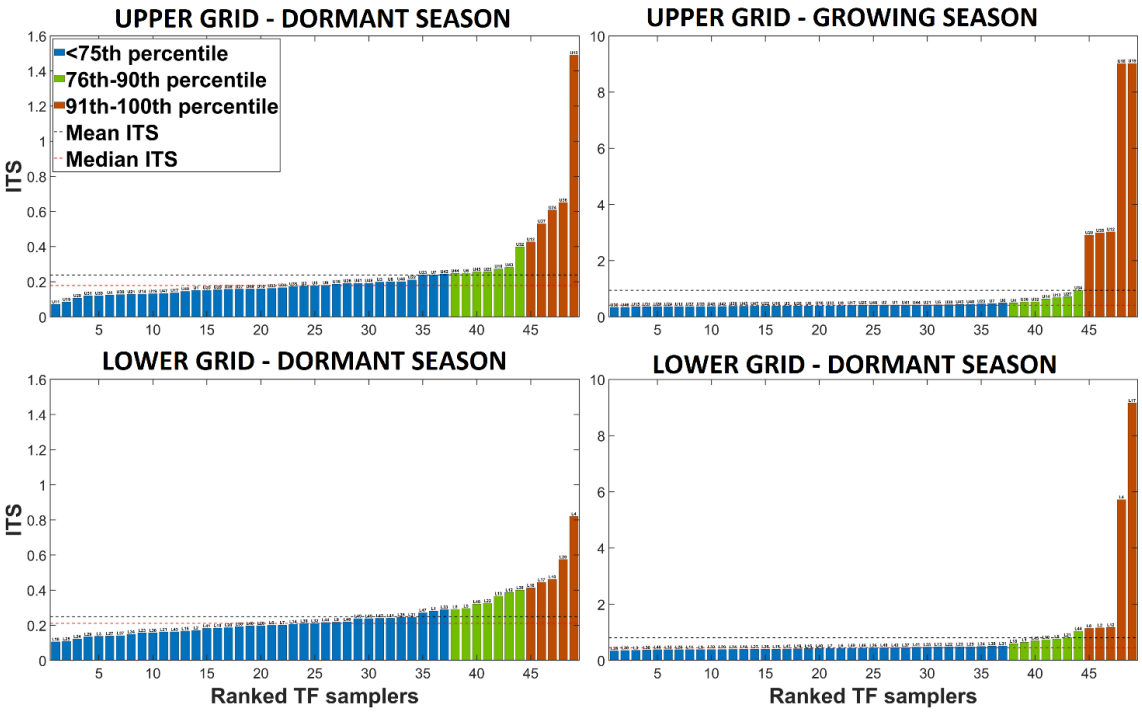

Figure S1. ITS of TF for the dormant (left column) and growing (right column) season in the upper and lower grid. Note that the TF samplers are ranked by ITS.

Appendix 1: Geostatistical and deterministic approaches to throughfall measurements

Matteo Verdone[*1,2], Anke Hildebrandt[3], Ilenia Murgia[1], Diletta Chirici[1], Christian Massari[2], Ilja van Meerveld[4], and Daniele Penna[1,2,5]

[1]Department of Agriculture, Food, Environment and Forestry, University of Florence, Italy
[2]Research Institute of the Geo–Hydrological Protection, National Research Council, Italy
[3]Institute of Geoscience, Friedrich Schiller University Jena, Deutschland.
[4]Department of Geography, University of Zurich, Switzerland
[5]Oregon State University, Forest Engineering Resources and Management Department, Corvallis, OR, USA

Disclaimer

This section will be part of a comparison work between throughfall data collected, with a comparable sampling design, in the Lecciona catchment (Italy) and in the Hainich Critical Zone Exploratory (CZE Hainich, Germany). Preliminary results presented here are based on data collected in the Lecciona site.

Throughfall data analysis

TF was monitored from February 2024 to March 2025 using plastic collectors with an opening of 60 cm^2, manually emptied roughly after each rainfall event since February 2024. The samplers were deployed on the Lecciona hillslope forming 18 squares of 10x10 m, for a total monitoring area of 1800 m^2 (Fig.1). In each square, two TF collectors were randomly placed ("kernel" collectors) and in six squares a transect made of four collectors with increasing distances one for each other (0.1 m, 0.4 m and 0.5 m) was positioned. Furthermore, nine trees were selected to host a radial transect made of three collectors with increasing distance from the tree stem (0.2 m, 0.6 m, and 1.1 m). Gross precipitation was measured by a weather station placed at the top of the hillslope. We divided the entire observation period into leafed and leafless periods (Verdone et al., 2025). The samplers on the short transects were used only for geostatistical analysis.

For each TF sampler, we geolocalized the position within the experimental plot using a total station, then we calculated the elevation and the distance from the closest stem for each one. We implemented forest surveys as shown in Section 1.2.2.3 with the positions of trees not included in previous experimental design.

To assest the effect of tree distance, we normalized TF data for each sampling day using the approach of Fischer-Bedtke et al.(2023). We divided the data in tree distance classes. The first class was for distances <0.25m, the other classes were 0.5 m wide each one and, the last classes aggregated values higher than 3.25 m to avoid classes with few samples.

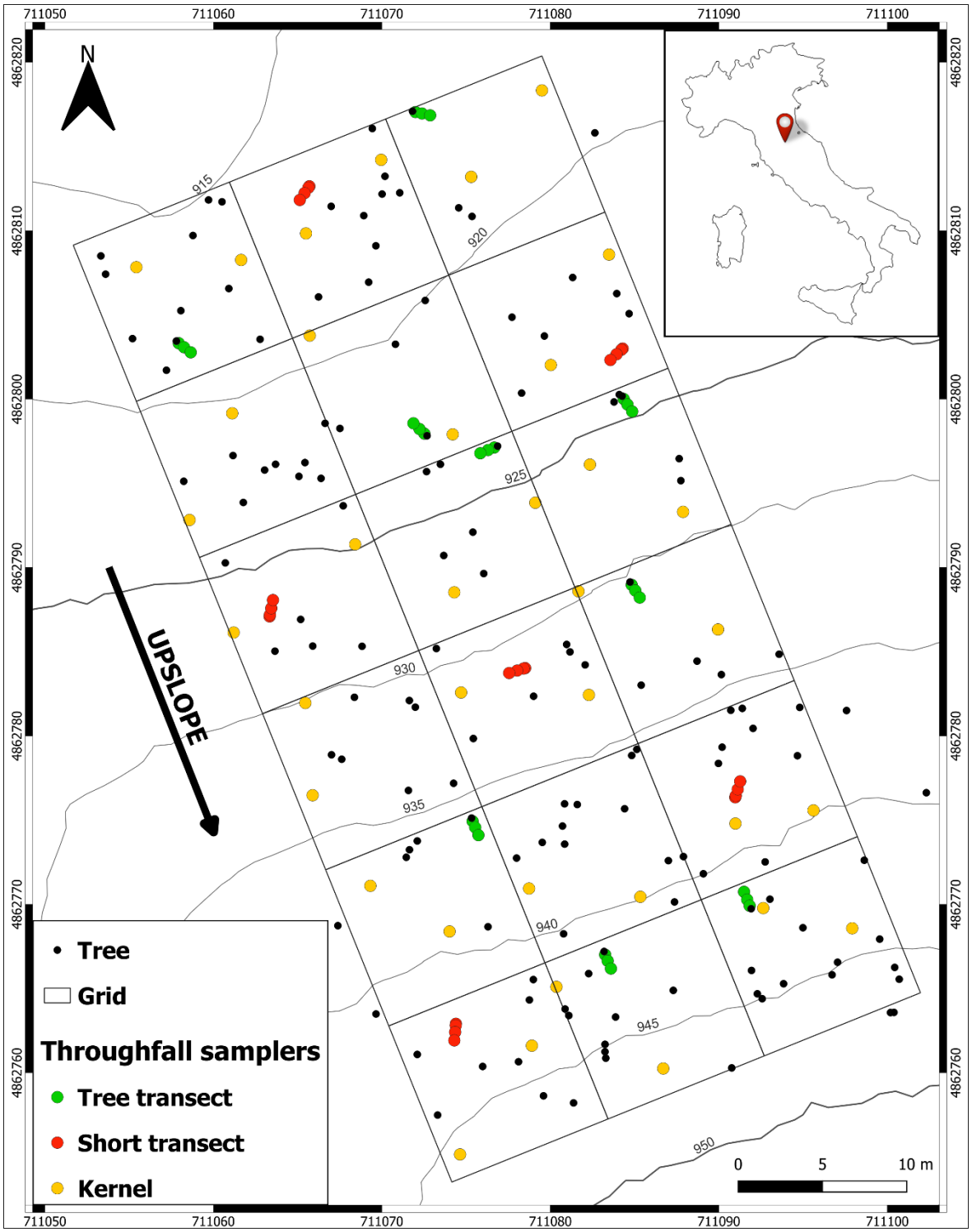

Fig.1. Map of the experimental plot. TF was monitored by 87 collectors distributed in a grid of 18 squares of 10x10 m. Two TF collectors ("kernel") were randomly placed in each square. In six squares, a "short transect" of four collectors with variable spacing was deployed. Nine trees were selected to host a "tree transect" made of three collectors with increasing distance from the stem. Forest surveys were conducted to measure the diameter and height of the trees in the plot.

We employed variograms to assess spatial patterns in event throughfall. Variogram analysis serves as a method for evaluating the continuity of spatial phenomena, quantifying the spatial variability as the mean squared difference between measurements taken at various locations (Keim et al., 2005). Variograms are defined

by the sill, which represents the maximum semivariance determined by the total variance of the dataset, and the range, which indicates the distance at which the variogram attains the sill. The range illustrates the scale of length over which TF quantities exhibit correlation, and is also referred to as the spatial correlation length (Keim et al., 2005). Variograms often present a "nugget", which refers to the anticipated variation between samples when the separation distance approaches zero. This phenomenon may be due to intrinsic small-scale spatial variability or inaccuracies in the data, such as sampling and database errors. First, we calculated four empirical TF variograms using four different variogram estimators. We used non-robust (Matheron, 1962) and robust (Cressie and Hawkins, 1980) models. Then, we fitted three models (spherical, exponential, and pure nugget) to each empirical variogram and chose the model with the lowest residual sum of squares (Fischer-Bedtke et al.,2023).
To investigate the temporal stability of TF, we used the temporal stability analysis approach (Vachaud et al., 1985, He et al., 2019). We calculated the Mean Relative Difference (MRD) of TF for each sampler and the corresponding Standard Deviation of the Relative Difference (SDRD) (Vachaud et al., 1985). The MRD represents the systematic bias in TF at a location relative to the spatial average. SDRD represents the persistence of the location in representing the TF spatial average. To take both the MRD and SDRD metrics into account, we used the Index of Temporal Stability (ITS) that combines the effect of both the MRD and SDRD (Penna et al., 2013, Rodrigues et al., 2022).

Results

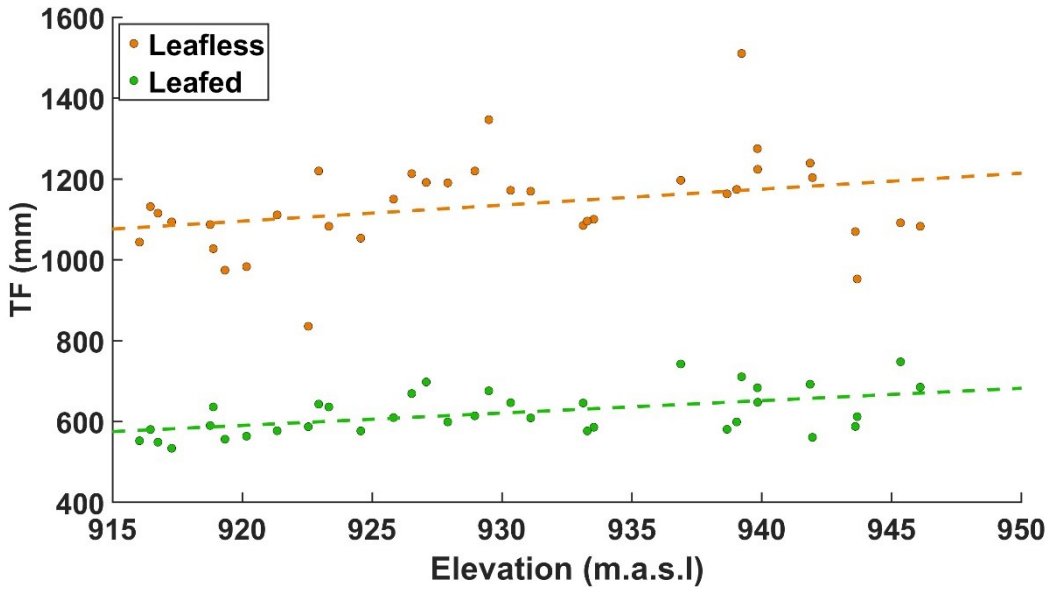

Fig.2. TF cumulative for each sampler divided by period with leaves and period without leaves. Only kernel samplers are considered to avoid bias induced by tree proximity.

TF amount increases linearly with elevation (Fig.2) in leafed and leafless periods, with a slightly higher slope for the leafless period. This confirms our observations with the previous experimental design Section 1.3.3 of this thesis).

Values for the leafed period appear less sparse than values for the leafless period, suggesting that without leaves, the TF ratio for each sampler persists across the events. On the other hand, canopy cover in the leafed period acts like a filter that randomly redistributes water. The temporal stability analysis confirms this observation, considering all samplers (Fig.3), or kernels only (Fig. 4), or tree transects only (Fig. 5). ITS was even lower for the leafless period, as for the previous design Sections 1.3.4 and 1.4.4).

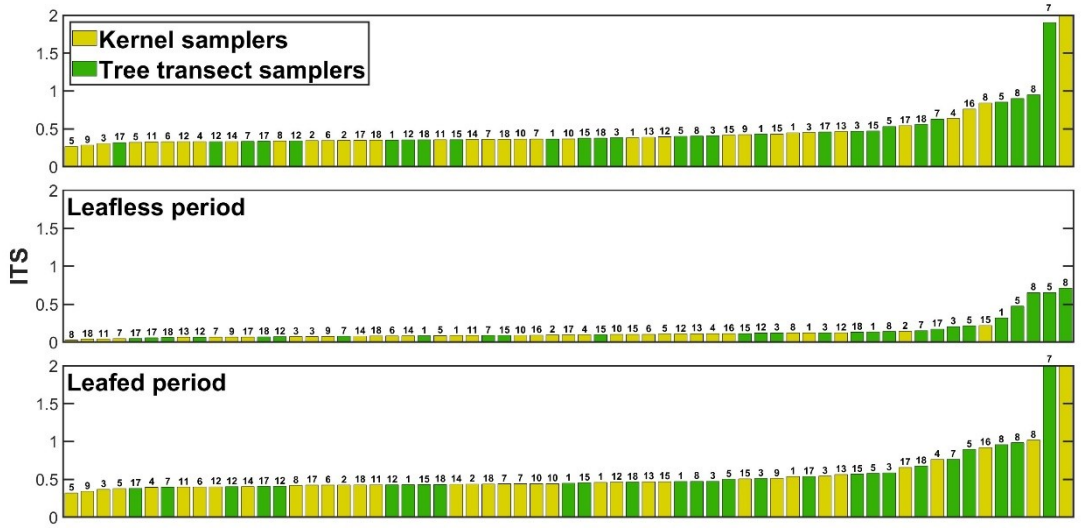

Fig.3. ITS of TF for all samplers for the leafless and the leafed period. The last two bars are not entirely shown to better appreciate the lower values. The number above each column indicates the square numbers, from 1 to 18. Lower numbers are associated with lower elevation.

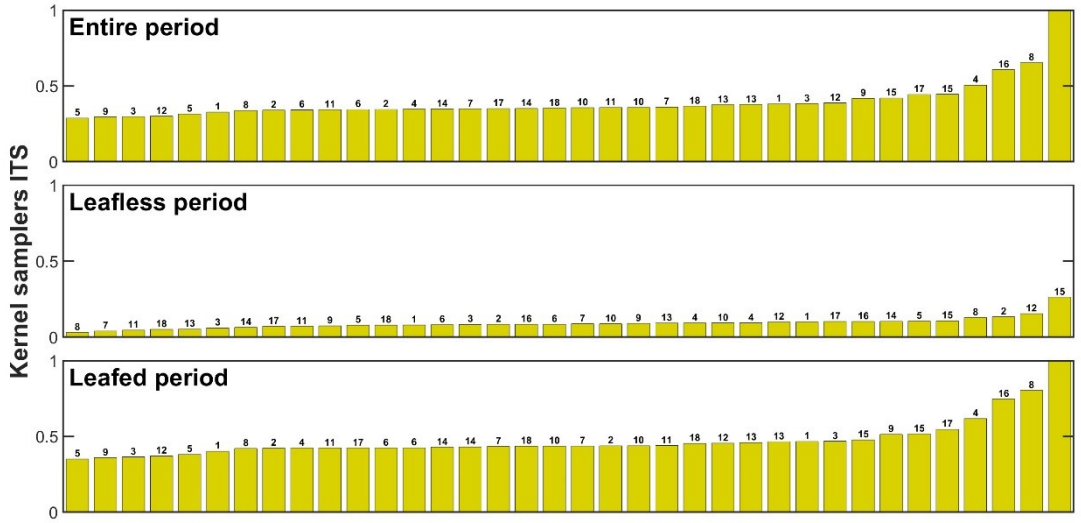

Fig.4. ITS of TF for the kernel samplers for the leafless and the leafed period. The last two bars are not entirely shown to better appreciate the lower values. The number above each column indicates the square numbers, from 1 to 18. Lower numbers are associated with lower elevation.

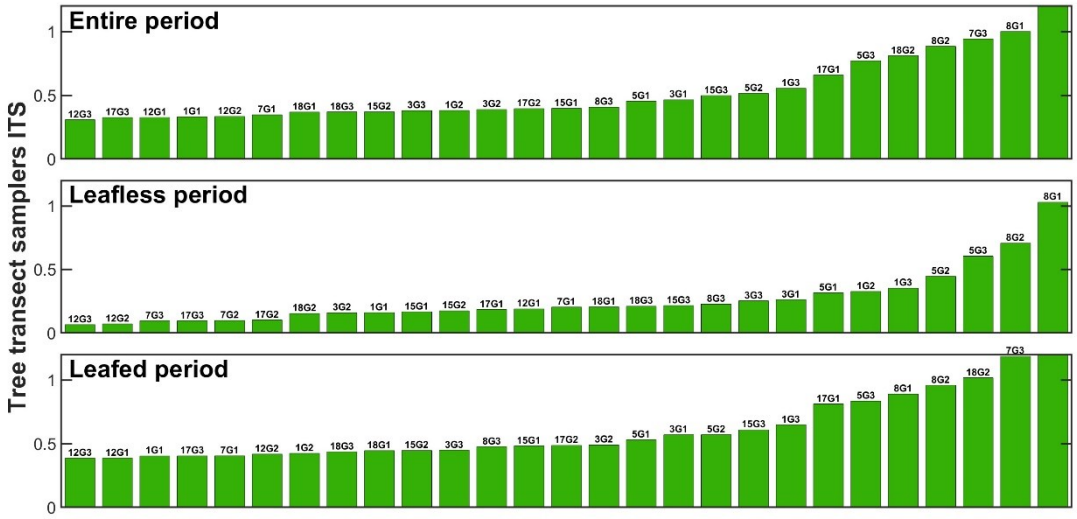

Fig.5. ITS of TF for the tree transect samplers for the leafless and the leafed period. The last two bars are not entirely shown to better appreciate the lower values. The number above each column indicates the square numbers, from 1 to 18. Lower numbers are associated with lower elevations. The first number in the label of each bar indicates the square number (Fig. 1); the letter indicates the type of sampler (G: green); and the last number indicates the distance from the stem ((1=0.2 m, 2=0.6 m and 3=1.1 m).

The relation between TF and stem distance (Fig. 6) shows that TF is affected by distance to the closest stem only for the first meter, in which TF increases with distance. For longer distances, TF variability decreases for each class, and the spatial trend disappears. This is a combined effect of crown architecture and large branches in creating dripping points and/or dry points for TF. A similar behaviour is observed in the leafed and leafless periods, with higher variability in the leafed period. Observing what happened in the first meter of distance from the stem (Fig.6), samplers in squares 3,5,7,15, and 18 show an increasing trend of TF amount with distance in both periods, while in square 12 there is an opposite trend. In squares 1 and 17, there is an increasing trend in the leafless period, but no trend in the leafed period. In square 8, the trend is decreasing during the leafless period. Our results are in partial agreement with those by Jochheim et al. (2022), who found that TF was lower near the stem than further away in summer and higher in winter, while in our study, the general trend is similar in both periods. The short and weak spatial correlation between tree distance and TF confirms previous studies conducted in other climates (Staelens et al., 2006; Nanko et al., 2011).

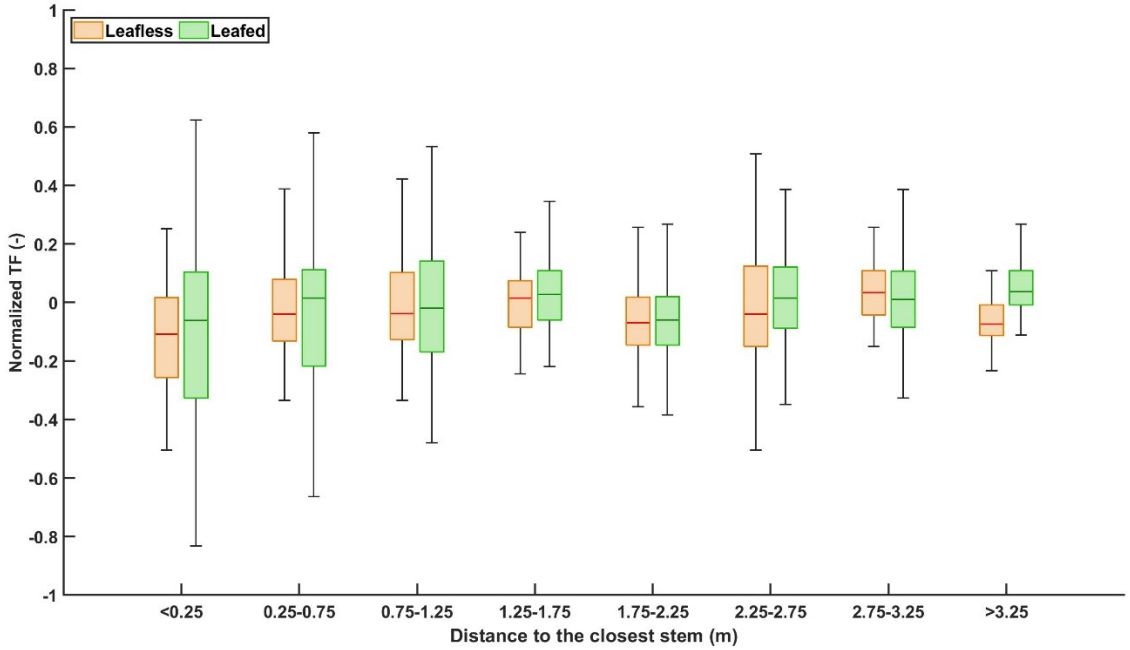

Fig.6. Relation between normalised TF values and distance to closest stem. The bottom and top of each box represent the 25th and 75th percentiles.

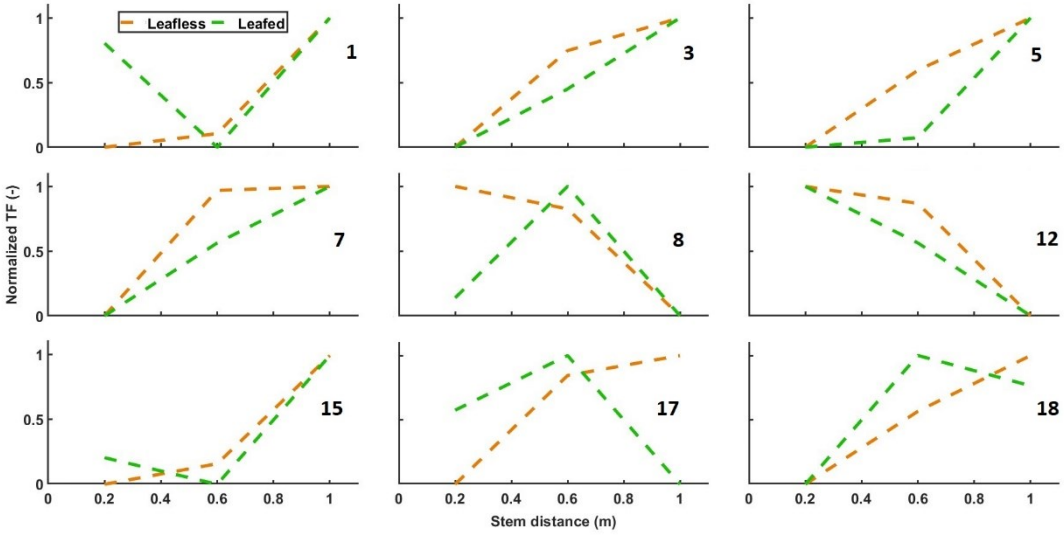

Fig.7. Relation between normalised TF values and distance to stem for the transect samplers divided into leafless and leafed periods.

The explorative variogram analysis for the leafless period shows median ranges of 5 m, while median ranges become around 2 m in the leafed period (Fig.8). This difference is caused by the effect of canopy cover when leaves are on branches in redistributing rain water (Keim et al., 2005). Boxplots are skewed upward due to the shape of the grid that extends along the topographic gradient (Fig.1), which generates a trend in TF values related to elevation (Fig.2) that increases the range. Short range explained how the previous experimental design was not able to catch the spatial correlation TF sampler's distance was indeed higher (and multiplier) than 2 m.

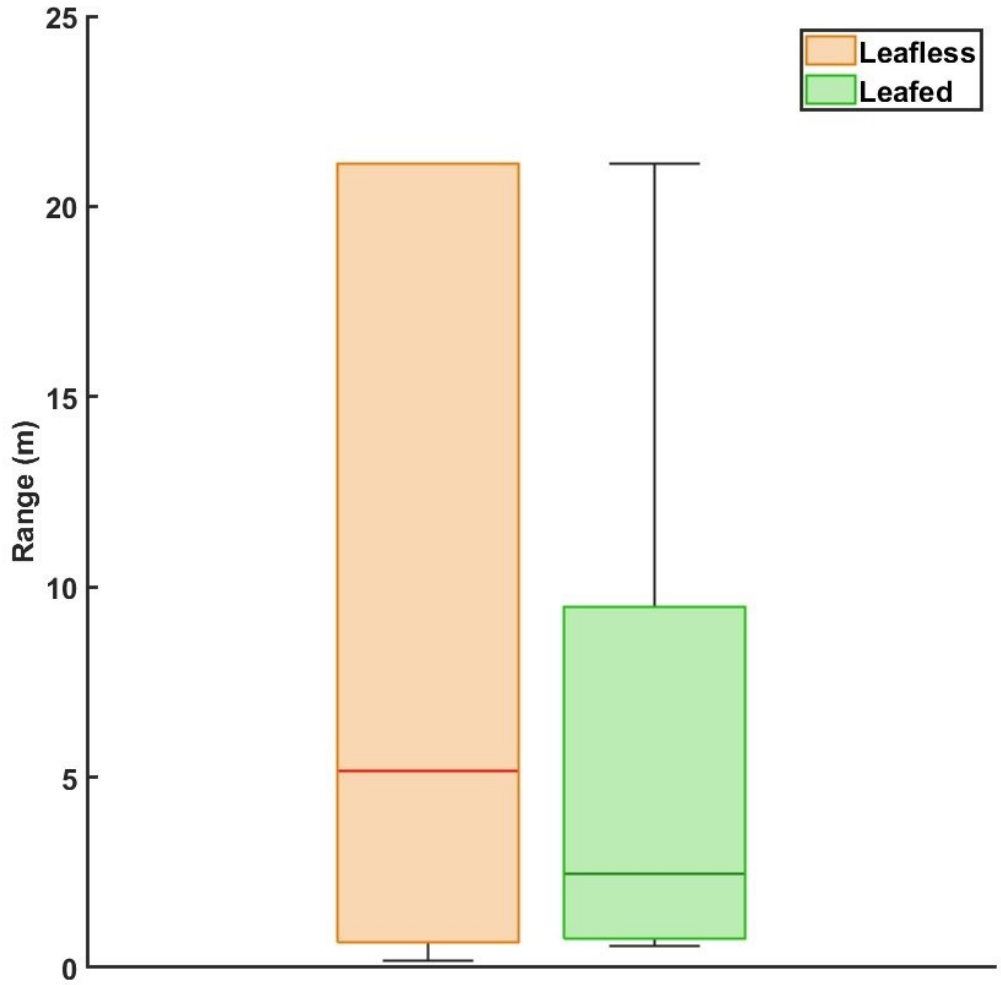

Fig.8. Variogram range for the leafless and leafed periods. The bottom and top of each box represent the 25th and 75th percentiles, the horizontal line marks the median. N=14 for the leafless period, and N=17 for the leaved period.

References

Cressie, N., Hawkins, D.M. Robust estimation of the variogram: I. Mathematical Geology 12, 115–125 (1980). https://doi.org/10.1007/BF01035243

Fischer-Bedtke, C., Metzger, J. C., Demir, G., Wutzler, T., and Hildebrandt, A.: Throughfall spatial patterns translate into spatial patterns of soil moisture dynamics – empirical evidence, Hydrol. Earth Syst. Sci., 27, 2899–2918, https://doi.org/10.5194/hess-27-2899-2023, 2023.

He, Z., Zhao, M., Zhu, X., Du, J., Chen, L., Lin, P., & Li, J. (2019). Temporal stability of soil water storage in multiple soil layers in high-elevation forests. *Journal of Hydrology*, *569*, 532-545. https://doi.org/10.1016/j.jhydrol.2018.12.024

Keim, R., Skaugset, A., & Weiler, M. (2005). Temporal persistence of spatial patterns in throughfall. Journal of Hydrology, 314(1-4), 263-274. https://doi.org/10.1016/j.jhydrol.2005.03.021

Matheron, G.: Traité de géostatistique appliquée, Éditions Technip, Paris, 333 pp., https://www.sudoc.fr/004651340 (last access: 24 July 2023), 1962.

Nanko, K., Onda, Y., Ito, A., & Moriwaki, H. (2011). Spatial variability of throughfall under a single tree: Experimental study of rainfall amount, raindrops, and kinetic energy. Agricultural and Forest Meteorology, 151(9), 1173-1182. https://doi.org/10.1016/j.agrformet.2011.04.006

Nanko, K., Onda, Y., Ito, A., & Moriwaki, H. (2011). Spatial variability of throughfall under a single tree: Experimental study of rainfall amount, raindrops, and kinetic energy. *Agricultural and Forest Meteorology*, *151*(9), 1173-1182. https://doi.org/10.1016/j.agrformet.2011.04.006

Penna, D., Brocca, L., Borga, M., & Dalla Fontana, G. (2013). Soil moisture temporal stability at different depths on two alpine hillslopes during wet and dry periods. *Journal of Hydrology*, *477*, 55-71. https://doi.org/10.1016/j.jhydrol.2012.10.052

Rodrigues, A. F., Terra, M. C., Mantovani, V. A., Cordeiro, N. G., Ribeiro, J. P., Guo, L., Nehren, U., Mello, J. M., & Mello, C. R. (2022). Throughfall spatial variability in a neotropical forest: Have we correctly accounted for time stability? Journal of Hydrology, 608, 127632. https://doi.org/10.1016/j.jhydrol.2022.127632

Staelens, J., De Schrijver, A., Verheyen, K., & Verhoest, N. E. (2006). Spatial variability and temporal stability of throughfall water under a dominant beech (Fagus sylvatica L.) tree in relationship to canopy cover. *Journal of Hydrology*, *330*(3-4), 651-662. https://doi.org/10.1016/j.jhydrol.2006.04.032

Vachaud, G., De Silans, A. P., Balabanis, P., & Vauclin, M. (1985). Temporal Stability of Spatially Measured Soil Water Probability Density Function. Soil Science Society of America Journal, 49(4), 822-828. https://doi.org/10.2136/sssaj1985.03615995004900040006x

Verdone, M., Van Meerveld, I., Massari, C., & Penna, D. (2025). Variability and temporal stability of throughfall along a hillslope. *Journal of Hydrology*, *647*, 132294. https://doi.org/10.1016/j.jhydrol.2024.132294

2. Topography controls the response of beech trees to atmospheric demand during summer droughts

This chapter is taken from: Verdone, M., Massari, C., Murgia, I., Cocozza, C., Van Meerveld, & Penna, D. (2025). Topography controls the response of beech trees to atmospheric demand during summer droughts. *Ecohydrology*. Under review.

Abstract

Droughts can significant impacting tree responses in Mediterranean forest ecosystems and will likely increase in frequency and intensity. To better understand the combined effects of landscape position, (topography and related variation in soil moisture) and atmospheric demand (vapor pressure deficit; VPD) on tree transpiration during drought periods, we examined the variations in sap flow velocity as a function of water availability, VPD and air temperature across a forested hillslope in central Italy. Our results show that sap flow velocity decreased during the hottest period for upslope trees but remained stable for the riparian trees. The sap flow velocity of trees on the midslope and upslope locations was mainly affected by soil moisture, while riparian trees responded more to variations in VPD and temperature. The analysis of the time lag between VPD and peak sap flow velocity showed that the trees were not stressed during low temperatures, but high temperatures caused stress for the mid- and upslope trees. These results suggest that the wet riparian zone limited tree water stress, resulting in greater sap flow velocities than for upslope and midslope trees, which experienced moderate stress during summer droughts. These results highlight the need to account for small scale topographic and moisture related differences when analysing the response of trees to droughts and in ecohydrological models that aim to capture the variability in evapotranspiration fluxes across the landscape. However, these results need to be validated in different climatic zones and for different tree species.

2.1 Introduction

Due to climate change, summer droughts are expected to become longer and more intense (Kukal and Hobbins, 2025; Shuai et al., 2025), causing stress on ecosystems (Van der Molen et al., 2011) and water resources (Orth et al., 2018; Teuling et al., 2013). Droughts pose a particular pressure on forests by directly inducing tree mortality or making trees more vulnerable to biotic stresses (Gazol and Camarero, 2022; Caudullo and Barredo, 2019; Rebollo et al., 2024).

The response of mountain forested ecosystems in the Mediterranean region to droughts can be very diverse due to the combined effects of the strong seasonality in the meteorological forcing (Lopez-Bustins et al., 2013) and complex topography (Macchioli et al., 2024; Wang et al., 2024). The seasonal variability in precipitation, air temperature, and vapour pressure deficit (VPD) drives the temporal variability of soil moisture and evaporation (Zeng et al., 2018), while topography influences water redistribution in the soil through surface and mainly subsurface flow paths (Han et al.,

2021). Therefore, a deeper understanding of the interactions between the seasonal variation in meteorological forcing and topography, and their combined effects on forest ecosystem responses, is essential for determining the conditions (in terms of drought severity and landscape position) under which trees are most vulnerable to summer drought stress. Understanding these interactions is also critical for enhancing the parametrization of ecohydrological models and forest growth models and the management of water and forest resources.

Soil moisture in the rooting zone is closely linked to tree transpiration (Hasselquist et al., 2018; Schaap et al., 1997) because it affects tree water uptake and is also directly affected by evapotranspiration. Trees can respond in different ways to critically low soil moisture availability by limiting water losses by closing their stomata(McDowell et al. 2008). Some trees can maintain their stomata open and have high photosynthetic rates for long periods, even in the presence of decreasing leaf water potentials (i.e., anisohydric response). Other trees maintain a constant leaf water potential when water is abundant, as well as under drought conditions, by reducing stomatal conductance to limit transpiration (i.e., isohydric response). There are also several intermediate responses between these two strategies (Ryan, 2011). The isohydric response results in a time shift between the diurnal variation in sap flow and climatic variables (e.g., daily temperature, VPD, solar radiation), with sap flow peaking earlier than temperature and VPD due to early stomata closure (Zhang et al., 2014). This time shift leads to hysteresis in the relation between sap flow and climatic variables. The longer the time lag (TL), the stronger the hysteresis. The analysis of hysteresis loops can thus help to understand the ecohydrological strategies adopted by trees to avoid excessive water loss and dehydration. If the hysteresis loop is clockwise, trees have an isohydric strategy; if the loop is anti-clockwise, trees have an anisohydric response or are not water stressed (Chen et al., 2011; Bai et al., 2015).

TLs between sap flow and VPD in *F. sylvatica* tree in the central part of Slovakia were analysed by Sitková et al. (2014), who observed a progressive decrease in sap flow as soil moisture decreased. TLs between sap flow and VPD were observed for five Mediterranean species in Spain, but the water use strategies differed for the five species. For instance, *Q. coccifera* was able to maintain a high daily sap flow rate regardless of soil moisture availability and atmospheric conditions, while the sap flow rate for *P. halepensis* reduced during dry periods (Chirino et al., 2011). Looker et al. (2018) evaluated microtopographic impacts on water use for five conifer species along a water availability gradient in western Montana (USA) and found hysteresis in the VPD-sap flow relations. At their sites, the TL increased as the growing season progressed and the soil dried out. Li et al. (2016) observed early stomatal closure for an arid region in northwest China, as indicated by the sap flow peak preceding the VPD peak with a TL of approximately 1.0 to 1.5 hours. They attributed this TL to stomatal closure in response to the high VPD. Similarly, Zhang et al. (2019) observed that the peak of diurnal sap flow for a deciduous forest in a subtropical humid karst regions generally lagged the photosynthetically active radiation but preceded the peak in air temperature, relative humidity, and VPD. They interpreted these TLs as an active physiological response of the trees during hot periods.

Thus, studying the timing of sap flow and meteorological parameters can help to detect and understand the short-term and long-term dynamics of the plant water balance, and important information on growth patterns and thus the sensitivity of plant transpiration to the environment (Cocozza et al., 2015).

A tree's response to water stress may vary at the small stand/hillslope scale due to differences in microclimatic conditions and local water availability (Fabiani et al., 2024). In mountain regions, topography can play an important role in moderating or enhancing stress conditions for trees (Eberbach and Burrows, 2006; Elliott et al., 2015). Fabiani et al. (2024) compared sap flow velocities on a gentle hillslope in the Weierbach catchment in Luxembourg (humid temperate climate) and on a steep hillslope in the Lecciona catchment in Italy (Mediterranean climate). They showed that the growing season was shorter for trees located on the upper part of the Italian hillslope, due to downslope water redistribution, leading to a different soil moisture status between the lower and upper part of the hillslope. Similarly, trees growing at the lower hillslope positions of a mixed forest in the southern Appalachian Mountains (USA) had a greater sapwood area than those in the upper hillslope (Hawthorne and Miniat, 2017). This difference was attributed to the drier soils at the top of the hillslope compared to those at the bottom. The higher daily transpiration rates for trees at the lower part of the hillslope indicated that local conditions, i.e. the higher water availability, protected trees against water stress during dry periods. However, Renner et al. (2016) observed for European beech trees growing on two opposite hillslopes in Luxembourg that sap flow and transpiration differed significantly between north-facing and south-facing hillslopes and that differences in stand structure also affected tree transpiration, hiding the potential effect of topography. Still, they found that topographic factors caused differences in tree responses during dry periods due to soil moisture limitation. Other studies have shown the effects of aspect and geology (Hassler et al. 2018) or soil depth (Tromp-van Meerveld et al., 2006) on sap flow rates.
Although many studies have focused on the relation between VPD and sap flow dynamics (e.g., Dhungel et al., 2021; Xu et al., 2022; Zhang et al.,2019; Liu et al., 2024; Wan et al., 2023; Roddy et al., 2013), only a few studies have so far analyzed the TL and hysteresis between VPD and sap flow for broadleaf trees in Mediterranean mountain catchments and how they depend on the seasonality in meteorological forcing (including summer drought episodes) and hillslope topography. Therefore, we investigated the changes in the VPD-sap flow relation for beech trees growing on different hillslope positions across a full summer period with periods of different drought severity for a hillslope in Central Italy. To better understand the response of forests to summer droughts. More specifically, we asked the following research questions:

1. How do soil moisture and sap flow vary along the hillslope during the growing season?
2. How does the VPD-sap flow relation vary during different drought conditions and with hillslope position?

Answering these questions will lead to a better understanding of the effect of topography, via its effect on soil water availability, on the response of trees to droughts. As sap flow is considered a proxy for tree transpiration (Granier and Bréda, 1996), assessing its spatial variability at the small scale is crucial for the correct measurement of mass and energy fluxes in densely forested catchments, and to understand differences in tree growth and drought impacts across the landscape.

2.2. Materials and methods

2.2.1. Study area

The data were collected on a steep hillslope called "Lecciona" in the Re della Pietra experimental catchment (43.878 °N, 11.622 °E), Tuscany Apennines, central Italy (Fig. 1a, b). The elevation of the hillslope varies between 910 and 960 m a.s.l., the aspect is predominantly North, and the average slope is 30° (Verdone et al., 2025). The study hillslope is densely vegetated by European beech trees (*Fagus sylvatica*), with a few inclusions of oak trees (*Quercus cerris*). The understory is sparse (Fig. 1c). The last thinning occurred in 1990 (Fabiani et al., 2024). A forest survey conducted in 2022 showed that trees in the riparian zone had a larger basal area and a more expanded and denser crown compared to trees on the upper part of the hillslope (26 vs 18 m^2/ha; $p<0.01$, for both characteristics), while tree height was relatively similar along the hillslope (19.2 m ± standard deviation: 2.3 m; n=138). The age of the trees (52 ± 6 years) did not vary systematically across the hillslope either (Verdone et al., 2025).

Soil depth, assessed by knocking pole measurements, varies from 1.5 m at the bottom of the hillslope to 0.8 m at the ridge (Verdone et al., 2025). Soils are Humic Dystrudepts (USDA, 1999), with an A-Bw-C-R profile and sandy loam texture. The soil is characterised by high organic matter content in the A profile and a high gravel content (Fabiani et al., 2024). The soils are underlain by fractured sandstone.

Average monthly temperatures vary from 2°C in January to 20°C in August. The average annual temperature is 10.5 °C (based on five years of data collected on-site; Macchioli Grande et al., 2024). Average annual precipitation is 1100 mm, but as is typical for the Mediterranean region, it is unevenly distributed over the year, with higher rainfall in autumn and less rainfall in summer.

2.2.2. Sap flow measurements

Sap flow velocity was measured from April to October 2021 in nine beech trees at three distinct topographic positions: riparian (Rip), midslope (Mid), and upslope (Up) (Fig. 1b). The trees are typical for the forest stand and crown structure and were chosen to have a similar phytosociological position and diameter (30 to 32 cm), to exclude the possible influence of tree size on the results.

Sap flow velocity was measured at 12.5 and 27.5 mm from the bark using heat pulse sap flow sensors (SFM1, ICT International Pty Ltd., Australia). In essence, a heater and two temperature sensors were inserted horizontally in the sapwood, with the sensors positioned at a fixed distance of 5 mm above and below the heated needle (Burgess et al. 2001). The heat pulse method employs heat as a tracer to determine sap velocity (Eq 1).

$$V_{SAP} = V_h \times \mathrm{B}\, \frac{\rho_b (c_w + m_c \times c_s)}{(\rho_s \times C_s)} \quad (1)$$

Where V_h is the heat pulse velocity (cm h^{-1}), B is the wound correction factor, ρ_b the basic density of wood, c_w the specific heat capacity of the wood matrix, c_s the specific heat capacity of water, ρ_s the density of sap water, and m_c the water content of sapwood (Brugess et al., 2001). To correct the mechanical disturbance caused by

sensor installation (B), we applied a correction factor of 0.13 cm to V_{SAP} values (Green et al., 2003). To prevent installation in tension wood, with lower lignification and eccentric growth in hardwood species on steep slopes (Fabiani et al., 2024), the sensors were installed on the west side of the trees. Data were taken at a 30-min time step and aggregated at a 1 h time step.

2.2.3. Soil moisture and weather data

Air temperature, relative humidity, precipitation, and solar radiation data were recorded at a 10-minute time step by a weather station located in an open area at 990 m a.s.l., upslope from the experimental hillslope (Macchioli Grande et al.,2024). We computed the daily mean VPD (kPa) from the relative humidity (RH) and temperature (T) as follows (Eq. 2):

$$VPD = 0.61375 \times e^{17.502} \frac{T}{(240.97 \times T)} \times \left(1 - \frac{RH}{100}\right) \quad (2)$$

Soil moisture was measured at a 10-min interval using six frequency domain reflectometry sensors (Teros 10, Meter Group, Pullman, USA) (Fig. 1b). The sensors were installed at 15 and 35 cm below the soil surface at three locations on a transect along the hillslope close to the monitored trees (5-10 m from each other): in the riparian area, the lower part of the hillslope, and in the middle part of the hillslope (Fig. 1b). The raw values were converted into volumetric water content (m^3/m^3) by applying the standard calibration for mineral soils suggested by the manufacturer (reported precision: 0.03 m^3/m^3). The soil moisture data for the two depths were fairly similar (mean absolute difference of 0.01-0.07 m^3/m^3) and therefore we averaged them to obtain one soil moisture value for each of the three hillslope positions.
We used the Soil Water Deficit Index (SWDI) proposed by Martínez-Fernández et al. (2015) to divide the study period into different periods. The SWDI is based on soil moisture and can also be used for relatively short time series of soil moisture data (Eq.3):

$$SWDI = \left(\frac{\theta - \theta_{FC}}{\theta_{AWC}}\right) \times 10 \quad (3)$$

where θ is the volumetric water content, θ_{FC} denotes the moisture content at field capacity, and θ_{AWC} is the available water content, which is based on the difference between the moisture content at field capacity (θ_{FC}) and moisture content at wilting point (θ_{WP}). Nine soil samples were taken at three depths (0-20, 20-40 and 40-60 cm below the surface) across the experimental hillslope to determine the soil texture based on sieving. The texture data (sand 71%, loam 22%, and clay 7%) were used to estimate θ_{WP} and θ_{FC} according to Saxton et al. (1986). Based on this method, θ_{WP} and θ_{FC} were estimated to be 0.074 m^3/m^3 and 0.176 m^3/m^3, respectively.
When the SWDI is positive, the moisture content is above field capacity, when it equals zero, the soil is at the field capacity, and when it is negative it indicates drought conditions. Values of SWDI ranging between 0 and -2 define a mild drought severity, values between -2 and -5 a moderate drought severity, values from -5 to -10 a severe drought severity, and values below -10 an extreme drought severity (-10 is the value at

which the soil moisture reaches the estimated WP). To define position-specific drought conditions, we determined the SWDI values separately for each soil moisture measurement location based on the average values for the two depths. For the period from April to October 2021, the maximum SWDI values was 11.22 and the minimum -8.25.

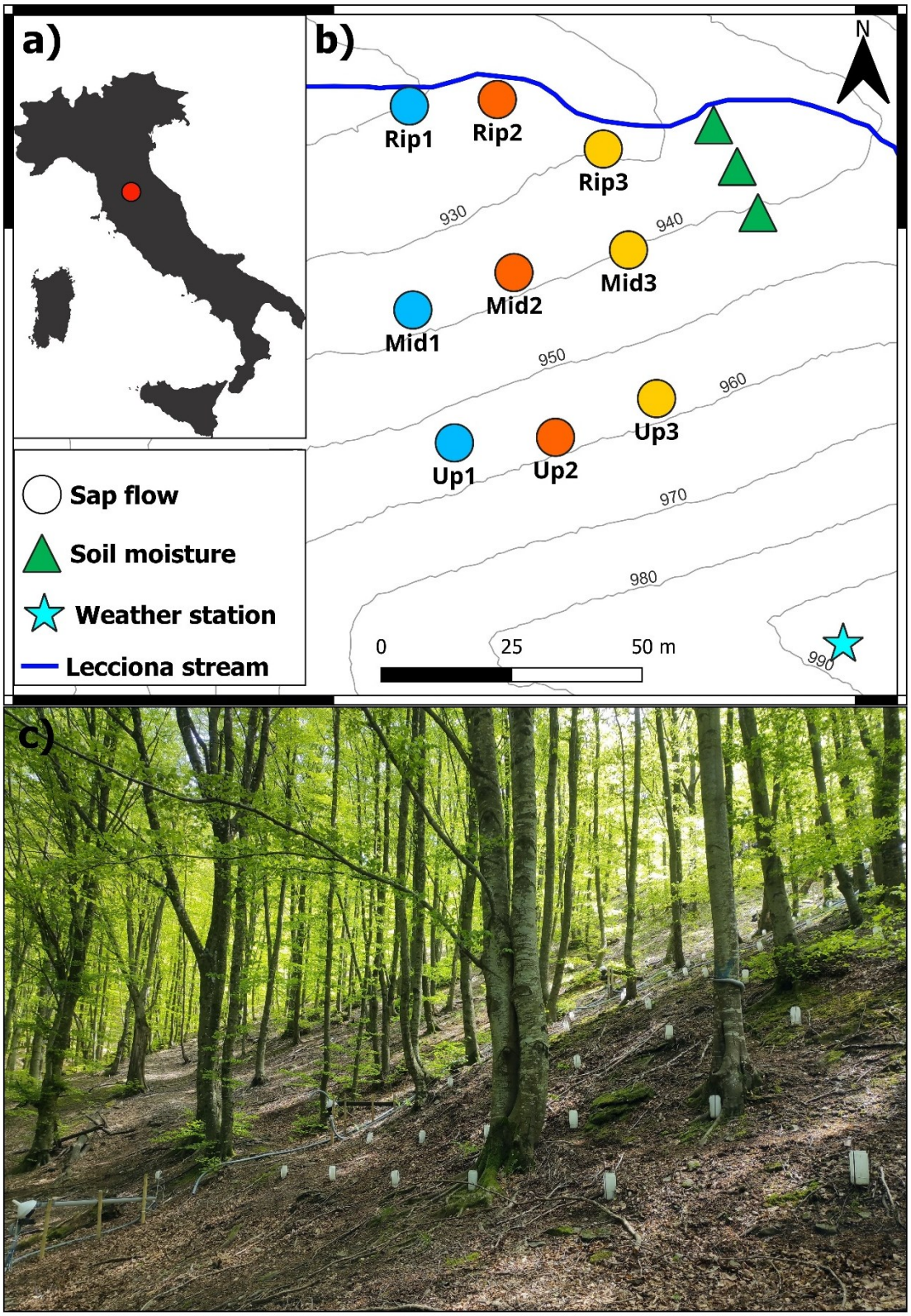

Figure 1. Overview of the experimental hillslope: location in Tuscany, Italy (a), map showing the location of the measurement equipment (b), and a picture of the study hillslope (c). The white jars are throughfall collectors used by Verdone et al. (2025).

2.2.4. Data analysis

For each monitored tree, we calculated the mean daily sap flow velocity as a proxy of the tree transpiration rate (Smith and Allen, 1996). Due to the non-normal distribution of sap flow velocity data, we used the non-parametric Kruskal-Wallis test (Kruskal and Allen Wallis 1952) to determine the statistical significance of the differences in the daily mean sap flow velocities among the nine trees for the different drought severity periods. Moreover, we related the daily mean sap flow to the daily mean values of the climatic variables and soil moisture using scatter plots and the Spearman rank correlation. In addition, we determined the relative importance of these factors for the daily mean sap flow velocity for each tree using the "relaimpo" package in R (Groemping, 2006). To avoid the influence of precipitation events on sapflow and rapidly changing soil moisture conditions, we did not consider days with rainfall in any of these analyses (cf. Renner et al., 2016). Finally, we used hourly data to determine the TL between the peak sap flow velocity and the time of the maximum i) VPD; ii) air temperature, and iii) solar radiation. This was done for each day for each tree. Negative values indicate that sap flow velocity peaked after the climatic variables, while positive values indicate that sap flow velocity peaked first. To analyse the effects of the temperature on the TL between sap flow velocity and VPD, we compared the TLs for days days with different daily mean temperatures. For this we divided the daily mean temperature into four quartiles.

2.3. Results

2.3.1. Seasonal variation in atmospheric conditions, soil moisture and sap flow across the hillslope

The variation in air temperature (29 - -5 °C) was typical for the Mediterranean climate, with peak values during the summer months. Rainfall events led to a temporary decrease in air temperature, after which temperatures rose again. This was particularly notable during the first ten days of August and in early September. VPD varied between 11 and 0 kPa and followed the temperature trend (and was highly correlated to the temperature; Figure S1a). It was highest at the end of June, in early and late July, and particularly in mid-August (Fig. 2).
Average soil moisture (over the two depths) varied across the hillslope: from 0.14 to 0.3 m^3/m^3 in the riparian zone, 0.09 to 0.26 m^3/m^3 on the lower hillslope, and 0.11 to 0.29 m^3/m^3 on the midslope. Soil moisture in the riparian zone responded less to precipitation compared to the other locations (Fig. 2c-e). Although soil moisture values were overall higher in the riparian zone, they decreased more abruptly between mid-May and early June. The riparian zone was at field capacity by the end of May, then dried out to what would be considered a moderate drought by early August, which persisted until late September, when soil moisture gradually increased again. The changes in soil moisture at the lower hillslope and midslope positions were similar, but soil moisture increased more rapidly in response to rainfall (e.g., in mid-July). Soil moisture at the hillslope positions dropped to what would be considered a severe drought by mid-August for the lower hillslope and by late August for the midslope, ending abruptly in mid-September after rainfall events. Although soil moisture did not drop to the

estimated wilting point at any of the locations, we noticed evidence of drought stress, such as yellowing leaves at the top of the trees growing on the upper part of the hillslope. This suggests that although the beech trees at our site did not reach a critical desiccation point and did not shed the leaves (as observed for other sites in Tuscany during the 2017 droughts; Pollastrini et al., 2019), they did experience periods of water stress.

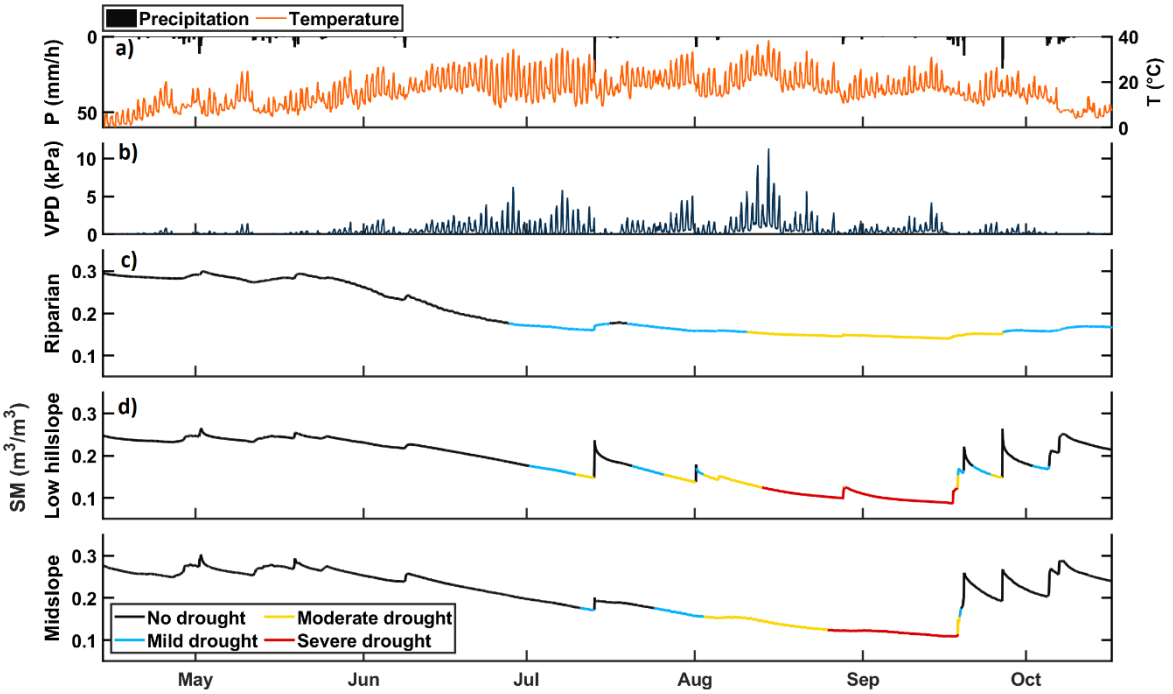

Figure 2. Time series of hourly precipitation, air temperature, vapor pressure deficit (VPD), and depth-averaged soil moisture (SM) for the three hillslope positions during the monitoring period (April-October 2021). The colours in the soil moisture time series indicate the drought severity according to the Soil Water Deficit Index (see Section 2.3).

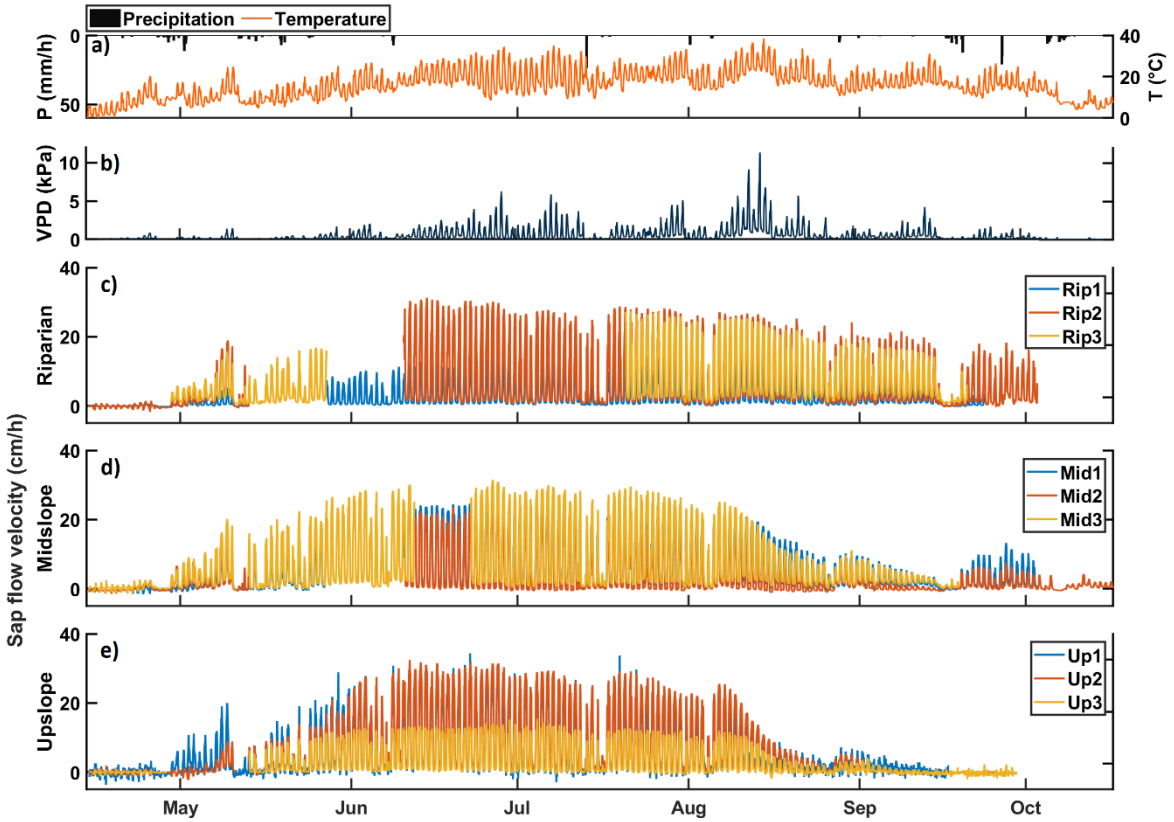

Figure 3. Time series of hourly precipitation and air temperature (a), vapor pressure deficit (VPD) (b), and sap flow velocity of three trees (1, 2, and 3) for each of the three hillslope positions (riparian (c), midslope (d), and upslope (e)) during the monitoring period.

Sap flow velocity dynamics also differed by location (Fig. 3). Sap flow increased at all locations at the beginning of May, as temperatures rose following rainy days in late April (Fig. 2; Fig S1b). They continued to increase during the early summer with rising temperatures and increasing VPD, which led to a decrease in soil moisture (that was exacerbated by the lack of rainfall) (Fig. 3).

In the riparian zone, sap flow increased with VPD until July, remained stable until mid-August, and then decreased (Figs.5 and S3). Notably, sap flow values in the Rip2 and Rip3 trees remained relatively high at the end of the observation period. In contrast, there was a significant drop in sap flow in the upslope trees from early August, in response to the marked increases in VPD and temperature(Fig. 2). From late August, sap flow increased again as VPD decreased, but more gradually for midslope trees than for upslope trees (Figs.5 and S3). Despite lower temperatures and increases in soil moisture in September (Fig. S2), sap flow for the trees on the upslope and the midslope continued to decrease (sharply for trees in the upslope).

The daily average sap flow velocities on days without precipitation were correlated with the climatic variables and soil moisture (Table 1). For the trees in the riparian zone, the correlation with VPD and temperature was higher (r_s= 48 - 69) than for trees on the midslope and upper slope (although tree Up2 was an outlier) (r_s= 21 - 30). Contrary, the correlations with radiation and soil moisture were higher for the trees on the midslope and upper slope (r_s= 46 – 56 and 11 – 53 respectively) than for the trees in the riparian zone (r_s= 0.37 - -0.28). The relative importance analysis (Fig. 4) indicated that the combination of these variables could explain half (riparian zone) to two-thirds (midslope and upper slope, except tree Mid3) of the observed variation in the daily average sap flow velocity. Similar to the results of the Spearman rank correlation (Table

1), the importance of soil moisture varied along the hillslope and was higher for the trees on the mid and upper part of the hillslope (Fig. 4).

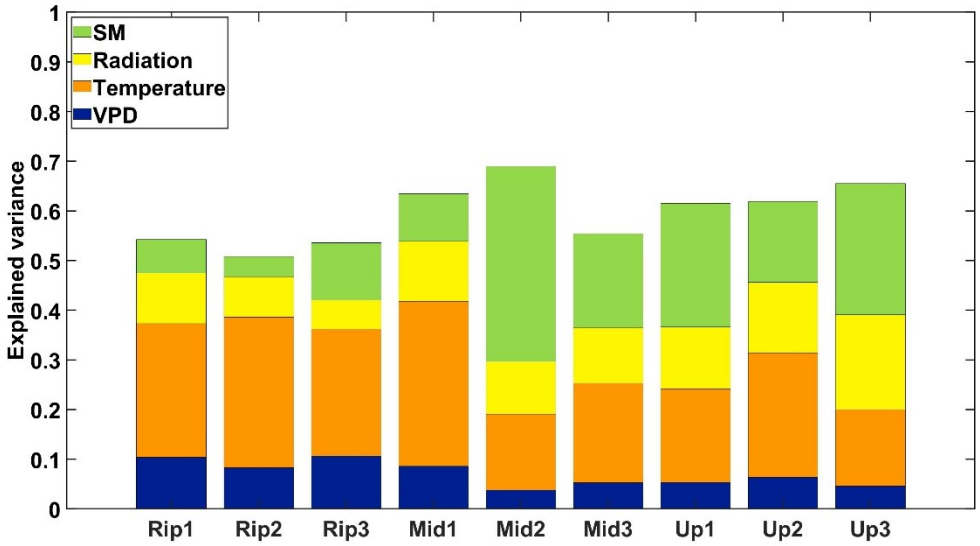

Figure 4. Fraction of the variance in the daily average sap flow explained by the vapor pressure deficit (VPD), temperature, solar radiation, and soil moisture (average of the measurement at 15 and 35 cm depth) for each tree.

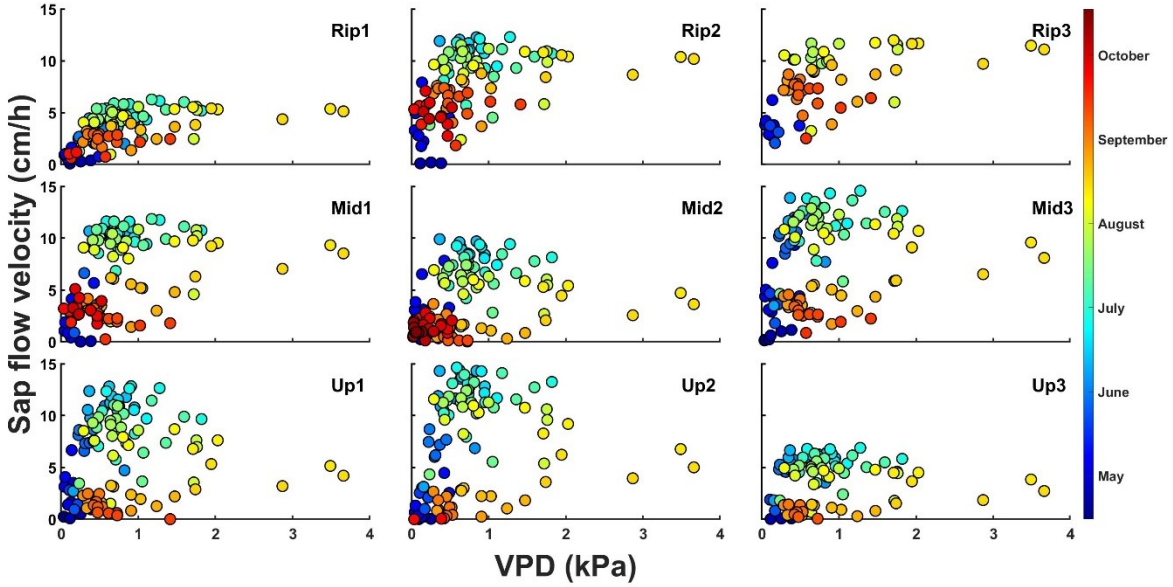

Figure 5. Relation between the daily average values of sap flow and vapor pressure deficit (VPD) for each monitored tree, colour coded by the date to highlight the seasonal hysteresis.

Table 1. Spearman rank correlation between the daily average sap flow and daily average VPD, temperature, radiation and average soil moisture (at either the riparian zone (Rip1-3), lower hillslope (Mid1-3) and middle hillslope (Up1-3) positions) for days without any precipitation.

Tree	VPD	Temperature	Radiation	Soil moisture
Rip1	0.63	0.67	0.38	-0.06
Rip2	0.48	0.59	0.43	0.20
Rip3	0.58	0.69	0.37	-0.28
Mid1	0.50	0.56	0.49	0.11
Mid2	0.22	0.29	0.50	0.57
Mid3	0.31	0.34	0.46	0.25
Up1	0.22	0.30	0.50	0.41
Up2	0.36	0.42	0.51	0.29
Up3	0.21	0.25	0.56	0.53

2.3.2. Temperature and topography affect the time lag between VPD and sap flow

The TL between peak VPD and peak sap flow varied considerably throughout the growing season ranging with a mean (± standard deviation) of -1.1 ± 2.7 hours, indicating that, on average, sap flow peaked earlier than VPD. Typically, relatively cold days led to sap flow and VPD peaks almost at the same time, resulting in very small TLs, or sap flow peaked after VPD, whereas during warmer days sap flow peaked earlier than VPD. This behaviour was consistent across all the hillslope positions (Fig. 6; Table 2).

Overall, the mean TL was positive (Fig. 7) at the beginning and end of the growing season, when mean temperatures (and VPD) were relatively low, indicating that VPD generally preceded sap flow. The differences in TLs for the different trees were not statistically significant during these periods (Table 2). During these days, sap flow continued to increase after VPD started to decline (leading to anti-clockwise hysteresis patterns), implying that trees did not need to restrict stomatal conductance.

The TL between VPD and sap flow also depended on the moisture conditions. In the riparian zone, the mean TL was positive under no drought conditions (0.7 ± 2.9 hours) and most negative during moderate drought conditions (-0.7 ± 1.7 hours, Fig. 8). In the midslope zone, the mean TL was negative during all drought conditions and ranged between-1.2 ± 2.6 hours under no drought conditions and -3.0 ± 1.9 hours during severe drought conditions to. Lastly, in the upslope zone, the mean TL was more negative during mild and moderate drought (-2.0 ± 1.8 hours in both cases) than under no drought (-1.0 ± 3.4 hours) and moderate drought (-2.0 ± 1.8 hours, Fig. 8).

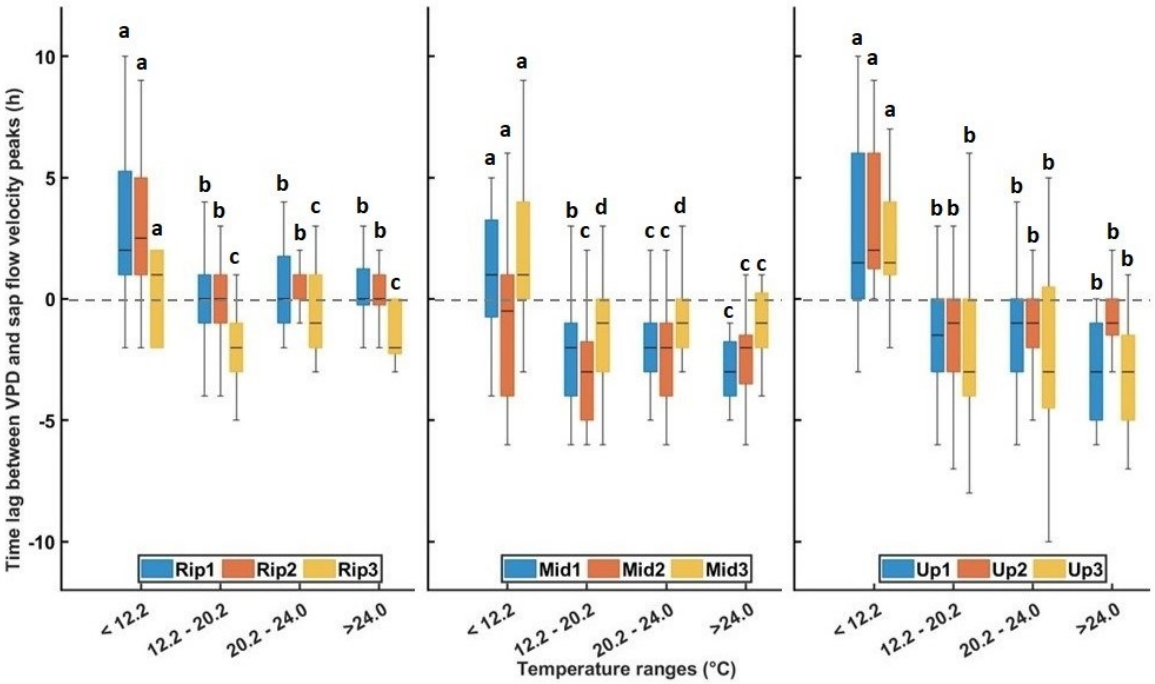

Figure 7. Box plots of the time lags between the maximum vapor pressure deficit (VPD) and sap flow for different air temperature classes for each tree (1, 2, and 3) at the three hillslope positions (riparian, midslope, and upslope). Positive values indicate that VPD peaked before sap flow. The boxes represent the interquartile range, the lines the median and the whiskers extend to 25th percentile and 75th percentile. Different letters above the boxes indicate that the lag times are statistically significantly different.

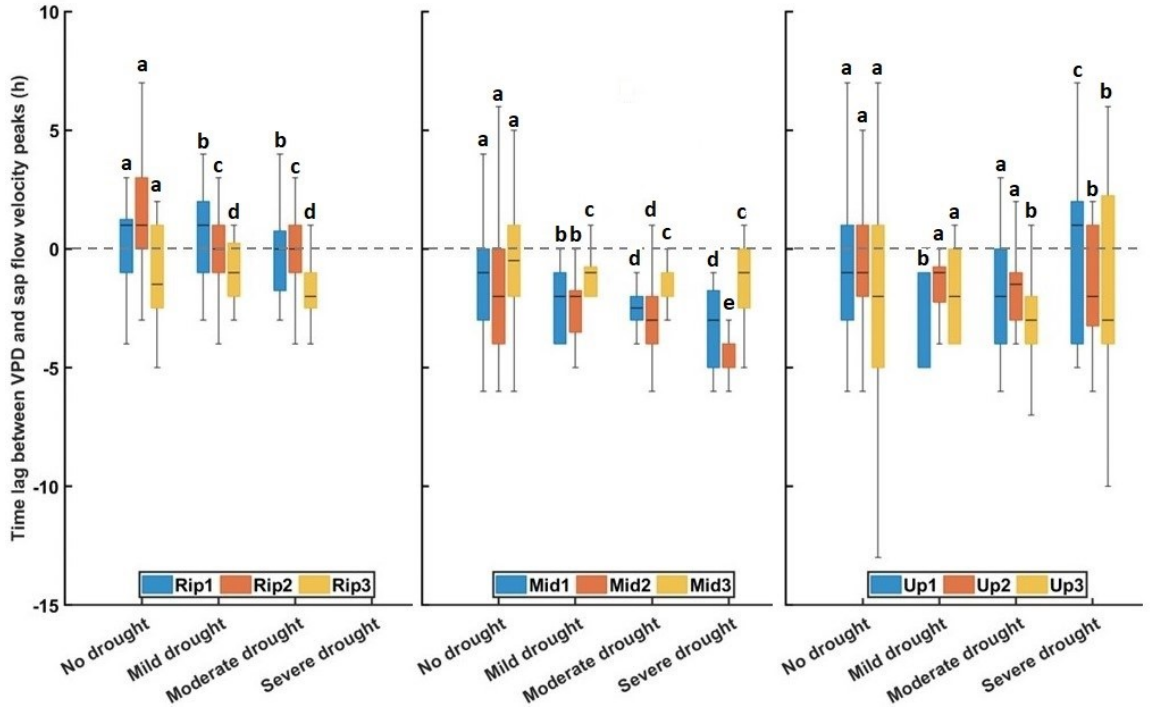

Figure 8. Box plots of the time lag between the peak vapor pressure deficit (VPD) and sap flow for different drought conditions according to the SWDI for each tree (1, 2, and 3) at the three hillslope positions (riparian, midslope, and upslope). Different letters above the boxes indicate that the time lags are statistically significantly different.

Table 2. Mean time lag ± standard deviation for each hillslope positions in relation to temperature and drought classes. Bold indicate significative differences among trees.

		Time lag (h)		
		Riparian	Mid hillslope	Upper hillslope
Temperature class	<12.2 °C	2.4 ±3.3	0.5 ± 3.5	2.6 ± 3.4
	12.2-20.2 °C	**0.6 ± 1.9**	**-2.2 ± 2.0**	-1.7 ± 2.9
	20.2-24.0 °C	**0.2 ± 1.6**	**-1.6 ± 1.7**	-1.6 ± 2.5
	>24.0 °C	**-0.4 ± 1.5**	-2.0 ± 2	**-2.3 ± 2.2**
Drought class	No drought	0.7 ± 2.9	-1.2 ± 2.6	**-1 ± 3.4**
	Mild drought	**0.1 ± 1.7**	-2.0 ± 1.6	**-2.0 ± 1.8**
	Moderate drought	**-0.7 ± 1.7**	**-2.0 ± 1.8**	**-2.0 ± 1.8**
	Severe drought	-	**-3 ± 1.9**	**-1.0 ± 3.6**

2.4. Discussion

2.4.1. Topographic effects on the seasonal variation in soil moisture and sap flow

The consistently wetter conditions in the riparian zone, compared to the mid and upper hillslope zones (Fig. 2), were likely due to the contribution of lateral flow from the upslope areas, the relatively flat area that limits drainage and facilitates water retention, the higher groundwater levels near the stream that keep soil moisture high, and the presence of a thick litter layer composed of beech tree leaves that reduce soil water evaporation during dry periods (Macchioli Grande et al., 2024; Zhu et al., 2020; Sato et al., 2004). In addition, there is more shading below the larger trees on the riparian zone due to the larger crowns reduces soil evaporation. However, the larger trees also cause higher interception losses (Verdone et al., 2025), which reduces the amount and intensity of rainfall reaching the riparian zone and thus the soil moisture response to precipitation (Penna et al., 2009). In mature beech stands, approximately 70% of fine roots are concentrated within the upper 30 cm of soil, while 95% are located within the first 60 cm (Bakker et al., 2008). In other words, the 15-35 cm depth where we measured soil moisture, effectively captures more than 75% of the root-accessible area (Bakker et al., 2008). Thus, the higher soil moisture measured soil moisture in the riparian zone indicates that more water is available for uptake by fine roots, and as the results show lead to more constant sap flow velocities over the season in the riparian zone, and sustained sapflow during dry periods (Fig. 3).
Although differences in soil moisture responses across the topographic gradient do not have to be directly related to the hillslope geometry (Lu et al., 2024), the transition from dry to wet periods occurred more rapidly on the hillslope than in the riparian zone, due

to the steeper gradient and lower water table that facilitate drainage and the lack of litter that increases soil evaporation (Dymond et al., 2021). Soil moisture explained more of the variation in sap flow for the trees on the mid and upper hillslope than for the trees on the riparian zone (Table 1 and Fig. 4). The role of topography on sap flow velocity became especially evident during mid-August (Fig. 3). The reduced soil moisture availability at the upslope and midslope locations during this period (with a SWDI of 0.10-0.11 for the mid slope and 0.14-0.15 for the lower slope) led to a marked decrease in sap velocity on the hillslope. Sap flow velocities in the riparian zone were higher than at upslope and midslope positions during this period. This is consistent with the results of Fabiani et al. (2024) and Renner et al. (2016), who noted that topographic factors amplify the transpiration response during droughts. More specifically, Renner et al. (2018), showed that for the first part of the season, sap flow velocities for eight trees on a north-facing hillslope in Attert catchment (Luxembourg) were not related to hillslope position. In the second part of the season, however, declines in soil moisture led to different tree responses, with less sap flow for trees on the upper hillslope positions declining.

Despite the improved soil moisture conditions, the lower VPD and temperature in September, sap flow velocities on the upper and midslope did not recover to pre-drought levels. This suggests a persistent water stress in the upper hillslope and lagged physiological recovery. Thus, the low soil moisture at upslope sites resulted in a shorter growth season (cf. Fabiani et al., 2024; Chen et al., 2014), which may explain the overall lower basal area for the upslope (cf. Tromp-van Meerveld and McDonnell, 2006).

2.4.2. Topographic effects on the diurnal variation in VPD and sap flow

Trees can avoid excessive water loss by closing their stomata, which leads to a reduction in sap flow (Chen et al., 2011). VPD strongly influences sap flow dynamics, but hydraulic limitations constrain the extent to which sap flow can respond to increasing VPD. Trees risk excessive desiccation beyond a VPD and soil moisture threshold, necessitating stomatal closure to prevent xylem cavitation (Link et al., 2014). On the mid and upper hillslope, sap flow velocity decreased soon after reaching peak values during periods of high VPD and limited water availability (Fig. 5). Contrary, for trees in the riparian zone of the Lecciona hillslope, with sufficient soil moisture availability for most of the time (although SM dropped to a minimum value of 0.14, indicating moderate drought in August-September), there was an asymptotic trend in the relation between sap flow velocity and VPD. The plateau for the trees in the riparian zone indicates that sap flow reached a maximum physiological limit and did not decrease further when VPD increased. This behaviour may correspond with the isohydric stomatal regulation strategy seen in beech trees, as isohydric trees maintain a fairly stable leaf water potential by closely regulating stomatal openings in reaction to environmental factors, thus preventing significant dehydration even in conditions of high VPD (Gessler, 2021; Magh et al., 2020; Grossiord et al., 2016).

The TLs for the trees in the riparian zone fluctuated around zero, even during periods with higher temperatures (Table 2) and there was limited hysteresis between sap flow and VPD (the relation was similar to a line), indicating that trees experienced only mild water stress (Chen et al., 2011). Contrary, for the trees on the midslope and upslope, TLs became more negative as temperatures and VPD increased (Table 2), which

suggests that trees proactively closed their stomata to avoid excessive water loss. For the trees on the midslope and upslope , the VPD-sap flow relation (Fig. 9) was characterised by clockwise hysteresis, consistent with trees closing their stomata early to mitigate dehydration risk (Chen et al., 2011; Bai et al., 2015). The slightly higher TLs for the days with the highest air temperatures may be caused by the higher soil moisture during months of June and July (Fig. 2). However, Renner et al. (2018), showed that TLs between sap flow and VPD were more related to temperature than soil moisture (Renner et al., 2018).

Trees in the upslope position appeared less stressed than the trees on the midslope early in the growing season (lower temperature ranges). However, upslope trees exhibited a rapid stress response as temperatures increased, likely due to rapid soil moisture depletion or distinct microclimatic conditions (e.g., increased solar radiation or temperature). However, contrary to other positions, the TL for the upslope trees was similar for no drought and severe drought conditions, and were more negative for mild and moderate drought conditions. During the severe drought conditions (especially during the second week of August), the temperatures were not as extreme, but sap flow values remained substantially reduced due to cumulative climatic stress. Under these circumstances, soil moisture may limit sap flow velocities more than the atmospheric conditions. This may lead to reduced tree transpiration later in the growing season, as supported by observations of yellowish leaves in the upper canopy.

Although previous studies described the controls on VPD-sap flow TL and analysed sap flow responses at the hillslope scale, we think that this is (one of) the first to show the difference in the VPD-sap flow velocity relation across a small (roughly 60 m) steep hillslope. These TLs between peak VPD and sap flow in midslope and upslope positions at Lecciona are consistent with those reported by Li et al. (2016) for nine trees in northwest China. The greater variability observed in our study may be attributed to the weather conditions, characterised by fluctuating cloud cover and some wetter periods. Although these variations may influence the daily VPD trends, we did not exclude cloudy days from the analysis to avoid reducing the number of observations.

Based on these observations, we propose a conceptual model to explain VPD-sap flow variability across topographic gradients (Fig. 10). When temperature and VPD increase, but soil moisture is not a limiting factor, beech trees reach their physiological transpiration limit, leading to a negative TL between VPD and sap flow (Fig. 9a). When soil moisture becomes a limiting factor, sap flow decreases because stomata are closed (anisohydric behaviour, Fig. 10b). Topography causes a redistribution of water in the soil (Fig. 10c) andmore water available for trees in the riparian zone, even under drought conditions. This leads to zero or negative TLs for trees in the riparian zone and high sap flow velocities (Fig. 3c). Contrary, on the hillslope position (Fig. 3d, e), sap flow velocity decreases in response to the higher moisture stress. The analysis of TLs across drought severity classes (Fig. 8) revealed that decreasing soil moisture resulted in decreasing TLs between peak VPD and peak sap flow, which is indicative of increasing water stress as soil moisture becomes depleted (Fabiani et al., 2024; Zhang et al., 2019; Bai et al., 2015). This model should be validated in future studies with observations from other hillslopes across different climatic zones and tree species

In addition to this general, across hillslope pattern, there was also considerable variation in the response of individual trees to temperature, VPD, and drought conditions (Fig. 3). The time lags between peak sap flow velocity and peak VPD varied considerably for the individual trees as well (see Table 2). This highlights the need to

analyse the response of multiple trees, and the necessity to interpret the results in this study with care as there were only three monitored trees in each hillslope zone. Differences in TLs for the Rip3 tree compared to the other two riparian trees (Fig. 7) for the low temperature class (Table 2) may largely stem from missing sap flow data for the Rip3 tree between mid-May and mid-July (Fig. 3). During the remainder of the observation period, sap flow velocities for the Rip3 tree were similar to those for the Rip2 tree (Fig. 3). However, TLs for the Rip3 tree were comparable to those for trees at the midslope and upslope trees, suggesting that, potentially due to variability in soil moisture availability (Yang and Tong, 2024), the Rip3 tree responded more similar to trees at higher hillslope positions. Tree traits could affect daily sap flow seasonal behaviour as well (Hassler et al., 2018). Thuse high variability in the explained variance in daily average sap flow for the individual trees (Fig. 3) suggests that other tree and site characteristics, such as contributing area and root status, which were omitted in the relative importance analysis for this study, are important factors for the variability in sap flow velocities as well (cf. Hassler et al., 2018).

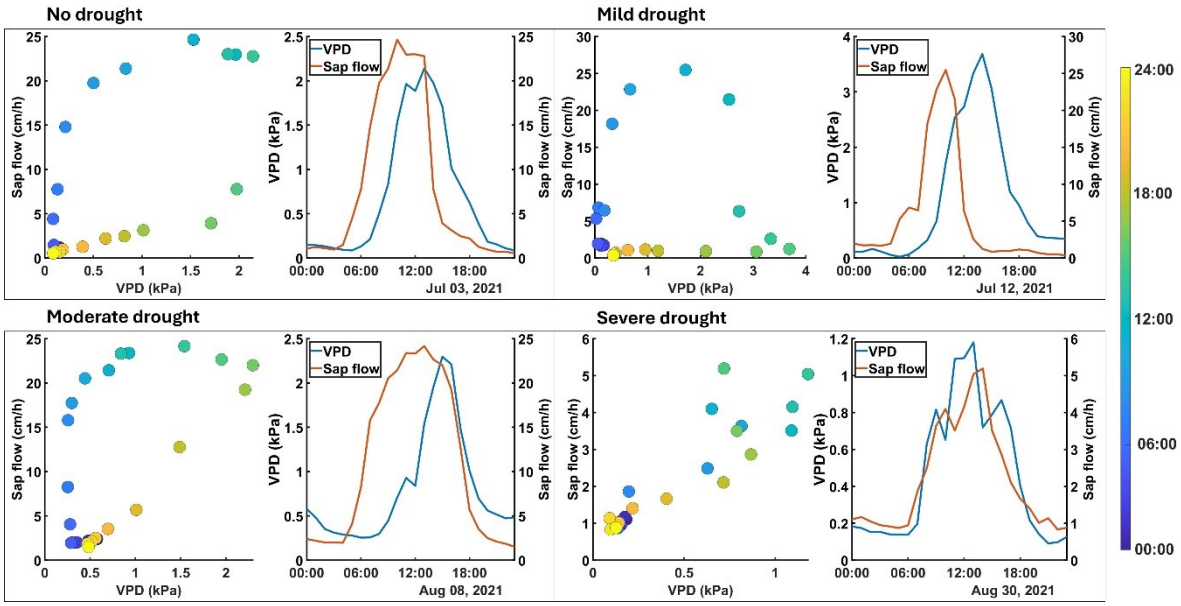

Figure 9. Time series of the vapor pressure deficit (VPD) and sap flow velocity for four selected days: during no drought, mild, moderate, and severe drought conditions (according to the SWDI), as well as the correlation between VPD and sap flow, colour-coded by the time of the day.

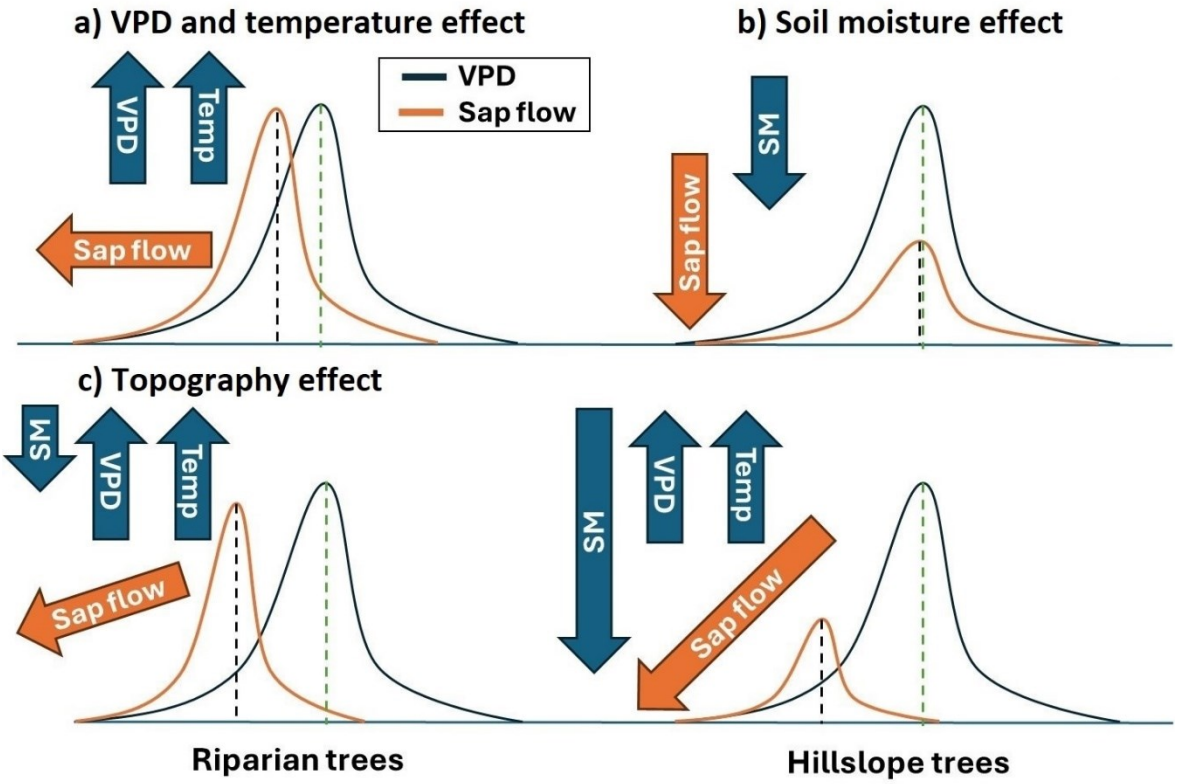

Figure 10. Conceptual model of the effect of VPD, temperature, soil moisture, and topography on sap flow velocity. The direction of the blue arrows indicates an increase (upward) or decrease (downward) of VPD, temperature (Temp), and soil moisture (SM), while the direction of the orange arrows indicates a decrease (downward) or a temporal shift (pointing left) of sap flow compared to VPD. Panel a) highlights the effect of increasing temperature and VPD on the sap flow. Panel b) indicates the effect of decreasing soil moisture on sap flow. In panel c), due to topography-induced redistribution of water in the soil, sap flow anticipates VPD and remains high in the riparian (and wetter) zone, but decreases markedly on the hillslope.

2.5. Conclusions

We investigated the combined effects of seasonality and topography on tree responses to atmospheric demand using a dataset of sap flow velocities collected across a monospecific forested hillslope in the Apennine Mountains, Central Italy. Time lags between VPD and sap flow responses decreased with increasing temperatures and VPD, indicating an anisohydric response of the beech trees. However, the relationship between VPD and sap flow is modulated by both climatic variables and soil moisture along the hillslope. For trees on the hillslope, soil moisture became a limiting factor, as indicated by limited sap flow velocities during periods with high temperatures and VPD and the presence of yellowish leaves. In contrast, trees in riparian zones experienced less water stress due to the overall higher soil moisture in the riparian zone. The proposed conceptual model explains the combined effects of temperature, VPD, soil moisture, and topography on sap flow responses and the VPD-sap flow relation (Fig. 10) and can be used to inform ecohydrological models that aim to capture fine-scale variability in evapotranspiration fluxes across the landscape. However, it should be validated in future studies with observations from hillslopes across different climatic zones and tree species.

Acknowledgements

This study was supported by the following research projects: “WATer mixing in the critical ZONe: observations and predictions under environmental changes – WATZON” (call PRIN 2017, code: 2017SL7ABC), funded by the Italian Ministry of University and Research (MUR); “Unravelling interactions between WATER and carbon cycles during drought and their impact on water resources and forest and grassland ecosySTEMs in the Mediterranean climate – WATERSTEM” (call PRIN 2020, code: 20202WF53Z), funded by the Italian Ministry of University and Research (MUR); “Carbon and water cycles interactions during drought and their impact on WAter and ForEst Resources in the Mediterranean region -WAFER” funded by the Italian National research Council (Consiglio Nazionale delle Ricerche – CNR); "Hydrological controls on carbonate-mediated CO2 consumptions – HYDRO4C (call PRIN 2022, code: 2022PFNNRS) funded by the European Union, Next Generation EU; "A new interdisciplinary approach to advance understanding of sediment and large wood transport in forested mountain catchments - TRANSFORM” (call MUR - D.M.737, code B55F21007810001) funded by the European Union, Next Generation EU; “Space It Up!” (call ASI n. 687/2022 of 26 July 2022, contract ASI N. 2024-5-E.0, master code: I53D24000060005, WP 7.6), funded by the Italian Space Agency (ASI) and the Italian Ministry of University and Research (MUR); and ESA CCI GLANCE: “AGricultural Land AbandoNment and ClimatE change impacts on the water, energy and vegetation carbon cycles in the Mediterranean region” ESA Contract no. 4000145543/24/I-LR CLIMATE-SPACE – THEME II: CROSS ECV ACTIVITIES
The authors thank the local Forest Service (Unione Comuni Valdarno e Valdisieve) for their logistical support in managing the Re della Pietra experimental catchment; Ginevra Fabiani and Julian Klaus for sap flow data collection and analysis; and Francesca Sofia Manca di Villahermosa and Andrea Dani for their help in field work.

Authors’ contribution

M. Verdone: Conceptualization; Data curation; Formal analysis; Investigation; Methodology; Visualization; Writing – original draft. **C. Massari**: Conceptualization; Funding acquisition; Project administration; Supervision; Validation; Writing – review and editing. **I. Murgia**: Data curation; Investigation; Writing – review and editing. **C. Cocozza**: Conceptualization; Validation; Writing – review and editing. **I. van Meerveld**: Conceptualization; Validation; Supervision; Formal analysis, Writing – review and editing. **D. Penna**: Conceptualization; Data curation; Funding acquisition; Methodology; Project administration; Supervision; Validation; Writing – review and editing.

References

Bai Y, Zhu G, Su Y, Zhang K, Han T, Ma J, Wang W, Ma T, Feng L. (2015). Hysteresis loops between canopy conductance of grapevines and meteorological variables in an oasis ecosystem. Agric For Meteorol, 214 215: 319–327

Bakker, M.R., Turpault, MP., Huet, S. et al. Root distribution of Fagus sylvatica in a chronosequence in western France. J For Res 13, 176–184 (2008). https://doi.org/10.1007/s10310-008-0068-6

Burgess, S. S. O., Adams, M. A., Turner, N. C., Beverly, C. R., Ong, C. K., Khan, A. A. H., and Bleby, T. M.: An improved heat pulse method to measure low and reverse rates of sap flow in woody plants, Tree Physiol., 21, 589–598, 2001.

Caudullo, G., Barredo, J.I., (2019). A georeferenced dataset of drought and heat-induced tree mortality in Europe. One Ecosystem 4, e37753.

Chen L, Zhang Z, Li Z, Tang J, Caldwell P, Zhang W. (2011). Biophysical control of whole tree transpiration under an urban environment in Northern China. J Hydrol, 402: 388–400

Chen, D., Wang, Y., Liu, S., Wei, X., & Wang, X. (2014). Response of relative sap flow to meteorological factors under different soil moisture conditions in rainfed jujube (Ziziphus jujuba Mill.) plantations in semiarid Northwest China. Agricultural Water Management, 136, 23-33. https://doi.org/10.1016/j.agwat.2014.01.001

Chirino, E., Bellot, J. & Sánchez, J.R. Daily sap flow rate as an indicator of drought avoidance mechanisms in five Mediterranean perennial species in semi-arid southeastern Spain. Trees 25, 593–606 (2011). https://doi.org/10.1007/s00468-010-0536-4

Cocozza, C., Marino, G., Giovannelli, A., Cantini, C., Centritto, M., & Tognetti, R. (2015). Simultaneous measurements of stem radius variation and sap flux density reveal synchronisation of water storage and transpiration dynamics in olive trees. Ecohydrology, 8(1), 33-45. https://doi.org/10.1002/eco.1483

Dhungel, R., Aiken, R., Evett, S. R., Colaizzi, P. D., Marek, G., Moorhead, J. E., et al. (2021). Energy imbalance and evapotranspiration hysteresis under an advective environment: Evidence from lysimeter, eddy covariance, and energy balance modeling. Geophysical Research Letters, 48(1). https://doi.org/10.1029/2020GL091203

Dymond, S. F., Wagenbrenner, J. W., Keppeler, E. T., & Bladon, K. D. (2021). Dynamic Hillslope Soil Moisture in a Mediterranean Montane Watershed. Water Resources Research, 57(11), e2020WR029170. https://doi.org/10.1029/2020WR029170

Eberbach, P. L., & Burrows, G. E. (2006). The transpiration response by four topographically distributed eucalyptus species, to rainfall occurring during drought in south eastern Australia. Physiologia Plantarum, 127, 483–493. doi:10.1111/j.1399-3054.2006.00762.x

Elliott, K. J., Miniat, C. F., Pederson, N., & Laseter, S. H. (2015). Forest tree growth response to hydroclimate variability in the southern Appalachians. Global Change Biology, 21, 4627–4641. doi:10.1111/gcb.13045

Fabiani, G., Klaus, J., and Penna, D., (2024). The influence of hillslope topography on beech water use: a comparative study in two different climates, Hydrol. Earth Syst. Sci., 28, 2683–2703, https://doi.org/10.5194/hess-28-2683-2024

Gazol, A., & Camarero, J. J. (2022). Compound climate events increase tree drought mortality across European forests. Science of The Total Environment, 816, 151604. https://doi.org/10.1016/j.scitotenv.2021.151604

Gessler, A. (2021). Water transport in trees—the importance of radial and circumferential transport, Tree Physiol., 1–3, https://doi.org/10.1093/treephys/tpab131

Granier, A., Bréda, N., (1996). Modelling canopy conductance and stand transpiration of an oak forest from sap flow measurements. Ann. Sci. For. 53, 537–546. https://doi.org/10.1051/forest:19960233.

Green, S., Clothier, B. and Jardine, B. (2003), Theory and Practical Application of Heat Pulse to Measure Sap Flow. Agron. J., 95: 1371-1379. https://doi.org/10.2134/agronj2003.1371

Groemping, U. (2006). Relative Importance for Linear Regression in R: The Package relaimpo. Journal of Statistical Software, 17(1), 1–27. https://doi.org/10.18637/jss.v017.i01

Grossiord, C., Sevanto, S., Dawson, T. E., Adams, H. D., Collins, A. D., Dickman, L. T., Newman, B. D., Stockton, E. A., & McDowell, N. G. (2016). Warming combined with more extreme precipitation regimes modifies the water sources used by trees. New Phytologist, 213(2), 584-596.https://doi.org/10.1111/nph.14192

Han, X., Liu, J., Srivastava, P., Liu, H., Li, X., Shen, X., & Tan, H. (2021). The Dominant Control of Relief on Soil Water Content Distribution During Wet-Dry Transitions in Headwaters. Water Resources Research, 57(11), e2021WR029587. https://doi.org/10.1029/2021WR029587

Hassler, S. K., Weiler, M., and Blume, T. (2018). Tree-, stand- and site-specific controls on landscape-scale patterns of transpiration, Hydrol. Earth Syst. Sci., 22, 13–30, https://doi.org/10.5194/hess-22-13-2018

Hawthorne, S., & Miniat, C. F. (2017). Topography may mitigate drought effects on vegetation along a hillslope gradient. Ecohydrology, 11(1), e1825. https://doi.org/10.1002/eco.1825

Kruskal, W. H., & Wallis, W. A. (1952). Use of Ranks in One-Criterion Variance Analysis. Journal of the American Statistical Association, 47(260), 583–621. https://doi.org/10.1080/01621459.1952.10483441

Kukal, M. S., & Hobbins, M. (2025). Thirstwaves: Prolonged periods of agricultural exposure to extreme atmospheric evaporative demand for water. Earth's Future, 13, e2024EF004870. https://doi.org/10.1029/2024EF004870

Li W, Yu T F, Li X Y, Zhao C Y. (2016). Sap flow characteristics and their response to environmental variables in a desert riparian forest along lower Heihe River Basin, Northwest China. Environ Monit Assess, 188: 561

Link, P., Simonin, K., Maness, H., Oshun, J., Dawson, T., & Fung, I. (2014). Species differences in the seasonality of evergreen tree transpiration in a Mediterranean climate: Analysis of multiyear, half-hourly sap flow observations. Water Resources Research, 50(3), 1869-1894. https://doi.org/10.1002/2013WR014023

Liu, Y., Chen, Z., Cheng, L., Qin, S., Wan, L., Yin, J., et al. (2024). Modelling of sap flux density of oak in a humid region in China. Ecohydrology. https://doi.org/10.1002/eco.2650

Looker, N., Martin, J., Hoylman, Z., Jencso, K., & Hu, J. (2018). Diurnal and seasonal coupling of conifer sap flow and vapour pressure deficit across topoclimatic gradients in a subalpine catchment. Ecohydrology, 11(7), e1994. https://doi.org/10.1002/eco.1994

Lopez-Bustins, J.A., Pascual, D., Pla, E. et al. Future variability of droughts in three Mediterranean catchments. Nat Hazards 69, 1405–1421 (2013). https://doi.org/10.1007/s11069-013-0754-3

Lu, S., Liu, M., Yi, J., Zhang, H., & Wan, J. (2024). Responses of soil moisture at different topographic positions to rainfall events along a steep subtropical forested hillslope. Hydrological Processes, 38(5), e15164. https://doi.org/10.1002/hyp.15164

Macchioli Grande, M., Kaffas, K., Verdone, M., Borga, M., Cocozza, C., Dani, A., Errico, A., Fabiani, G., Gourdol, L., Klaus, J., Manca di Villahermosa, F., Massari, C., Murgia, I., Pfister, L., Preti, F., Segura, C., Tailliez, C., Trucchi, P., Zuecco, G., Penna, D. (2024). Seasonal meteorological forcing controls runoff generation at multiple scales in a Mediterranean forested mountain catchment. Journal of Hydrology, 639, 131642. https://doi.org/10.1016/j.jhydrol.2024.131642

Magh, R.-K., Eiferle, C., Burzlaff, T., and Dannenmann, M. (2020). Competition for water rather than facilitation in mixed beech-fir forests after drying-wetting cycle, J. Hydrol., 587, 124944, https://doi.org/10.1016/j.jhydrol.2020.124944

Martínez-Fernández, J., González-Zamora, A., Sánchez, N., & Gumuzzio, A. (2015). A soil water based index as a suitable agricultural drought indicator. Journal of Hydrology, 522, 265-273. https://doi.org/10.1016/j.jhydrol.2014.12.051

McDowell N. Pockman W.T. Allen C.D.et al. 2008. Mechanisms of plant survival and mortality during drought: why do some plants survive while others succumb to drought? New Phytol. 178:719–739.

Michael G. Ryan, Tree responses to drought, Tree Physiology, Volume 31, Issue 3, March 2011, Pages 237–239, https://doi.org/10.1093/treephys/tpr022

Orth, R., Destouni, G. Drought reduces blue-water fluxes more strongly than green-water fluxes in Europe. Nat Commun 9, 3602 (2018). https://doi.org/10.1038/s41467-018-06013-7

Penna, D., Borga, M., Norbiato, D., & Dalla Fontana, G. (2009). Hillslope scale soil moisture variability in a steep alpine terrain. Journal of Hydrology, 364(3-4), 311-327. https://doi.org/10.1016/j.jhydrol.2008.11.009

Pollastrini, M., Puletti, N., Selvi, F., Iacopetti, G., & Bussotti, F. (2019). Widespread Crown Defoliation After a Drought and Heat Wave in the Forests of Tuscany (Central Italy) and Their Recovery—A Case Study From Summer 2017. Frontiers in Forests and Global Change, 2, 486030. https://doi.org/10.3389/ffgc.2019.00074

Rebollo, P., Moreno-Fernández, D., Cruz-Alonso, V. et al. Recent increase in tree damage and mortality and their spatial dependence on drought intensity in Mediterranean forests. Landsc Ecol 39, 38 (2024). https://doi.org/10.1007/s10980-024-01837-9

Renner, M., Hassler, S. K., Blume, T., Weiler, M., Hildebrandt, A., Guderle, M., Schymanski, S. J., and Kleidon, A.: Dominant controls of transpiration along a hillslope transect inferred from ecohydrological measurements and thermodynamic limits, Hydrol. Earth Syst. Sci., 20, 2063–2083, https://doi.org/10.5194/hess-20-2063-2016, 2016.

Roddy, Adam & Dawson, T. (2013). Novel patterns of hysteresis in the response of leaf-level sap flow to vapor pressure deficit. Acta horticulturae. 991. 261-267. 10.17660/ActaHortic.2013.991.32.

Sato, Y., Kumagai, T. O., Kume, A., Otsuki, K., & Ogawa, S. (2004). Experimental analysis of moisture dynamics of litter layers—the effects of rainfall conditions and leaf shapes. Hydrological Processes, 18(16), 3007-3018. https://doi.org/10.1002/hyp.5746

Saxton, K. E., Rawls, W. J., Romberger, J. S., & Papendick, R. I. (1986). Estimating Generalized Soil-water Characteristics from Texture. Soil Science Society of America Journal, 50(4), 1031-1036. https://doi.org/10.2136/sssaj1986.03615995005000040039x

Shuai, H., Li, F., Zhu, J., Tingen, W. J., & Mukherjee, S. (2025). Hydroclimate-coupled framework for assessing power system resilience under summer drought and climate change. Renewable and Sustainable Energy Reviews, 213, 115397. https://doi.org/10.1016/j.rser.2025.115397

D.M. Smith, S.J. Allen, Measurement of sap flow in plant stems, Journal of Experimental Botany, Volume 47, Issue 12, December 1996, Pages 1833–1844, https://doi.org/10.1093/jxb/47.12.1833

Sitková, Zuzana & Nalevanková, Paulína & Střelcová, Katarína & Fleischer, Peter & Ježík, Marek & Sitko, Roman & Pavlenda, Pavel & Hlásny, Tomáš. (2014). How does soil water potential limit the seasonal dynamics of sap flow and circumference changes in European beech?. Lesnícky časopis – Forestry Journal. 60. 19-30. 10.2478/forj-2014-0002.

Teuling, A. J., Van Loon, A. F., Seneviratne, S. I., Lehner, I., Aubinet, M., Heinesch, B., Bernhofer, C., Grünwald, T., Prasse, H., & Spank, U. (2013). Evapotranspiration amplifies European summer drought. Geophysical Research Letters, 40(10), 2071-2075. https://doi.org/10.1002/grl.50495

Tong, Y., Liu, J., Han, X., Zhang, T., Dong, Y., Wu, M., Qin, S., Wei, Y., Chen, Z., & Zhou, Y. (2023). Radial and seasonal variation of sap flow and its response to meteorological factors in sandy Pinus sylvestris var. Mongolica plantations in the Three North Shelterbelt of China. Agricultural and Forest Meteorology, 328, 109239. https://doi.org/10.1016/j.agrformet.2022.109239

Tromp-van Meerveld, H., & McDonnell, J. (2006). On the interrelations between topography, soil depth, soil moisture, transpiration rates and species distribution at the hillslope scale. Advances in Water Resources, 29(2), 293-310. https://doi.org/10.1016/j.advwatres.2005.02.016

Van der Molen, M., Dolman, A., Ciais, P., Eglin, T., Gobron, N., Law, B., Meir, P., Peters, W., Phillips, O., Reichstein, M., Chen, T., Dekker, S., Doubková, M., Friedl, M., Jung, M., Van den Hurk, B., De Jeu, R., Kruijt, B., Ohta, T.,Wang, G. (2011). Drought and ecosystem carbon cycling. Agricultural and Forest Meteorology, 151(7), 765-773. https://doi.org/10.1016/j.agrformet.2011.01.018

Verdone, M., Van Meerveld, I., Massari, C., & Penna, D. (2025). Variability and temporal stability of throughfall along a hillslope. Journal of Hydrology, 647, 132294. https://doi.org/10.1016/j.jhydrol.2024.132294

Wan, L., Zhang, Q., Cheng, L., Liu, Y., Qin, S., Xu, J., & Wang, Y. (2023). What determines the TLs of sap flux with solar radiation and vapor pressure deficit? Agricultural and Forest Meteorology, 333, 109414. https://doi.org/10.1016/j.agrformet.2023.10941

Wang, H., Guan, H., Xu, X., Gao, L., Gutiérrez-Jurado, H. A., & Simmons, C. T. (2024). Topographic regulations on ecohydrological dynamics in a montane forest catchment and the implications for plant adaptation to environment. Journal of Hydrology, 637, 131412. https://doi.org/10.1016/j.jhydrol.2024.131412

Xu, S., McVicar, T. R., Li, L., Yu, Z., Jiang, P., Zhang, Y., et al. (2022). Globally assessing the hysteresis between sub-diurnal actual evaporation and vapor pressure deficit at the ecosystem scale: Patterns and mechanisms. Agricultural and Forest Meteorology, 323, 109085. https://doi.org/10.1016/j.agrformet.2022.109085

Yang, Y., & Tong, X. (2024). Spatial variability and uncertainty associated with soil moisture content using INLA-SPDE combined with PyMC3 probability programming. Scientific Reports, 14(1), 1-14. https://doi.org/10.1038/s41598-024-74624-w

Zeng, X., Song, Y., Zhang, W. et al. (2018). Spatio-temporal Variation of Soil Respiration and Its Driving Factors in Semi-arid Regions of North China. Chin. Geogr. Sci. 28, 12–24 https://doi.org/10.1007/s11769-017-0899-1

Zhang Q, Manzoni S, Katul G, Porporato A, Yang D. (2014). The hysteretic evapotranspiration-Vapor pressure deficit relation. J Geophys Res Biogeosci, 119: 125–140

Zhang, R., Xu, X., Liu, M. et al. (2019). Hysteresis in sap flow and its controlling mechanisms for a deciduous broad-leaved tree species in a humid karst region. Sci. China Earth Sci. 62, 1744–1755. https://doi.org/10.1007/s11430-018-9294-5

Zhu, H., Wang, G., Yinglan, A., & Liu, T. (2020). Ecohydrological effects of litter cover on the hillslope-scale infiltration-runoff patterns for layered soil in forest ecosystem. Ecological Engineering, 155, 105930. https://doi.org/10.1016/j.ecoleng.2020.105930

Supplementary material 2

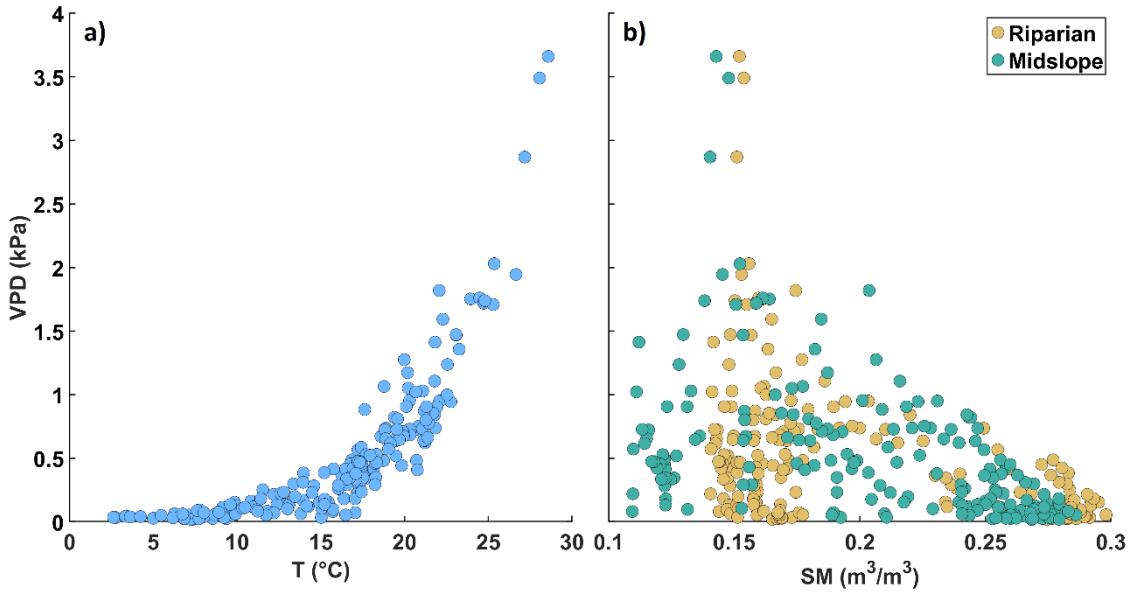

Figure S1. Scatterplot between mean daily temperature and mean daily vapour pressure deficit (VPD), highlighting that VPD is highly correlated to the air temperature (a), and between mean daily soil moisture (SM) measured in the riparian zone and midslope locations and mean daily VPD to highlight that low soil moisture occurred during days with high and low VPD (b).

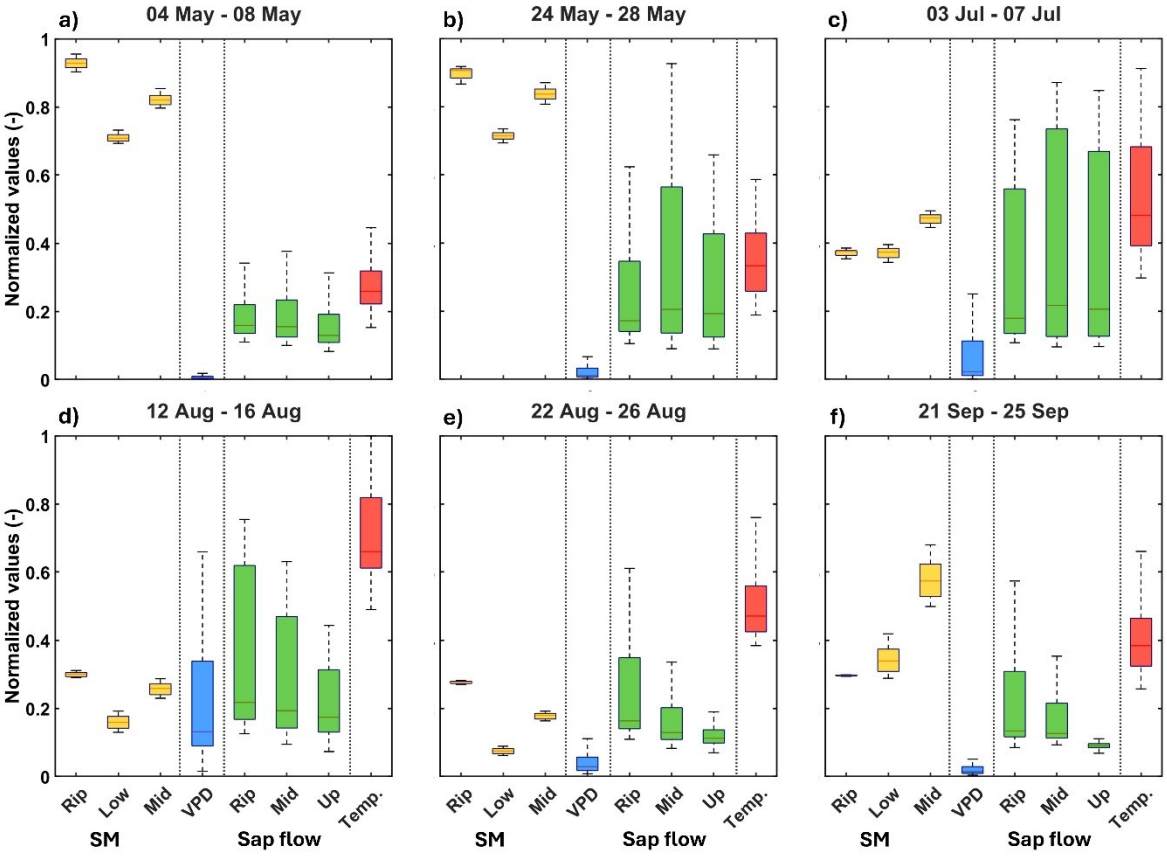

Figure S2. Box plots of the hourly soil moisture (SM), vapour pressure deficit (VPD), sap flow, and air temperature during six key 5-day periods during the growing season. Each variable is normalised between 0 and 1, based on the minimum and maximum value during the 5-day monitoring period to better visualize the differences. The boxes represent the interquartile range, the lines the median and the whiskers extend to 25th percentile and 75th percentile.

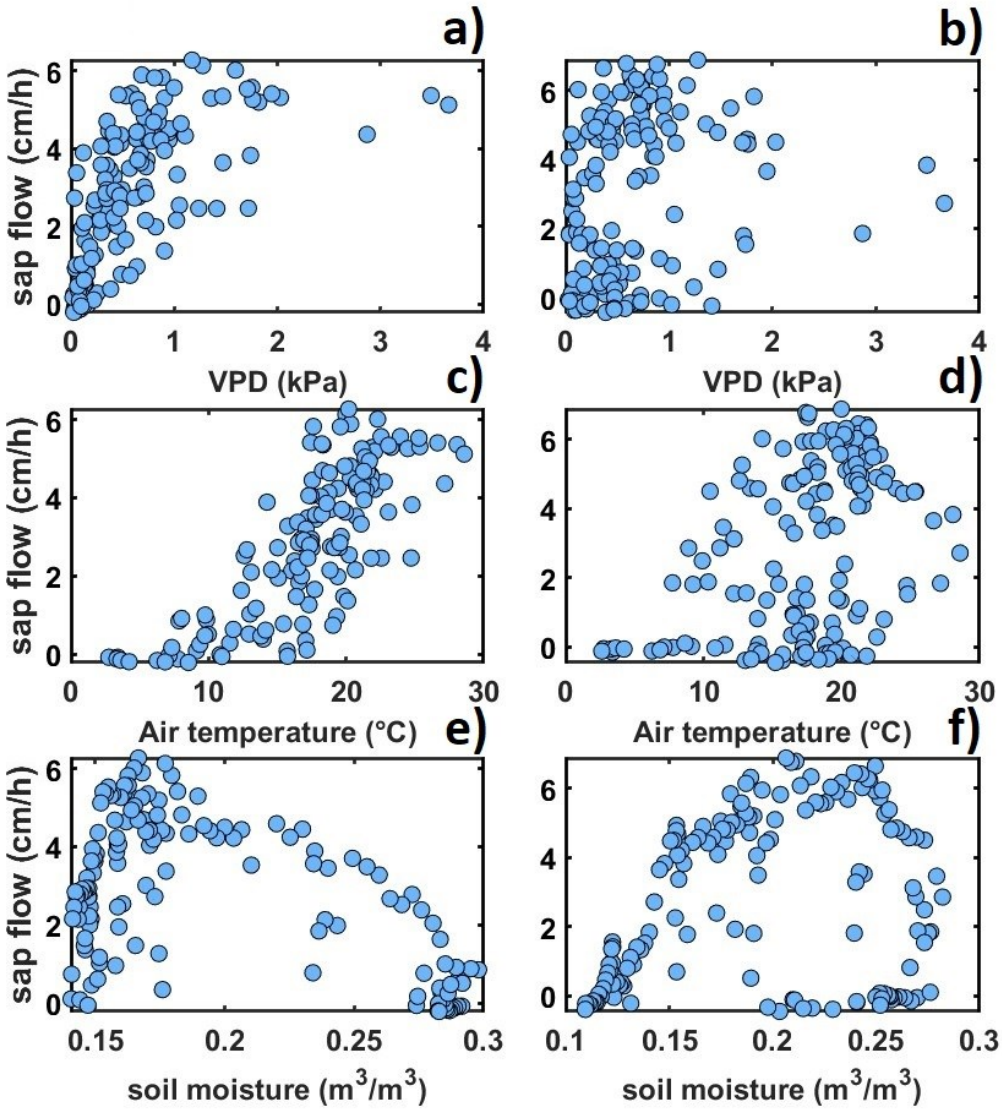

Figure S3. Scatter plot between the daily average sap flow and daily average vapor pressure deficit (VPD) (top), daily average air temperature (middle), and daily average soil moisture (bottom) for a tree in the riparian zone (Rip3; left column), and an upslope tree (Up2; right column).

3. Seasonal meteorological forcing controls runoff generation at multiple scales in a Mediterranean forested mountain catchment

This chapter is taken from: Macchioli Grande, M., Kaffas, K., **Verdone, M.**, Borga, M., Cocozza, C., Dani, A., Errico, A., Fabiani, G., Gourdol, L., Klaus, J., Manca di Villahermosa, F., Massari, C., Murgia, I., Pfister, L., Preti, F., Segura, C., Tailliez, C., Trucchi, P., Zuecco, G., Penna, D. (2024). Seasonal meteorological forcing controls runoff generation at multiple scales in a Mediterranean forested mountain catchment. Journal of Hydrology, 639, 131642. https://doi.org/10.1016/j.jhydrol.2024.131642

Abstract

Understanding hydrological processes during dry periods in Mediterranean mountain catchments is critical due to the increasing frequency of drought episodes. In this work, we aimed at characterizing the effect of the seasonal variability of meteorological forcing on the hydrological response of a small mountain forested catchment in the Mediterranean region. We analyzed the hydrological response and its timing based on hydrometric and electrical conductivity (EC) data for a year in the nested (0.31–2 km2) Re della Pietra catchment, in Central Italy. We used a soil moisture-based metric to distinguish between wet and dry periods and performed EC-based hydrograph separations during these two periods. The results revealed the important role of seasonality as a meteorological forcing affecting soil moisture, groundwater, streamflow response, and stream event water fractions. Wet and dry periods were distinctly characterized by different streamflow, soil moisture, and groundwater responses. Event water fractions in streamflow also highlight the relevance of the seasonality in the meteorological forcing on runoff generation. Particularly, at the rainfall-runoff event scale, the combination of antecedent soil moisture and precipitation depth controlled the non-linear response of streamflow, groundwater, and different event water fractions in the wet and dry periods.
Stream stages and event water fractions also varied across nested spatial scales. Antecedent moisture conditions triggered a faster streamflow response due to higher connectivity along the hillslope in the wet period, with higher event water fractions in the upper sub-catchments (25 %) compared to the lower sub-catchments (15 %). Conversely, in the dry period, higher event water fractions were registered at the outlet (11 %) than at the headwaters (7 %). Time lags between peak flows observed across the nested catchment showed a complex pattern, suggesting the interaction of multiple factors controlling the timing of streamflow peaks in the study area. These findings contributed to improve our mechanistic insights into the elusive seasonal hydrological patterns observed in Mediterranean mountain forested catchments.

3.1. Introduction

The hydrological functioning of catchments is influenced by complex interactions between meteorological forcing, geomorphological features, soil properties, geology, vegetation cover, and land use (Bracken and Croke, 2007; Llorens et al., 2018; Wei et al., 2020; Birch et al., 2021; Massari et al., 2023). Despite the body of literature investigating the main controls on catchment hydrological response, our understanding of how runoff generation changes between dry and wet periods and across multiple spatial scales is still limited. Particularly, two processes that are related to the mechanistic fundamentals of runoff generation in mountain catchments are (i) the role of antecedent moisture conditions in controlling streamflow and groundwater response under dry and wet conditions, and (ii) the change in event water fractions in streamflow (the proportion of water input to the catchment, i.e., rainfall or snowmelt) compared to pre-event water fractions (i.e., water stored in the catchment prior to the rainfall or snowmelt event) across nested catchments. Although these processes can be case-sensitive depending on factors like climate and physiographic properties of the study area, their characterization is essential for a detailed understanding of rainfall-runoff dynamics at the catchment scale (Ries et al., 2017, Wei et al., 2020).

Previous studies have addressed the influence of antecedent soil moisture and storm characteristics on streamflow, shallow groundwater response, and event water contributions in mountain forested catchments. Llorens et al. (2018) reported extensive monitoring for 30 years at the Vallcebre experimental catchment, a small partly forested mountain catchment in the Catalan Pre-Pyrenees, northeastern Spain. The authors stressed the combined effect of antecedent moisture conditions, precipitation depth and intensity, and forest cover on the catchment hydrological response. Detty and McGuire (2010) identified hydrologic connectivity as a key control for catchment runoff response in a small, forested catchment in New Hampshire, USA. They showed that seasonal variations of hydrologic connectivity were related to dynamics in evapotranspiration, soil moisture storage, and groundwater recharge. Scaife and Band (2017) reported stormflow threshold behavior influenced by antecedent soil moisture and gross precipitation at forested mountain catchments of the Coweeta Hydrologic Laboratory, North Carolina, USA, finding differences between the dormant and the growing season. Thresholds in stormflow generation were also identified in a humid forested catchment in China, revealing the importance of antecedent conditions on the swift changes from slow to rapid runoff response (Zhang et al., 2021).

Hydrological processes in Mediterranean catchments, in particular, are affected by the strong seasonality in the meteorological forcing (i.e., alternance between a wet period in fall/winter and a dry period in spring/summer) and are thus extremely sensitive to drought episodes which are increasing both in frequency and severity (Giorgi and Lionello, 2008; Vasiliades and Loukas, 2009; Sellami et al., 2016; Massari et al., 2022). Nanda and Safeeq (2023) analyzed 129 rainfall-runoff events in Mediterranean headwater catchments in California (USA) and showed that runoff was eventually triggered when the total wetness (storage plus precipitation) exceeded specific thresholds. Their analysis also indicated that storage was higher at the downslope than at the upslope position, yielding higher runoff values. Dymond et al. (2021) studied water movement and storage on a forested Mediterranean slope. They observed that

near-stream locations (riparian and footslope) were the wettest during the wet period, as well as ridges, with similar contents at 15, 35, and 100 cm of depth. However, during the dry period, soil moisture exhibited high variability among all depths and topographic positions, with higher influence of local factors, plant water use, soil texture, and climatic forcing.

The analysis of event water contribution provides insight into runoff response to precipitation in catchments (Buttle, 1994, Pellerin et al., 2008), and allows process identification when studying the seasonal differences in the contributions of various sources to streamflow (e.g., Penna et al., 2015). Event and pre-event water fractions at the rainfall-runoff event scale or at seasonal, annual, or multiannual time scales are typically computed through tracer-based (e.g., stable isotopes of hydrogen and oxygen, or electrical conductivity) hydrograph separation techniques (Klaus and McDonnell, 2013). Hydrograph separation analysis in a partially forested mountain headwater catchment in Switzerland revealed that pre-event water fractions were mainly controlled by rainfall amount with a limited influence of antecedent moisture conditions (Fischer et al., 2017). On the contrary, von Freyberg et al. (2018) found unclear relationships between antecedent moisture and storm characteristics and event or pre-event water contributions in another steep mountain forested catchment in Switzerland. Two- and three-component hydrograph separation was also performed in a small, forested catchment in the Italian Pre-Alps, revealing a strong seasonality in runoff generation (Penna et al., 2015). Summer streamflow was mainly generated through direct channel precipitation and saturation overland flow from the riparian zone. In contrast, fall and winter streamflow was predominantly fed by groundwater and hillslope soil water contributions. Mosquera et al. (2018) compared the use of different tracers in hydrograph separation in the catchments of the Mediterranean HJ Andrews Experimental Forest (Oregon, USA), but did not address specific seasonal hydrological responses.

In addition to quantifying the role of antecedent soil moisture and threshold behaviors on runoff generation, and event fraction contributions to streamflow, the analysis of stream response timing across nested spatial scales can provide valuable insights into possible changes in hydrological processes controlling discharge with increasing catchment size. However, studies focusing on this aspect performed in forested mountain catchments with Mediterranean climates remain scarce. McGlynn et al. (2004) studied the streamflow response in micro- and small-scale mountain forested catchments at Maimai (<1–280 ha) in New Zealand. These authors did not observe any consistent pattern of new water contribution with increasing catchment area, but their findings revealed an increment of time lag responses with increasing catchment size. For small (7–147 ha) forested catchments in Québec, Canada, event water contributions were found to be unrelated to catchment size but dependent on rainfall intensity and storm size, with higher event water transit time with increasing areas (Segura et al., 2012). Contrarily, Guastini et al. (2019) observed an overall decreasing trend of specific streamflow and runoff coefficients moving from a small grassland catchment to larger forested catchments (0.14–109 km^2) in the Dolomites, in northern Italy. However, they did not find any distinct relationship between lag times and catchment scales, suggesting interactions of multiple factors on response times.

The literature inspection reported above clearly reveals that only few studies have been carried out on the role of antecedent moisture conditions on catchment response during dry and wet periods, and on changes in event water fractions and timing of

stream response across spatial scales. Most importantly, no studies have been conducted on these aspects in Mediterranean mountain forested catchments. To fill these knowledge gaps on the role of antecedent conditions on hydrological processes in meteorological contrasting periods, and on runoff volume timing across multiple spatial scales, we conducted a study based on hydrometeorological and tracer data collected in the small forested and nested Re della Pietra catchment, in the Apennine mountains, Central Italy. This catchment can be considered representative of Mediterranean mountain forested catchments due to its physiographic and climatic characteristics, thus making it an ideal setting for investigating seasonal patterns in hydrological responses. We aim to achieve a better mechanistic understanding of how the seasonal variability of the meteorological forcing affects the hydrological response at the headwater catchment scale, and between different spatial scales. In particular, we addressed the following questions:

I. How do antecedent moisture conditions control streamflow and shallow groundwater response during dry and wet periods?

II. How do event water fractions and timing of stream response change with increasing spatial scales?

3.2. Study area

The Re della Pietra is a 2 km^2 experimental forested catchment located in the Tuscan Apennines, Central Italy (Fig. 1a). The area is part of the International Model Forest network (https://imfn.net/) and is managed by the local Forest Service. The climate is temperate Mediterranean with wet (approximately October–May) and dry (approximately June–September) periods. The average annual precipitation depth is 1316 mm (1992–2022) based on data available from a weather station located at 1005 m a.s.l. (12 km south from the catchment) and operated by the Regional Hydrological Service. The year 2021, which covers most of the data collected for this study, was characterized by an annual precipitation of 1212 mm, i.e., slightly less than the long-term average. Therefore, the study period can be considered representative of the long-term hydrometeorological conditions in the study area. Average monthly temperatures vary from 2 °C in January to 20 °C in August, and the average annual temperature is 10.5 °C, according to data from the aforementioned weather station. Elevations range from 634 to 1320 m a.s.l., the average slope (from headwater to outlet) is 27.5°, and the stream channel is approximately 3000 m long. The catchment geology consists of sandstones corresponding to the Late Oligocene – Early Miocene Macigno Formation (Amendola et al., 2016). The soil is well drained and typically deeper than 50–80 cm, as assessed by spatially distributed knocking pole measurements. Soil texture in the upper headwater portion of the catchment was determined through the analysis of 11 soil samples collected in March 2021 at 0–20 cm (four samples), 20–40 cm (four samples), and 40–60 cm (three samples) close to the soil moisture sensors (see Section 3.1). Sand content in the 11 samples ranged between 57 and 76 %, and clay content between 4 and 11 %. Soil texture in all samples resulted in sandy loam, according to the USDA (1999) classification. The catchment area is predominantly covered by forests (>95 %), dominated by beech trees (Fagus sylvatica), oaks (Quercus cerris), and conifers (Pseudotsuga menziesii and Pinus nigra).

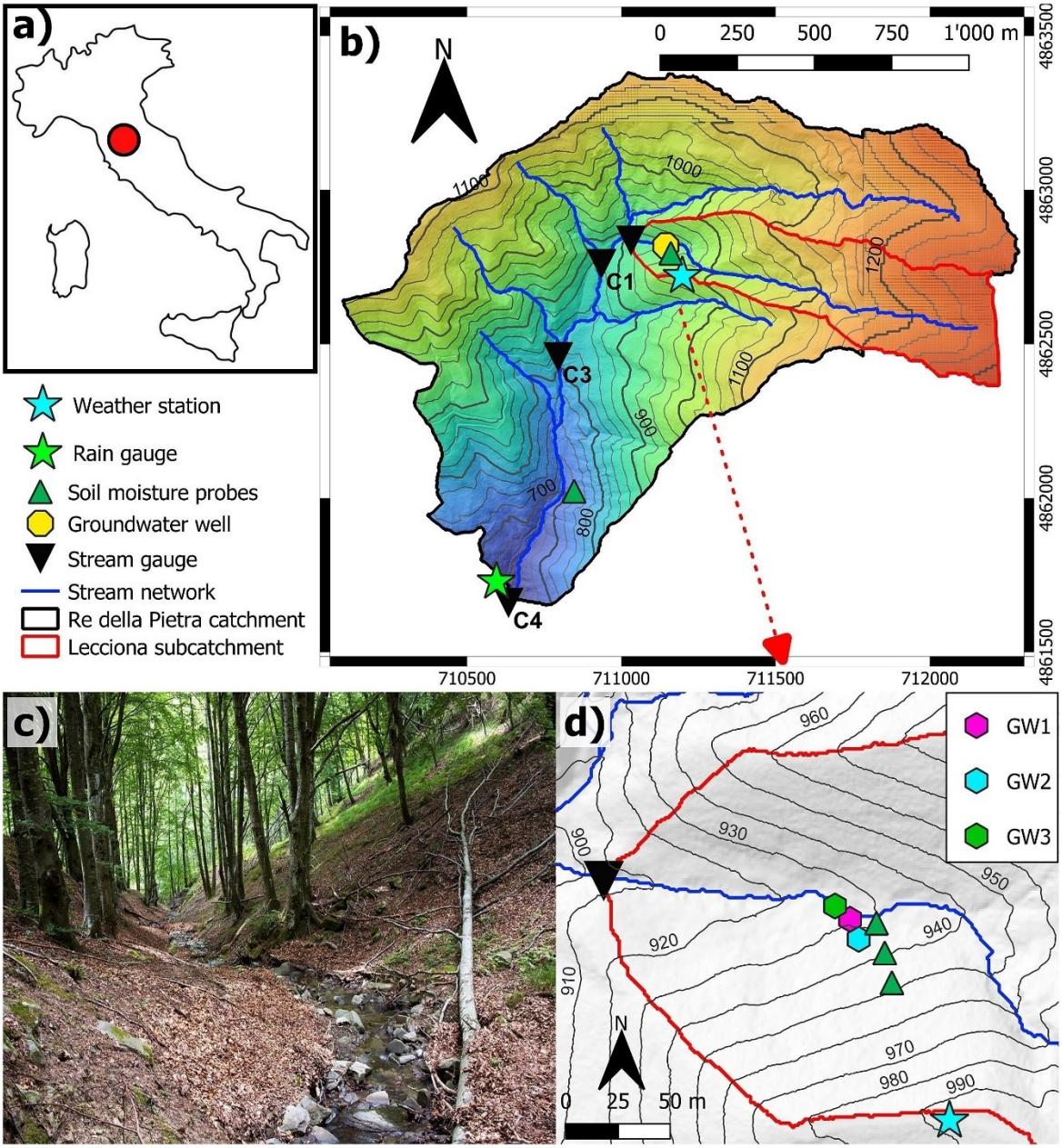

Figure 1. a) Study area in the Tuscan Apennines (Italy). b) Map of the Re della Pietra experimental catchment, showing the position of the monitoring instruments (stream and rain gauges, groundwater wells, weather stations, and soil moisture probes. c) Field picture of the Lecciona sub-catchment. d) Detailed map of the Lecciona sub-catchment, showing the location of the instruments, including the weather station, the soil moisture probes, the three groundwater wells (GW1, GW2, and GW3), and the stream gauge.

3.3. Materials and methods

3.3.1. Hydrometeorological measurements

Hydrometeorological data were collected during one calendar year, from 19 January 2021 to 20 January 2022. Four sub-catchments, from the headwater to the outlet, were selected to investigate the hydrological response across nested scales (Fig. 1b). The sub-catchments drain 0.31–2 km^2, with average slopes varying between 23.2 and 27.5°, and stream lengths ranging from 1357 to 3001 m (Table 1). Most of the

instruments were installed in the Lecciona sub-catchment, in the headwater portion of the Re della Pietra. A representative field picture of the Lecciona stream is shown in Fig. 1c. A weather station installed in a forest clearing near the boundary of the Lecciona sub-catchment at 991 m a.s.l. (Fig. 1d) records precipitation depth, air temperature, air humidity, solar radiation, wind speed, and wind direction at a 10-minute time step (reported precision for precipitation of 0.2 mm). Precipitation depth and air temperature were also recorded in another tree-free area at the outlet (C4) of the Re della Pietra catchment, at 634 m a.s.l. (Fig. 1b). Given their different elevations and the small size of the Re della Pietra catchment, the two rain gauges were deemed representative of the precipitation amount in the study area. Because of a two-week technical malfunction of the weather station at Lecciona, data from the rain gauge at C4 were used to fill in the gaps.

Table 1. General characteristics of the Re della Pietra (RdP) catchment at different spatial scales.

Sub-catchment name	Size (km^2)	Elevation range (m asl)	Average slope (°)	Main stream length (m)*	Main tree species
Lecciona	0.31	913–1313	23.2	1357	*F. sylvatica*
RdP at C1	0.99	873–1320	23.6	1554	*F. sylvatica*
RdP at C3	1.34	815–1320	24.9	1994	*F. sylvatica* – Mixed deciduous forest
RdP at C4	2.00	634–1320	27.5	3001	*F. sylvatica* – Mixed deciduous forest

*stream length was defined as the length of the channel measured in GIS environment from a digital elevation model (1x1 m, except in the upper part of the catchment where only 10x10 m2 resolution was available).

Stream stage, water temperature, and water electrical conductivity (EC) data were recorded at a 10-min interval by a CTD (conductivity, temperature, depth, with precisions of ± 0.5 % µS/cm, ± 0.3 °C, and ± 0.05 % mm, respectively, SEBA Hydrometrie GmbH) probe at Lecciona, C1, and C4, whereas at C3 only the stream stage was registered (reported precision of ± 0.05 % mm). At the Lecciona sub-catchment, a sharp crested weir with a composite triangular-rectangular shape was built to convert stream stage data into streamflow. The equations for the sharp crested weir were validated through multiple discharge measurements carried out using the salt dilution method under different hydrological conditions.
Soil moisture was measured as volumetric water content by six probes (Teros 10, Meter Group) installed in the Lecciona sub-catchment and recorded at a 10-min interval (Fig. 1d). The probes were installed in a transect along the hillslope, in three positions separated by 5 m each: the riparian area at the bottom of the hillslope, the lower part of the hillslope, where a gentle break in slope was evident, and in the middle part of the hillslope. In each position, two probes were installed, one at 15 cm and another at 35 cm depth. The raw values of the probes were converted into volumetric water content

(m3/m3) by applying a standard calibration for mineral soils suggested by the manufacturer (reported precision: 0.03 m3/m3). Soil moisture data among the three hillslope positions (riparian, low-slope, and mid-slope) were averaged by depth (15 and 35 cm) to assess the effect of soil moisture at the hillslope scale on the catchment hydrological response.

The influence of antecedent soil moisture conditions on the hydrological response was evaluated by computing the antecedent soil moisture index (ASI, Haga et al., 2005) given in Eq. (1):

$$ASI = \theta \times D \quad (1)$$

where θ is the volumetric soil moisture content at a given depth (m3/m3), and D is the installation depth (m). ASI was calculated based on soil moisture values recorded over one hour before the beginning of a precipitation event and averaged between the two depths and hillslope positions.

Pressure transducers measured groundwater levels in the Lecciona sub-catchment at a 15-min interval in three wells (reported precision is ± 0.05 mm). Two wells (GW1 and GW3) were located in the riparian zone, and a third one (GW2) was located at the foot of the hillslope (Fig. 1d).

3.3.2. Separation between wet and dry periods

We used the soil moisture-based metric proposed by Segura et al. (2023) to distinguish between wet and dry periods. First, we computed the hillslope spatial average soil moisture, i.e., among the three hillslope positions. Next, we determined the difference between the hillslope-average soil moisture at 35 and 15 cm depths. Upward positive peaks indicate that soil moisture at 35 cm is higher and responds earlier to precipitation than soil moisture at 15 cm, and were assigned to the wet period, while downward negative peaks indicate that soil moisture at 35 cm is lower and responds later than at 15 cm, and were assigned to the dry period (Fig. 2).

3.3.3. EC-based hydrograph separation

We used a tracer-based hydrograph separation approach to estimate the contribution of water originated from precipitation events (“event water”) and the contribution of water already stored in the catchment (“pre-event water”) to total streamflow. The latter is assumed to be a mixture of soil water and groundwater (Sklash and Farvolden, 1979, Laudon and Slaymaker, 1997, Penna et al., 2015). We used EC as a tracer in the hydrograph separations due to its simplicity in data acquisition and the high-resolution recording (e.g. Pellerin et al., 2008, Mosquera et al., 2018, Lazo et al., 2023). Hydrograph separation was performed i) at the yearly time scale at the stream gauges in Lecciona, C1, and C4; and ii) at the rainfall-runoff time scale during selected events in Lecciona only (see Section 3.4). At the yearly time scale, EC might behave as a non-conservative tracer due to dilution (during high flow) and concentration (during low flow) effects, resulting in non-stationary values of the pre-event water end-member signature over time, which is one of the prerequisites of the two-component

hydrograph separation technique (Buttle, 1994). In our case, we found a slight differences in the EC signature during baseflow conditions, between the wet and the dry periods, being 1, <1, and 13 µS/cm for Lecciona, C1, and C4 respectively (Fig. S1).

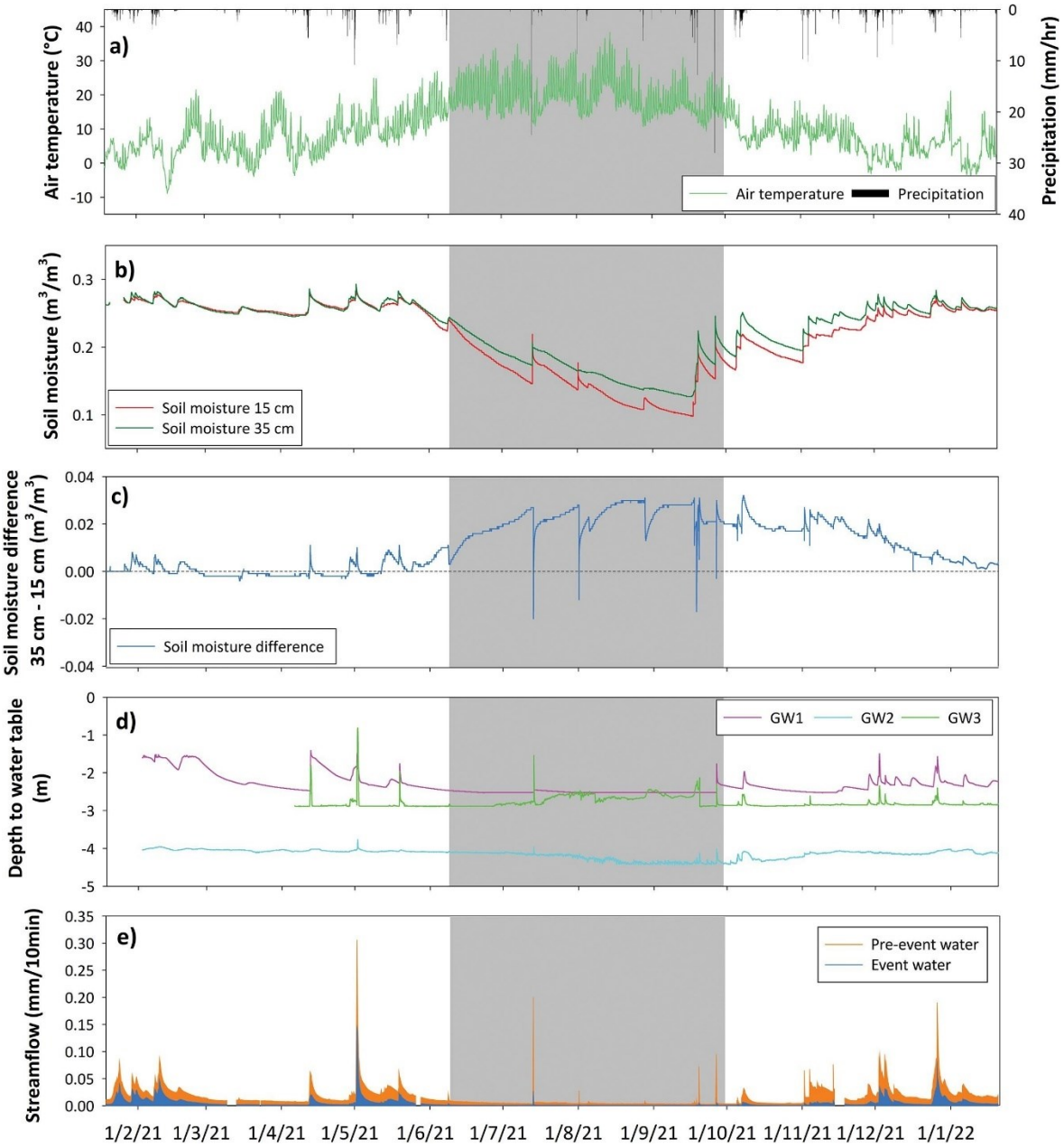

Figure 2. Time series of hydrometeorological variables in the Lecciona sub-catchment. The grey shaded area shows the dry period as defined by the soil moisture-based metric (described in Section 3.2). a) Precipitation and hourly air temperature registered by the weather station. b) Spatial average (among the three hillslope positions) soil moisture at 15 cm and 35 cm. c) Soil moisture difference between 35 cm and 15 cm. d) Groundwater level in the three wells. e) Event and pre-event water for the studied period.

Therefore, we applied EC-based hydrograph separation for wet and dry periods separately, identifying the pre-event water EC signature as the highest EC values measured in each stream section during base flow conditions. Because of its short duration, the seasonal dilution/concentration effect becomes negligible at the time scale of rainfall and runoff events, and EC can be considered a conservative tracer (Birch et al., 2021). In this case, the EC signature of pre-event water was identified as

the highest EC value one hour before the event onset or during the initial phase of the event (Penna et al., 2016, Buttle, 1994). For both approaches (annual and event scale hydrograph separation), the EC of event water was represented by the average EC from precipitation water monthly collected by an evaporation-free sampler installed close to the weather station.
The hydrograph separation was carried out employing the following equation:

$$f_e = \frac{C_s - C_p}{C_e - C_p} \quad (2)$$

where f_e is the event water fraction, C_s is the electrical conductivity of stream water, C_e is the electrical conductivity of precipitation, and C_p is the electrical conductivity of pre-event water.

3.3.4. Identification of precipitation-runoff events and time-lag analysis

Precipitation-runoff events were defined as events with a precipitation depth > 1 mm, which yielded a streamflow response > 0.01 mm/10 min. Based on these criteria, 34 events were identified during the study period in the Lecciona sub-catchment (Table S1). At the event scale, the distinction between baseflow and stormflow was performed using the constant-k method (Blume et al., 2007). The recession constant k was calculated at the time t of the event, and the time when this value remains constant marks the end of the event (Eq. (3)):

$$k = -\frac{dQ}{dt} \times \frac{1}{Q(t)} \quad (3)$$

where Q is the streamflow, and t is the time.
A time-lag analysis was conducted to assess the hydrological response time at each spatial scale (i.e., the time of the peak streamflow) from the Lecciona stream gauge to the outlet at C4. Stream stages at a 10-min time step were normalized to the highest value for comparability purposes. The time difference between the start of the event (Q_0) and the time at peak flow (Q_p) was computed at each stream section. Additionally, time lag differences in the peak streamflow (Q_p) occurrence between stream sections at different locations of the Re della Pietra catchment were also calculated.
To address the possible influence of the catchment shape on the timing of peak streamflow response, the Gravelius index (Gravelius, 1914, Bendjoudi and Hubert, 2002) was calculated for each sub-catchment (Bendjoudi and Hubert, 2002, Zemzami et al., 2013). The Gravelius index is the ratio of the catchment perimeter to the circumference of a circle with an area equal to that of the given catchment. The higher the index, the more elongated the catchment shape, while conversely, the closer the index to 1, the more rounded the catchment shape.

3.4. Results

3.4.1. Seasonal hydrological responses in the Lecciona sub-catchment

The strong seasonality characterizing the meteorological forcing in the study area was eventually reflected in the hydrological response of the Lecciona sub-catchment (Fig. 2). The soil moisture-based metric (Section 3.2) clearly identifies two distinct periods characterized by different precipitation depths and hydrological conditions (Table 2). Dominating positive values with upward peaks in the time series of the soil moisture difference are associated to periods with high precipitation depth, high and coupled soil moisture at both depths, and large streamflow, typical of winter, early spring, and late fall conditions. On the contrary, dominating downward peaks mainly reaching negative values of soil moisture difference coincide with spells characterized by low precipitation, low and decoupled soil moisture between the two soil depths, and low streamflow, typical of late spring and summer conditions (Fig. 2). This clear pattern allowed us to use the soil moisture difference between the two depths to distinguish between wet periods (i.e., periods with mainly upward peaks) and dry periods (i.e., periods with mainly downward peaks) in the time series. During the wet period, event precipitation depth ranged between 1.5 and 72 mm with low to moderate intensity (from 1.9 to 10.8 mm/h), while during the dry period, there were fewer events but with higher precipitation intensity (from 5.4 to 28.0 mm/h) (Table S1).

Reflecting the seasonal intermittency of precipitation, soil moisture varied considerably during the wet than during the dry period, with a significant decreasing trend during rainless periods and fewer responses (Fig. 2a). Soil moisture probes recorded comparable moisture content at 15 cm and 35 cm during the first part of the wet period, namely from January until the first week of June. They displayed different water content for the entire duration of the dry period (Fig. 2b), resulting in a coupling (matching) and decoupling (separation) behavior during the wet and dry periods, respectively. After the dry period (late September), there was again a converging trend which lasted until mid-late December, when soil moisture at the two depths exhibited similar values again.

Table 2. Average and standard deviation (SD) of the measured hydrometeorological variables in the wet (254 days, from 19 January 2021 to 7 June 2021 and from 27 September 2021 to 20 January 2022) and the dry period (111 days, from 8 June 2021 to 26 September 2021) in the Lecciona sub-catchment.

	Wet period		**Dry period**	
Cumulative precipitation depth (mm)	**1128.1**		**152.4**	
	Average	**SD**	**Average**	**SD**
Air temperature (°C)	6.9	5.6	19.9	5.2
Soil moisture at 15 cm (m^3/m^3)	0.238	0.045	0.151	0.036
Soil moisture at 35 cm (m^3/m^3)	0.245	0.042	0.173	0.031
Streamflow at Lecciona (mm/10 min)	0.026	0.023	0.006	0.003
Groundwater level – GW1 (m)	−2.22	0.27	−2.51	0.03
Groundwater level – GW2 (m)	−4.11	0.09	−4.25	0.12
Groundwater level – GW3 (m)	−2.84	0.12	−2.71	0.14
Event water fraction (dimensionless)	0.25	0.12	0.07	0.05

The water table also showed a certain degree of seasonal variability (Fig. 2d). Even though GW3 and GW1 wells are both located on a relatively flat area (14°) in the riparian zone, 1 and 3 m away from the Lecciona stream, respectively, they displayed noticeably different patterns. The groundwater level was most responsive at GW3, with a flashy response to precipitation with high peaks throughout the study period. The frequency and the magnitude of the peaks were consistent with the frequency and the magnitude of the major storm events. While showing a similar pattern during rainy periods, GW1 was almost unresponsive to even the largest precipitation events when these were preceded by periods with very little or no precipitation. This behavior was evident for the entire dry period, where the groundwater level was relatively stable with a slightly declining rate, but also during wet periods with long inter-storm times. It is worth noticing, however, that GW1 was highly responsive in the second part of the wet period (October 2021 onwards), resulting in higher peaks than GW3. GW2 is located at the footslope at a slightly higher altitude, 12 m from the stream, with a local slope of 26°. It had the deepest water table (1–2 m deeper than the other two wells) and displayed peaks of very low magnitude compared to GW1.

A clear seasonality in the Lecciona streamflow was evident as well (Fig. 2e), with streamflow being highly responsive to precipitation in the wet period and with very few but extreme responses in the dry period. This seasonal behavior was further characterized by longer recession times in the wet period in contrast with the dry period, which exhibited quick responses with very steep recessions. The highest peak in the dry period (13 July 2021) occurred after a prolonged period of dry conditions and was accompanied by a sharp peak in soil moisture (Fig. 2). Interestingly, the three following events —not preceded by a prolonged rainless spell— with higher precipitation depths in the dry period (1 and 28 August 2021, and 18–19 September 2021) resulted in lower streamflow. Pre-event water was dominant in the hydrograph throughout the year. However, proportionally larger fractions of event water were observed during the wet period (Fig. 2e and Table 3).

Table 3. Average and standard deviation (SD) of event water fraction (dimensionless) at Lecciona, C1, and C4 for the wet and dry period.

	Wet period		**Dry period**	
Stream gauge	**Average**	**SD**	**Average**	**SD**
Lecciona	0.25	0.12	0.07	0.05
C1	0.23	0.10	0.10	0.04
C4	0.15	0.11	0.11	0.07

3.4.2. Soil moisture and precipitation controls on seasonal hydrological response

The effect of 15 and 35 cm soil moisture on streamflow revealed contrasting behaviors in the wet and dry periods (Fig. 3). During the wet period, streamflow increased at soil moisture approximately at 0.25 m^3/m^3 for both depths, resulting in a non-linear behavior (Fig. 3a, b). An earlier —but lower in magnitude— rise of streamflow with instant peaks occurred at soil moisture values between 0.20 and 0.25 m^3/m^3, likely due to a large storm event in the wet period between the end of April and the beginning of

May (28 April 2021, Event 7, Table S1). Conversely, during the dry period, there was little effect of soil moisture on streamflow generation, with an abrupt peaking of streamflow for soil moisture values around 0.20 m^3/m^3 for both depths, corresponding to the intense storm events in mid-July and late September (Fig. 3a, b; events 14 (13 July 2021) and 21 (26 September 2021), Table S1). The relation between soil moisture at the two depths and event water fraction was characterized by a marked non-linearity, especially in the dry period (Fig. 3c and 3d). Event water fractions varied greatly during the wet period but showed an overall increasing trend with instant peaks between soil moisture values of 0.17 and 0.25 m^3/m^3 at 15 cm depth (Fig. 3c), while a more rapid increase was observed for soil moisture values between 0.23 and 0.24 m^3/m^3 at 35 cm depth (Fig. 3d). A higher increment in event water fractions was observed for soil moisture values ranging between 0.26 and 0.28 m3/m3 at 15 cm depth, and between 0.27 and 0.29 m^3/m^3 at 35 cm depth.

A clear non-linear behavior was observed in the relation between ASI and stormflow, with high stormflow values recorded only during wet conditions with ASI > 60 mm. However, some events had ASI > 60 mm but low stormflow values (Fig. 4a). The addition of precipitation depth to ASI led to a threshold behaviour with a linear increase of stormflow with ASI + P above 80 mm (Fig. 4b). ASI + P also showed a linear relation with stormflow for the dry period events (inset in Fig. 4b). Antecedent soil moisture conditions at 15 and 35 cm, especially with the addition of precipitation depth, also influenced the maximum event water fraction during both dry and wet periods (Fig. 4c and 4d). Events in the dry and wet periods were quite well grouped in two different clusters in both cases, but it is interesting to notice that the maximum event water fraction increased with increasing ASI + P at an overall higher rate in the dry season compared to the wet season.

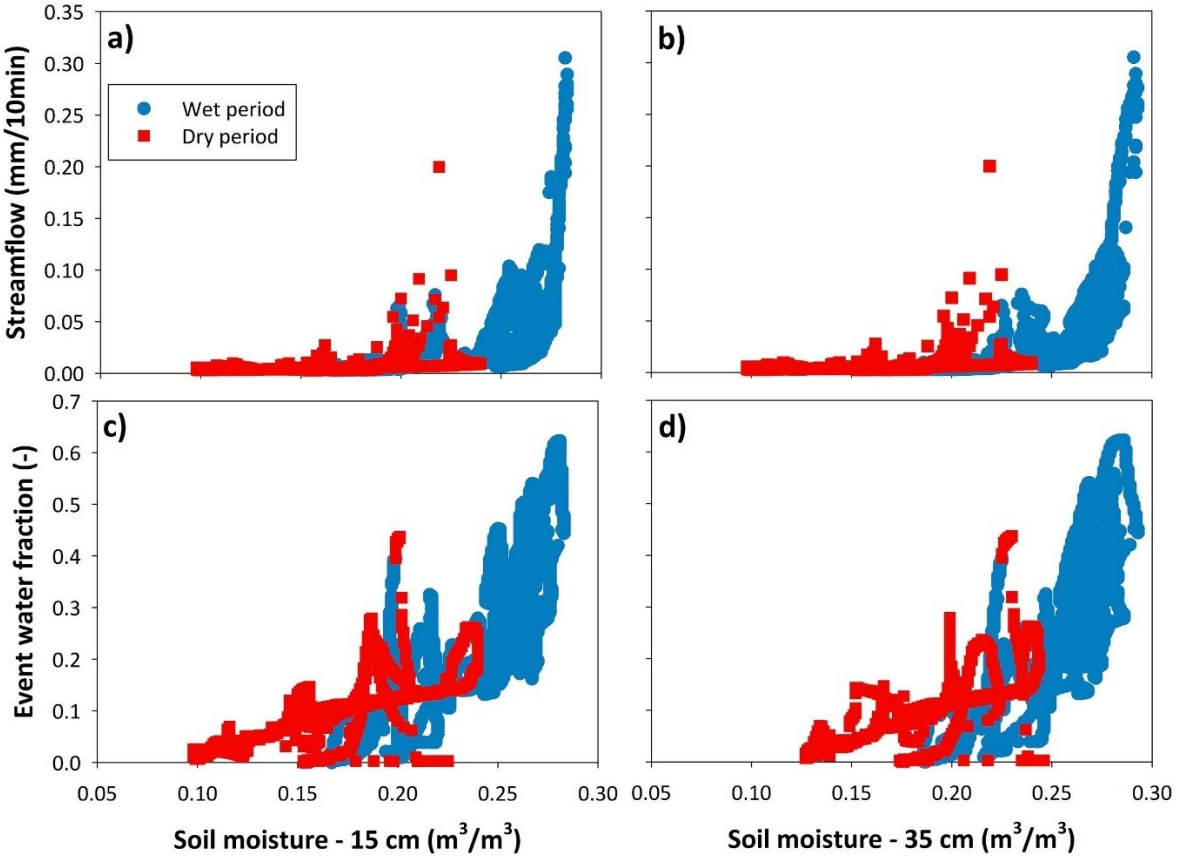

Figure 3. Non-linear behavior between hillslope-averaged soil moisture and streamflow (panels a and b) and event water fraction (panels c and d) at Lecciona catchment.

Water table peaks in GW1 were unrelated to ASI during the dry period (Fig. 5a). During the wet period, GW1 peaks showed a threshold response with marked increases above 60 mm in ASI (Fig. 5a). For the dry period, this behavior was in perfect agreement with the GW time series (Fig. 2d), i.e., the water level at GW1 remained stable even during large rainwater inputs. The only exception to this pattern was observed for two events indicated by red and blue arrows, which correspond to the highest precipitation events in the dry and wet periods. Specifically, a precipitation event of 36.3 mm and ASI slightly above 40 mm in the dry period (19 September 2021, event 21, Table S1) was responsible for a water table rise up to ~ 1.8 m from the soil surface, while 72 mm (highest precipitation event of the entire study period; 6 October 2021, event 24, Table S1) with ~ 53 mm ASI resulted in a rise of water table up to ~ 2 m from the soil surface. Excluding these two events, the vertical rise of GW1 peaks for ASI values in the 62–67 mm range indicates a threshold behavior of GW1 peaks' response to ASI during the wet period. Adding precipitation to ASI (Fig. 5b) eliminated this threshold behavior in the wet period, generating a linear relation between ASI + P and GW1 peaks, with a slight dispersion for ASI + P above 100 mm. The situation in the dry period was almost identical. A linear relationship was also observed between the maximum event water fraction and the water table peaks at GW1 in the dry period (Fig. 5c). Interestingly, during the dry period, a streamflow response was not coupled with a groundwater response, and a corresponding increase of GW1 peaks did not accompany the rise of the maximum event water fraction in streamflow.

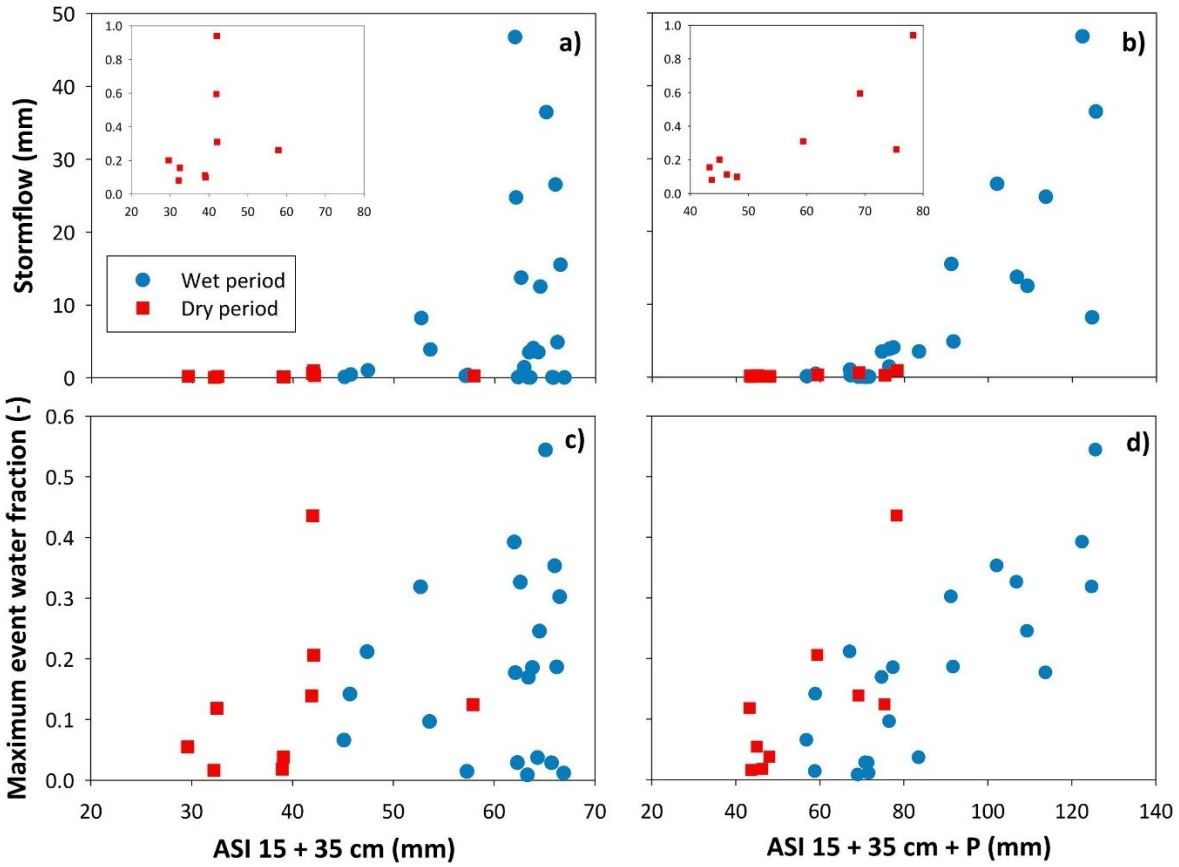

Figure 4. Relations between a) the 15-35 cm-averaged antecedent soil moisture index (ASI) and stormflow; b) the sum of the 15-35 cm-averaged ASI and precipitation depth and stormflow; c) the 15-35 cm-averaged ASI and maximum event water fraction; d) the sum of the 15-35 cm-averaged ASI and precipitation depth and maximum event water fraction. The insets in panel a) and b) refer to the red points shown in the same panel and plotted on an expanded y scale.

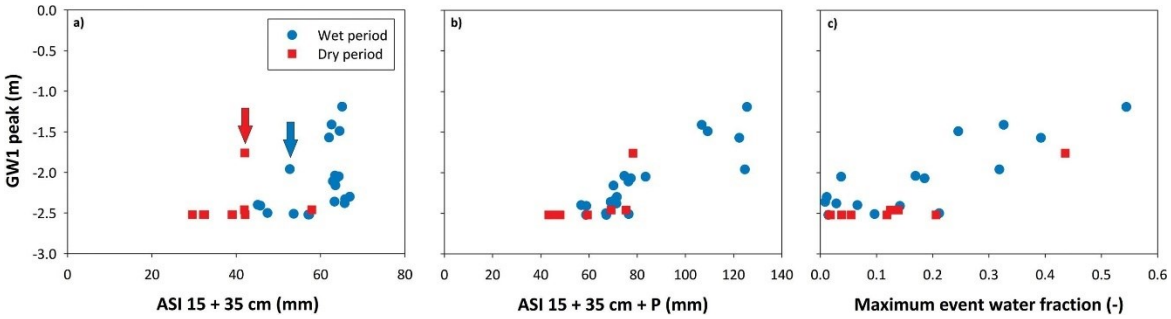

Figure 5. Relationships at the event scale between a) ASI, b) ASI + P, and c) maximum event water fraction, and water table peaks at GW1 well. The red and blue arrows in panel a) indicate two events in the dry (19 September 2021) and wet (6 October 2021) periods, respectively, which deviate from the overall threshold behavior.

3.4.3. Streamflow response across multiple spatial scales

Stream stages at C1, C3, and C4, and streamflow at Lecciona displayed seasonal patterns, with moderate to high peaks and long recessions in the wet period and smaller and flashy responses in the dry period (Fig. 6a). Event water fractions at Lecciona and C1 were very similar (Fig. 6b). However, the event water fraction was often higher at Lecciona during the wet period, while the event water fraction was regularly higher at C1 during the dry period (Table 3). The event water fraction at C4 varied more widely than in C1 and Lecciona, being noticeably lower during the wet season (before May) and noticeably higher from mid-May onwards and for most of the dry season. Between October 2021 and January 2022, the event water fractions in C4 fluctuated differently than in Lecciona and C1, remaining generally lower (Fig. 6b).

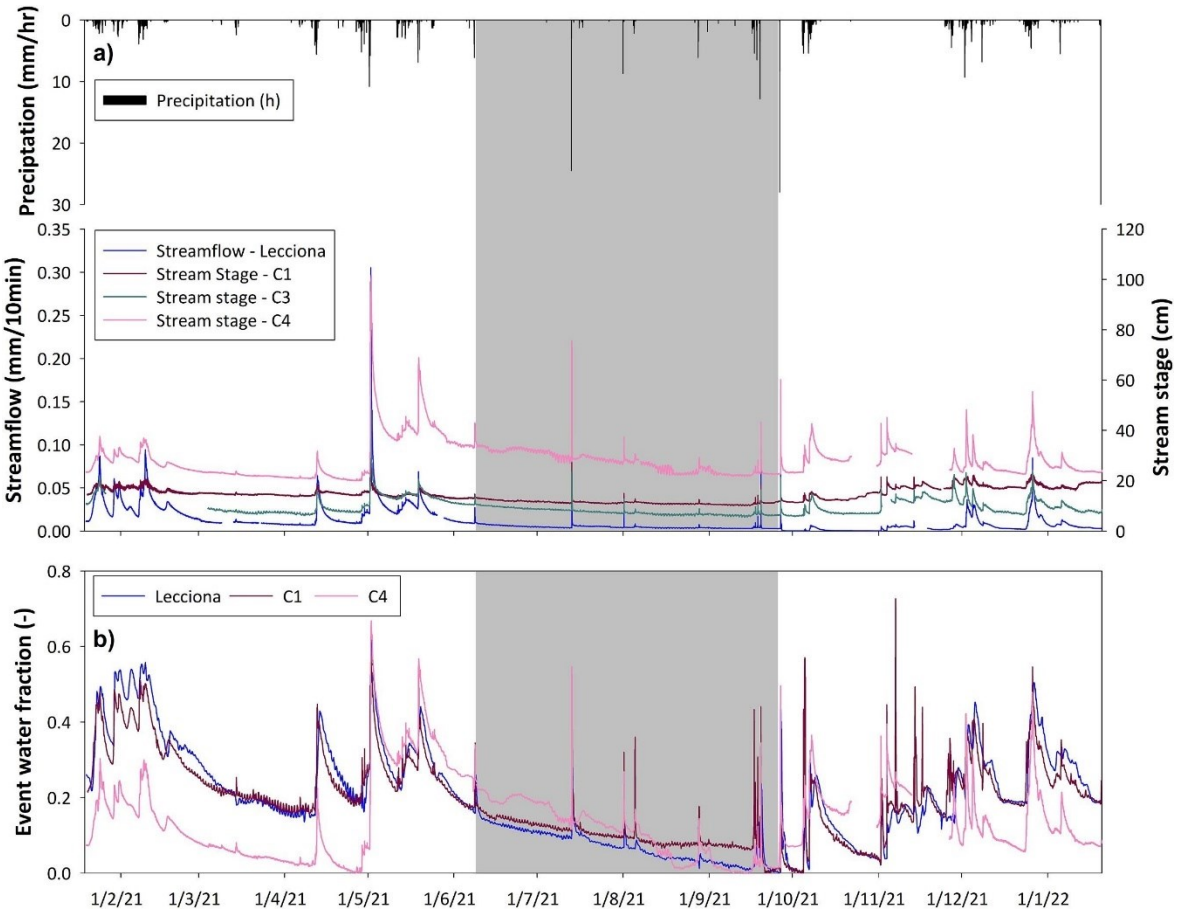

Figure 6. a) Time series of precipitation, Lecciona streamflow, and stage at C1, C3 and C4. b) EC-based time series of event water fraction at Lecciona, C1, and C4. Weighted average precipitation of the two rain gauges is shown. The grey shaded area marks the dry season. Note that the water level sensors at C1, C3, and C4 were installed at different depths, therefore the reported stage values cannot be directly compared.

The timing of stream response was variable across the catchment (Fig. 7). Positive values indicate that the upstream stream gauge peaked earlier than the downstream one, and negative values indicate the opposite. From Lecciona to C1, C3, and C4, the time lags consistently increase with greater differences in each sub-catchment's drainage area and stream length. Conversely, the small catchment area between C1 and C3 is counterbalanced by the long stream segment, which shifts the median value higher despite the high variability (long lower whisker). However, the relationships between stream length and catchment size with time lags are disrupted when considering C3-C4 and C1-C4 (Fig. 7).

Drainage area Δ (km^2)	0.68	1.03	1.69	0.35	0.66	1.01
Stream length (m)	165	605	1612	440	1007	1447

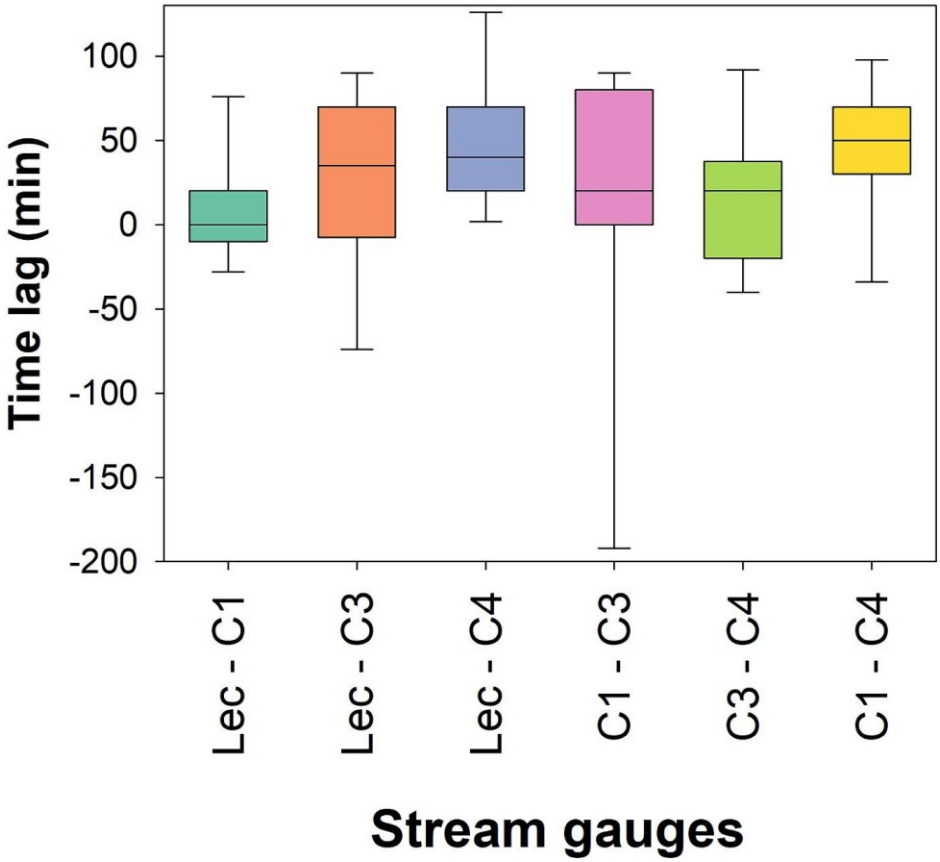

Figure 7. Peak response timing (i.e., difference between the time of peak stage in two stream gauges) across spatial scales (Lecciona, C1, C3, and C4). The symbol "Δ" indicates the difference between the areas of the compared sub-catchments. Stream length was computed based on the digital elevation model of the catchment and refers to the length of the stream between the two stream gauges indicated below each boxplot. The boxplots represent the first and third quartiles, the horizontal lines depict the median value of each dataset and the whiskers the 5-95% confidence interval.

3.5. Discussion

3.5.1. Effect of antecedent conditions on streamflow and groundwater response in wet and dry periods

The Lecciona sub-catchment showed a clear seasonal response to antecedent conditions during the studied period. The soil moisture difference between the measured depths allowed us to define temporal boundaries for dry and wet periods. Soil moisture responded quickly and had similar content at the two depths during the wet period (Fig. 2b). By contrast, soil moisture was decoupled between the two depths during the dry period, with higher values in the deeper soil, although with a responsive topsoil. The lower soil moisture content at 15 cm depth compared to the 35 cm depth observed during the dry period (Fig. 2b) could be due to the high evaporative demand on the soil surface and preferential tree water use in the shallower soil compared to the deeper layer (Fabiani et al., 2023). Although no soil-specific calibration was applied

to our soil moisture probes, and therefore the results should be interpreted with some caution, the decoupling of soil moisture at 15 and 35 cm depths in the Lecciona sub-catchment was similar to the decoupling observed in the forested Weierbach catchment for soil moisture measured at 10 and 40 cm depths (Segura et al., 2023). On the contrary, our results differ with the opposite decoupling dynamics observed for the Mediterranean mountain Can Vila catchment, where soil moisture was often higher in the shallow soil layer than in the deep layer (Segura et al., 2023). The disagreement between our results and those found for the Can Vila catchment suggests that different soil characteristics and water uptake by vegetation (that may lead to a marked vertical hydraulic redistribution of soil water) can affect soil moisture dynamics at different depths together with climatic characteristics.

Similar findings were presented by Dymond et al. (2021) for a Mediterranean forested catchment in Northern California, where soil moisture manifested a clear seasonality. During the wet period soil moisture was more similar between 15, 30, and 100 cm depths at all topographic positions, while the soil layer at 30 cm maintained a uniform higher water content than the layer at 15 cm in most hillslope positions throughout the dry period, thus evidencing a higher variability among depths. Studying the dependence of soil respiration's temperature on soil moisture in a Mediterranean riparian forest Northeast in Spain, Chang et al. (2014) found that during dry conditions, the soil at 5 cm depth suffered a 45–63 % reduction of water content when the soil at 30 cm depth only 14–35 %. Penna et al. (2015) documented a seasonal variability in the mountain forested Ressi catchment in Northern Italy, with higher precipitation depth, soil moisture, and streamflow in wet periods characterized by slow recessions and moderately high peak flows, compared to dry periods, which showed a flashy response, with quick recessions, and high peak flows. Other forested catchments showed a similar seasonal response (Fenicia et al., 2014, Douinot et al., 2022).

The non-linear relation between antecedent soil moisture and streamflow at Lecciona was more evident in the wet than in the dry period, likely due to the upper soil moisture limit that bounded further soil moisture increase (Fig. 3a, b). Previous work reported non-linear threshold effects in the relation between antecedent soil moisture and streamflow in forested catchments as a result of the activation of gravity-driven subsurface flow that connects hillslope to the streams (Penna et al., 2015, Zhang et al., 2021). In particular, Zhang et al. (2021) reported two distinct thresholds in a forested humid catchment in China, documenting a shift from a slow response with unsaturated soil water storage to a fast response with gravity-driven water movement through the soil along the hillslope reaching the stream. This behaviour is also in agreement with the "fill-and-spill" conceptual model (McDonnell et al., 2021), which proposes that only when storage reaches its critical level (fill), interconnection occurs, and outflow pathways activate (spill). However, as far as we know, our study is the first to document the distinct behavior of the antecedent soil moisture-streamflow relation in seasonally different dry and wet periods.

The effect of seasonality on streamflow generation was also evident in the relation between antecedent conditions, obtained by combining antecedent soil moisture and event precipitation (ASI + P), and stormflow (Fig. 4). During the dry period, when soil moisture was low, and during short events, the amount of stormflow in relation to precipitation depth was low, and relations between stormflow and ASI were weak (Fig. 4a). However, the linear response of stormflow to ASI + P for the events in the dry period suggests that the effect of precipitation depth became critical in producing stormflow

when antecedent moisture conditions were low (Fig. 4b). This basically stresses the important role of intense summer thunderstorms in generating runoff in this small catchment. Nevertheless, high stormflow values were always reached when wet soil and storm events were long (Fig. 4b). This observation agrees with the study of von Freyberg et al. (2018), which stresses the importance of controlling antecedent moisture conditions on streamflow and storm characteristics (precipitation depth and duration) in forested mountain catchments. The key role of wet antecedent conditions on streamflow generation was observed in other forested and not forested mountain catchments (e.g., Penna et al., 2011, Farrick and Branfireum, 2014, Wei et al., 2020). However, the distinct effect of seasonality on this behavior is shown here for the first time.

Antecedent soil moisture (ASI), and especially the combination of soil moisture and precipitation depth (ASI + P), had a clear effect on maximum event water fraction (Fig. 4c, d). This agrees with the findings by Fischer et al. (2017), who observed that event water contribution correlated positively to precipitation depth in a wet mountain and partially forested catchment in Switzerland, and with McGlynn et al. (2004), who showed increasing event water fractions with increasing antecedent moisture conditions in a forested catchment in New Zealand. In the Lecciona sub-catchment, non-linear behavior seemed to be controlled by antecedent soil moisture conditions combined with precipitation depth, suggesting the important role of hillslope-stream connectivity in delivering event water to the stream and in generating runoff (Fig. 4). Interestingly, the linear relation between ASI + P and maximum event water fractions was valid for events in both dry and wet periods. This new outcome can be valuable in understanding seasonal hydrological response in small catchments.

Groundwater in the Lecciona sub-catchment showed a different behavior in the riparian area, where the groundwater level was more responsive at GW3, closer to the stream (approximately 1 m distance) than GW1 (Fig. 2d). Additionally, a vertical increase of GW1 peaks above 62 mm of ASI (Fig. 5a) revealed a threshold behavior of GW1 response to antecedent moisture conditions during the wet period, while below that range of values, a considerable amount of rainfall would be necessary to elevate the water table. Noticeably, the groundwater level at the footslope was lower compared to the other two wells and not very responsive to precipitation (Fig. 2d). Despite the relatively small number of wells, which require some caution in the data interpretation, the observed response could imply less infiltration and more lateral flow at the hillslope, conducting water downwards and recharging the riparian zone. This process could be more effective in the wet period, when shorter transit times and larger connectivity between the riparian zone and the stream may control the event water fraction, particularly at the headwaters (Blume and van Meerveld, 2015, Nanda and Safeeq, 2023, Zuecco et al., 2019).

3.5.2. Event water fractions and streamflow timing at different spatial scales

A seasonal response was observed across all studied spatial scales in the Re della Pietra catchment. Stream stages were higher during the wet period than in the dry period, except at the outlet (C4), where the opposite was observed. Moreover, stream stages increased across spatial scales, from the Lecciona sub-catchment to the outlet of the Re della Pietra. Streamflow was dominated by pre-event water at all spatial

scales (85 % on a yearly average), and event water contributions were smaller than pre-event water contributions (Fig. 2e and 6, and Table 3). Similar event water fractions were reported by Laudon et al. (2007) for a forested catchment in Sweden, while Dusek and Vogel (2018) reported pre-event water contribution comprising hillslope preferential flow of 52–84 % (i.e., event water fractions of 16–48 %) in a mountain forested catchment.

In our study area, event water fractions varied seasonally and within spatial scales, with decreasing event water contribution with increasing drainage area in the wet period (being Lecciona and C1 more similar). Conversely, during the dry period the opposite behavior was observed (in which C1 and C4 were more similar). Wetter antecedent conditions could help to mobilize pre-event water rather than the fast transmission of event water (von Freyberg et al., 2018), and thus could explain the overall prevalence of pre-event water on streamflow. Nevertheless, event water contribution showed both seasonal and spatial variations (Fig. 6b). The average event water fractions calculated for Lecciona and C1 sub-catchments were higher in the wet period (24 and 23 %, respectively) than in the dry period (8 and 10 %), whereas event water fractions at C4 were lower in the wet period (10 %) than in the dry period (28 %). Blume et al., 2007, James and Roulet, 2009, and Penna et al. (2015) reported for small forested catchments a similar behavior to that observed at C4, with higher event water fractions occurring during the dry period and with dry antecedent conditions. This could result from shallow-subsurface stormflow (which drives a fast delivery of event water as quick flow) and catchment geomorphology (James and Roulet, 2009). Direct channel precipitation and overland flow could be favored at the outlet by its lower topographic position, increasing event water fraction, as Muñoz-Villers and McDonnell (2012) suggested. Although we have no evidence, litter cover (pretty thick in the lower hillslope position of the Lecciona sub-catchment) may also play a role in overland flow paths, as in other steep mountain catchments (Douinot et al., 2022).

Considering that a large drainage area favors lateral connectivity between the stream and upper hillslopes (Zhang et al., 2021), a wetter and highly connected hillslope to the stream during the wet period can explain the greater pre-event water fraction at C4, compared to Lecciona and C1. Thus, large areas integrate more lateral flow (McGlynn et al., 2004), which controls higher pre-event water fraction and higher stream stage at the outlet. In wetter conditions, there might be a larger contribution of the hillslope and riparian zones (i.e., greater pre-event water contribution, Fig. 6), meaning higher hydrological hillslope-riparian-stream connectivity (Zuecco et al., 2019). Therefore, the different seasonal response at multiple spatial scales in the Re della Pietra catchment seems to be controlled by catchment size, topography, and differences in soil transmissivity and antecedent conditions, as also observed by Shanley et al. (2002) for steep, partly forested catchments in the North-Eastern USA.

Other forested catchments also exhibited a seasonal pattern in hillslope-stream hydrological connectivity. For instance, Detty and McGuire (2010) and Bonanno et al. (2021) described hillslopes hydrologically disconnected from the main channel during the dry period, and connected during the wet period in mountain forested catchments. Similarly, at the Re della Pietra catchment, the response of shallow groundwater and soil moisture drives these seasonal variations, controlled by antecedent conditions and soil/bedrock characteristics. The underlying bedrock consists of fractured sandstones below the soil, which promotes both vertical percolation and lateral subsurface flow within the hillslope at the soil–bedrock interface. Moreover, soil

moisture response in the riparian area could control the higher event water fraction at Lecciona in the wet period, characterized by longer events and greater precipitation depths. By contrast, with increasing catchment size, higher connectivity during the wet period, which integrates lateral flow from a larger area, could lead to the decreasing event water contribution in the wet period. During the dry period, dry antecedent conditions, coupled with the presence of a hydrophobic litter cover and a bedrock of fractured sandstone draining a larger area, could lead to quick flows (Douinot et al., 2022), thus augmenting both the event water fraction and the stream stage with increasing catchment size.

Table 4. Gravelius index calculated for the four sub-catchments of the Re della Pietra catchment.

	Size (km^2)	Perimeter (km)	Gravelius index (–)
Lecciona	0.31	3.89	1.95
C1	0.99	6.10	1.72
C3	1.34	7.06	1.71
C4	2.00	9.22	1.83

The analysis of time lags of peak flow between multiple scales reveals a relatively complex pattern. On the one hand, the median time lag of peaks between Lecciona and C1, C3, and C4 increased with decreasing average catchment slope (Table 1), contrary to what was expected (Overton, 1971, Amiri et al., 2019). On the other hand, poor relations between time lags and catchment slope were found in other nested catchments with fractured geological settings (Penna et al., 2017). Further, the median time lag of peaks between all the stream gauges showed a consistent pattern of increasing lag times with increasing drainage area only in the upper part of the catchment, as observed elsewhere (McGlynn et al., 2004, Penna et al., 2017). Conversely, the relation between size and stream network and time lags weakened for the lower part of the catchment. The more elongated shape of the Lecciona sub-catchment, with a higher Gravelius index (Table 4), suggests that in the headwaters of the Re della Pietra, travel times are mainly a function of the stream length. The more rounded shape and more developed dendritic stream patterns of the other sub-catchments, in addition to catchment size and longer hillslopes, might lead to longer travel times (Bergstrom et al., 2016, van Meerveld et al., 2019).

Considering these results, the time lags between spatial scales appear to be controlled by time-variant hillslope hydrological connectivity, antecedent conditions, catchment size and shape, likely overlapping with soil properties and geology (Shanley et al., 2002, Haga et al., 2005, McGlynn et al., 2004). This combination of factors results in the large variability in streamflow peak time lags from upper headwater catchments to the outlet. Guastini et al. (2019) also reported a complex pattern in Alpine nested catchments, with an overall decrease in runoff coefficients and specific streamflow with increasing catchment area. In their case, however, a change in spring time was associated with a high snowmelt contribution to streamflow, which is missing in our case. The presented results thus suggest that more detailed studies are necessary to understand the interplay of different factors in the resulting time lags of peak response at different spatial scales.

3.6. Conclusions

Analyzing the dataset collected in the Re della Pietra experimental catchment improved the mechanistic fundamentals of seasonal hydrological patterns observed during dry and wet conditions across multiple spatial scales. These patterns revealed new findings on the effect of the seasonal meteorological forcings on streamflow generation and the event water contributions during both wet and dry periods, which are still missing in Mediterranean mountain forested catchments. This is a first attempt to understand how runoff response propagates across multiple spatial scales in small, forested catchments – therefore integrating both temporal and spatial variability in hydrological processes.

Our findings highlighted different soil moisture behaviors in shallow and deeper layers as a function of the overall catchment wetness. Antecedent soil moisture and its seasonality, often in combination with precipitation depth, control in a non-linear way streamflow generation and the fraction of event water delivered to the stream, ensuring groundwater response and subsurface hydrological connectivity under wet conditions. Streamflow peaks propagate downstream following a consistent spatial pattern only in the upper part of the catchment, mainly reflecting the catchment structure, indicating that more complex and interacting processes govern the timing of the hydrological response across multiple spatial scales, even in such a small catchment. Further investigations over a longer period in this and other mountain forested catchments are required to corroborate our conclusions and better understand the hydrology of climate change-sensitive Mediterranean catchments.

Funding

This study was supported by the research projects: “WATer mixing in the critical ZONe: observations and predictions under environmental changes – WATZON” (call PRIN 2017, code: 2017SL7ABC), funded by the Italian Ministry of University and Research (MIUR); “Unravelling interactions between WATER and carbon cycles during drought and their impact on water resources and forest and grassland ecosySTEMs in the Mediterranean climate – WATERSTEM” (call PRIN 2020, code: 20202WF53Z), funded by the Italian Ministry of University and research (MIUR); Hydrological Controls on Carbonate-mediated CO2 Consumption – Hydro4C (call PRIN 2022, code 2022PFNNRS), funded by the European Union – Next Generation EU; “Carbon and water cycles interactions during drought and their impact on WAter and ForEst Resources in the Mediterranean region –WAFER” funded by the Italian National research Council (Consiglio Nazionale delle Ricerche – CNR); “Space-time patterns of tree water uptake at hillslopes with contrasting climate and geology- STEP-UP” (code: AFR/STEP-UP ID 12546983), funded by the Fonds National de la Recherche Luxembourg; and “A new interdisciplinary approach to advance understanding of sediment and large wood TRANSport in FORested Mountain catchments – TRANSFORM” (call D.R. n. 328 on 11/03/2022, code: CUP B55F21007810001) funded by Next Generation EU and the University of Florence. MMG acknowledges a grant awarded by the National program for brief research internships abroad for postdoctoral students of the National Scientific and Technical Research Council of Argentina (Consejo Nacional de Investigaciones Científicas y Técnicas – CONICET), and a

research project awarded by the National Agency of Research and Development of Chile (call FONDECYT POSTDOCTORADO 2022, code: 3220318, Agencia Nacional de Investigación y Desarrollo – ANID).

Authors' contribution

M. Macchioli Grande: Writing – review & editing, Writing – original draft, Visualization, Data curation, Conceptualization. **K. Kaffas**: Writing – review & editing, Writing – original draft, Visualization, Formal analysis, Conceptualization. **M. Verdone**: Writing – review & editing, Visualization, Validation, Software, Methodology, Investigation, Formal analysis, Data curation. **M. Borga**: Writing – review & editing, Methodology, Investigation. **C. Cocozza**: Writing – review & editing, Methodology, Investigation. **A. Dani**: Writing – review & editing, Methodology, Investigation. **A. Errico**: Writing – review & editing, Methodology, Investigation. **G. Fabiani**: Writing – review & editing, Methodology, Investigation. **L. Gourdol**: Writing – review & editing, Methodology, Investigation. **J. Klaus**: Writing – review & editing, Funding acquisition, Conceptualization. **F.S. Manca di Villahermosa**: Writing – review & editing, Methodology, Investigation, Data curation. **C. Massari**: Writing – review & editing, Funding acquisition, Conceptualization. **I. Murgia**: Writing – review & editing, Methodology, Investigation, Data curation. **L. Pfister**: Writing – review & editing, Funding acquisition. **F. Preti**: Writing – review & editing, Methodology, Investigation. **C. Segura**: Writing – review & editing, Conceptualization. **C. Tailliez**: Writing – review & editing, Methodology, Investigation. **P. Trucchi**: Writing – review & editing, Methodology, Investigation. **G. Zuecco**: Writing – review & editing, Funding acquisition, Conceptualization. **D. Penna**: Writing – review & editing, Writing – original draft, Visualization, Methodology, Investigation, Funding acquisition, Conceptualization.

Acknowledgements

The authors thank the local Forest Service (Unione Comuni Valdarno e Valdisieve) for their logistical support that allowed the development of the Re della Pietra experimental catchment. The authors also extend their thanks to Dr. Ilaria Zorzi and to many undergraduate students who contributed to field work. The dataset is available upon request.

References

Amendola, U., Perri, F., Critelli, S., Monaco, P., Cirilli, S., Trecci, T., Rettori, R., 2016. Composition and provenance of the Macigno Formation (Late Oligocene - Early Miocene) in the Trasimeno Lake area (northern Apennines). Marine and Petroleum Geology 69, 146-167, doi: 10.1016/j.marpetgeo.2015.10.019

Amiri, B.J., Gao, J., Fohrer, N., Adamowski, J., Huang, J., 2019. Examining lag time using the landscape, pedoscape and lithoscape metrics of catchments. Ecological indicators 105, 36-46, doi: 10.1016/j.ecolind.2019.03.050

Bendjoudi, H., Hubert, P., 2002. The Gravelius compactness coefficient: critical analysis of a shape index for drainage basins. Hydrological Sciences Journal 47, 921-930. https://doi.org/10.1080/02626660209493000

Bergstrom, A., McGlynn, B., Mallard, J., Covino, T., 2016. Watershed structural influences on the distributions of stream network water and solute travel times under baseflow conditions. Hydrological Processes 30, 2671-2685. https://doi.org/10.1002/hyp.10792

Birch, A., Stallard, R., Barnard, H., 2021. Precipitation characteristics and land cover control wet season runoff source and rainfall partitioning in three humid tropical catchments in Central Panama. Water Resources Research 57(2), e2020WR028058, https://doi.org/10.1029/2020WR028058

Blume, T., Zehe, E., Bronstert, A., 2007. Rainfall-runoff response, event-based runoff coefficients and hydrograph separation. Hydrological Sciences Journal 52, 843–862. https://doi.org/10.1623/hysj.52.5.843

Blume, T., van Meerveld, H.J., 2015. From hillslope to stream: methods to investigate subsurface connectivity. WIREs Water 2, 177-198. https://doi.org/10.1002/wat2.1071

Bonanno, E., Blöschl, G., Klaus, J., 2021. Flow directions of stream-groundwater exchange in a headwater catchment during the hydrologic year. Hydrological Processes 35(8), e14310. https://doi.org/10.1002/hyp.14310

Buttle, J.M., 1994. Isotope hydrograph separations and rapid delivery of pre-event water from drainage basins. Prog. Phys. Geogr. 18, 16–41, doi: 10.1177/030913339401800102

Chang, C. T., Sabaté, S., Sperlich, D., Poblador, S., Sabater, F., Gracia, C., 2014. Does soil moisture overrule temperature dependence of soil respiration in Mediterranean riparian forests? Biogeosciences 11(21), 6173-6185. doi: 10.5194/bg-11-6173-2014

Detty, J.M., McGuire, K.J., 2010. Topographic controls on shallow groundwater dynamics: implications of hydrologic connectivity between hillslopes and riparian zones in a till mantled catchment. Hydrological Processes 24(16), 2222-2236, doi: 10.1002/hyp.7656

Douinot, A., Iffly, J.F., Tailliez, C., Meisch, C., Pfister, L., 2022. Flood patterns in a catchment with mixed bedrock geology: causes for flashy runoff contributions during storm events. Hydrology and Earth System Sciences 26, 5185–5206. https://doi.org/10.5194/hess-26-5185-2022

Dusek, J., Vogel, T., 2018. Hillslope hydrograph separation: The effects of variable isotopic signatures and hydrodynamic mixing in macroporous soil. Journal of Hydrology 563, 446-459, doi: 10.1016/j.jhydrol.2018.05.054

Dymond, S. F., Wagenbrenner, J. W., Keppeler, E. T., Bladon, K. D., 2021. Dynamic hillslope soil moisture in a Mediterranean montane watershed. Water Resources Research 57(11), e2020WR029170. doi: 10.1029/2020WR029170

Fabiani, G., Klaus, J., Penna, D., 2023. Contrasting water use strategies of beech trees along two hillslopes with different slope and climate. Hydrology and Earth System Sciences Discussions (preprint), https://doi.org/10.5194/hess-2023-225, in review.

Farrick, K.K., Branfireum, B.A., 2014. Soil water storage, rainfall and runoff relationships in a tropical dry forest catchment. Water Resources Research 50, 9236–9250, doi:10.1002/2014WR016045

Fenicia F., Kavetski, D., Savenije H.H.G., Clark, M.P., Schopus, G., Pfister, L., Freer, J., 2014. Catchment properties, function, and conceptual model representation: Is there a correspondence? Hydrological Processes 28, 2451–2467, doi: 10.1002/hyp.9726

Fischer B.M.C., Stähli, M., Seibert, J., 2017. Pre-event water contributions to runoff events of different magnitude in pre-alpine headwaters. Hydrology Research 48, 58–47, doi: 10.2166/nh.2016.176

Fu, C., Chen, J., Jiang, H., Dong, L., 2013. Threshold behavior in a fissured granitic catchment in southern China: 1. Analysis of field monitoring results. Water Resources Research 49, 2519–2535, doi:10.1002/wrcr.20191

Giorgi, F., Lionello, P., 2008. Climate change projections for the Mediterranean region. Global and Planetary Change 63, 90–104, doi: 10.1016/j.gloplacha.2007.09.005

Gravelius, H., 1914. Rivers, in: “Compendium in Hydrology”, 1 (in German). Göschen, Berlin, Germany

Guastini, E., Zuecco, G., Errico, A., Castelli, G., Bresci, E., Preti, F., Penna, D., 2019. How does streamflow response vary with spatial scale? Analysis of controls in three nested Alpine catchments. Journal of Hydrology 570, 705-718, doi: 10.1016/j.jhydrol.2019.01.022

Haga, H., Matsumoto, Y., Matsutani, J., Fujita, M., Nishida, K., Sakamoto, Y., 2005. Flow paths, rainfall properties, and antecedent soil moisture controlling lags to peak discharge in a granitic unchanneled catchment. Water Resources Research 41, W12410, doi: 10.1029/2005WR004236

James, A.L., Roulet, N.T., 2009. Antecedent moisture conditions and catchment morphology as controls on spatial patterns of runoff generation in small forest catchments. Journal of Hydrology 377, 351–366, doi: 10.1016/j.jhydrol.2009.08.039

Jin, Z., Guo, L., Yu, Y., Luo, D., Fan, B., Chu, G., 2020. Storm runoff generation in headwater catchments on the Chinese Loess Plateau after long-term vegetation rehabilitation. Science of the Total Environment 748, 141375, doi: 10.1016/j.scitotenv.2020.141375

Klaus, J., McDonnell, J., 2013. Hydrograph separation using stable isotopes: Review and evaluation. Journal of Hydrology 505, 47-64, doi: 10.1016/j.jhydrol.2013.09.006

Lazo, P.X., Mosquera, G.M, Cárdenas, I., Segura, C., Crespo, P., 2023. Flow partitioning modelling using high-resolution electrical conductivity data during variable flow conditions in a tropical montane catchment. Journal of Hydrology 617, 128898, doi: 10.1016/j.jhydrol.2022.128898

Laudon, H., Slaymaker, O., 1997. Hydrograph separation using stable isotopes, silica and electrical conductivity: an alpine example. Journal of Hydrology 201, 82–101, doi: 10.1016/S0022-1694(97)00030-9

Laudon, H., Sjöblom, V., Buffam, I., Seibert, J., Mörth, M., 2007. The role of catchment scale and landscape characteristics for runoff generation of boreal streams. Journal of Hydrology 344, 198-209, doi: 10.1016/j.jhydrol.2007.07.010

Llorens, P., Gallart, F., Cayuela, C., Roig-Planasdemunt, M., Casellas, E., Molina, A.J., Moreno de las Heras, M., Bertran, E., Sánchez-Costa, E., Latron, J., 2018. What have we learnt about Mediterranean catchment hydrology? 30 years observing hydrological processes in the Vallcebre research catchments. Geographical Research Letters 44, 475-502, doi: 10.18172/cig.3432

Massari, C., Avanzi, F., Bruno, G., Gabellani, S., Penna, D., Camici, S., 2022. Evaporation enhancement drives the European water-budget deficit during multi-year droughts. Hydrology and Earth System Sciences 26(6), 1527-1543, doi: 10.5194/hess-26-1527-2022

Massari, C., Pellet, V., Tramblay, Y., Crow, W.T., Gründemann, G.J., Hascoetf, T., Penna, D., Modanesi, S., Brocca, L., Camici, S., Marra, F., 2023. On the relation between antecedent basin conditions and runoff coefficient for European floods. Journal of Hydrology 625(B), 130012, doi: 10.1016/j.jhydrol.2023.130012

McDonnell, J.J., Spence, C., Karran, D., van Meerveld, H.J., & Harman, C., 2021. Fill-and-Spill: A Process Description of Runoff Generation at the Scale of the Beholder. Water Resources Research, 57, e2020WR027514. https://doi.org/10.1029/2020WR027514

McGlynn, B.L., McDonnell, J.J., Seibert, J., Kendall, C., 2004. Scale effects on headwater catchment runoff timing, flow sources, and groundwater-streamflow relations. Water Resources Research, 40, 1-14, doi: 10.1029/2003WR002494

Mosquera, G., Segura, C., Crespo, P., Mosquera, G.M., Segura, C., Crespo, P., 2018. Flow Partitioning Modelling Using High-Resolution Isotopic and Electrical Conductivity Data. Water 10, 904, doi: 10.3390/w10070904

Muñoz-Villers, L.E., McDonnell, J.J., 2012. Runoff generation in a steep, tropical montane cloud forest catchment on permeable volcanic substrate. Water Resources Research 48(9), doi: 10.1029/2011WR011316

Nanda, A., Safeeq, M., 2023. Threshold controlling runoff generation mechanisms in Mediterranean headwater catchments. Journal of Hydrology 620, 129532, doi: 10.1016/j.jhydrol.2023.129532

Overton, D.E., 1971. Estimation of surface water lag time from the kinematic wave equations. Journal of the American Water Resources Association 71038, doi: 10.1111/j.1752-1688.1971.tb05776.x

Pellerin, B.A., Wollheim, W.M., Feng, X., Vörösmarty, C.J., 2008. The application of electrical conductivity as a tracer for hydrograph separation in urban catchments. Hydrological Processes 22, 181-1818, doi: 10.1002/hyp.6786

Penna, D., Tromp Van-Meerveld, H.J., Gobbi, A., Borga, M., Dalla Fontana, G., 2011. The influence of soil moisture on threshold runoff generation processes in an alpine headwater catchment. Hydrology and Earth System Sciences 15, 689-702, doi: 10.5194/hess-15-689-2011

Penna, D., van Meerveld, H. J., Oliviero, O., Zuecco, G., Assendelft, R. S., Dalla Fontana, G., Borga, M., 2015. Seasonal changes in runoff generation in a small forested mountain catchment. Hydrological Processes 29(8), 2027-2042, doi: 10.1002/hyp.10347

Penna, D., van Meerveld, H.J., Zuecco, G., Dalla Fontana, G., Borga, M., 2016. Hydrological response of an Alpine catchment to rainfall and snowmelt events. Journal of Hydrology 537, 382–397, doi: 10.1016/j.jhydrol.2016.03.040

Penna D., Zuecco G., Crema S., Trevisani S., Cavalli M., Pianezzola L., Marchi L., Borga M., 2017. Response time and water origin in a steep nested catchment in the Italian Dolomites. Hydrological Processes 31, 768-782, doi:10.1002/hyp.11050

Ries, F., Schmidt, S., Sauter, M., Lange, J., 2017. Controls on runoff generation along a steep climatic gradient in the Eastern Mediterranean. Journal of Hydrology: Regional Studies 9, 18-33, doi: 10.1016/j.ejrh.2016.11.001

Scaife, C.I., Band, L.E., 2017. Nonstationarity in threshold response of stormflow in southern Appalachian headwater catchments. Water Resources Research 53, 6579-6596, doi:10.1002/2017WR020376

Segura, C., Penna, D., Borga, M., Hissler, C., Iffly, J. F., Klaus, J., Latron, J., Llorens, P., Marchina, C., Martínez-Carreras, N., Pfister, L., Zuecco, G. 2023. Comparing hydrological responses across catchments using a new soil water content metric. Hydrological Processes 37(10), e15010, https://doi.org/10.1002/hyp.15010

Sellami, H., Benabdallah, S., La Jeunesse, I., Vanclooster, M., 2016. Quantifying hydrological responses of small Mediterranean catchments under climate change projections. Science of the Total Environment 543, 924-936, doi: 10.1016/j.scitotenv.2015.07.006

Shanley, J.B., Kendall, C., Smith, T.E., Wolock, D.M., McDonnell, J.J., 2002. Controls on old and new water contributions to stream flow at some nested catchments in Vermont, USA. Hydrological Processes 16, 589-609, doi: 10.1002/hyp.312

Sidle, R.C., Tsuboyama, Y., Noguchi, S., Hosoda, I, Fujieda, M., Shimizu, T., 1995. Seasonal hydrologic response at various spatial scales in a small forested catchment, Hitachi Ohta, Japan. Journal of Hydrology 168, 227-250, doi: 10.1016/0022-1694(94)02639-S

Sklash, M.G., Farvolden, R.N., 1979. Role of groundwater in storm runoff. Journal of Hydrology 43(1–4): 45–65, doi: 10.1016/0022-1694(79)90164-1

Vasiliades, L., Loukas, A., 2009. Hydrological response to meteorological drought using the Palmer drought indices in Thessaly, Greece. Desalination 237(1-3), 3-21, doi: 10.1016/j.desal.2007.12.019

van Meerveld, H.J.I., Kirchner, J.W., Vis, M.J.P., Assendelft, R.S., Seibert, J., 2019. Expansion and contraction of the flowing stream network alter hillslope flowpath lengths and the shape of the travel time distribution. Hydrology and Earth System Sciences 23, 4825–4834, doi: 10.5194/hess-23-4825-2019

von Freyberg, J., Studer, B., Rinderer, M., & Kirchner, J.W., 2018. Studying catchment storm response using event- and pre-event-water volumes as fractions of precipitation rather than discharge. Hydrology and Earth System Sciences 22, 5847-5865, doi: 10.5194/hess-22-5847-2018

Wei, L., Qiu, Z., Zhou, G., Kinouchi, T., Liu, Y., 2020. Stormflow threshold behaviour in a subtropical mountainous headwater catchment during forest recovery period. Hydrological Processes 34(8), 1728-1740, doi: 10.1002/hyp.13658

Zhang, G., Cui, P., Gualtieri, C., Zhang, J., Bazai, N. A., Zhang, Z., Wang, J., Tang, J., Chen, R., Lei, M., 2021. Stormflow generation in a humid forest watershed controlled by antecedent wetness and rainfall amounts. Journal of Hydrology 603, 127107, doi: 10.1016/j.jhydrol.2021.127107

Zuecco G., Rinderer M., Penna D., Borga M., van Meerveld H.J., 2019. Quantification of subsurface hydrologic connectivity in four headwater catchments using graph theory. Science of the Total Environment 646, 1265-1280, doi: 10.1016/j.scitotenv.2018.07.269

Zemzami, M., Benaabidate, L., Layan, B., & Dridri, A., 2013. Design flood estimation in ungauged catchments and statistical characterization using principal components analysis: application of Gradex method in Upper Moulouya. Hydrological Processes, 27(2), 186-195, doi: https://doi.org/10.1002/hyp.9212

Supplementary material 3

Table S1. Main characteristics of the selected rainfall-runoff events at the Lecciona sub-catchment. Q_e/P index = event water fraction multiplied by total stormflow divided by precipitation depth; ASI = Antecedent soil moisture index; ASI + P = Antecedent soil moisture index plus Precipitation depth

ID	Date	Period	Cumulative Precipitation (mm)	Precipitation Duration (h)	Average Rainfall Intensity (mm/h)	Peak streamflow (mm/10 min)	Total stormflow (mm)	ASI (mm)	ASI + P (mm)	Maximum Event Water Fraction (-)	Total streamflow (mm)
1	20 January 2021	Wet	36.1	180	0.2	0.105	26.530	66.0	102.1	0.49	39.135
2	28 January 2021	Wet	24.7	121	0.2	0.073	15.520	66.5	91.2	0.54	27.517
3	7 February 2021	Wet	51.6	126	0.4	0.113	24.750	62.1	113.7	0.56	37.253
4	14 March 2021	Wet	8.5	15	0.6	0.017	0.082	62.3	70.8	0.20	1.018
5	12 April 2021	Wet	44.3	94	0.5	0.077	13.740	62.6	106.8	0.43	17.774
6	26 April 2021	Wet	6.7	9	0.8	0.013	0.038	63.5	70.2	0.20	0.516
7	28 April 2021	Wet	60.6	135	0.4	0.366	36.457	65.1	125.6	0.62	44.342
8	11 May 2021	Wet	5.6	4	1.4	0.028	0.045	63.3	69.0	0.24	0.565
9	13 May 2021	Wet	5.6	3	1.7	0.040	0.080	65.7	71.4	0.26	0.595
10	14 May 2021	Wet	4.8	2	2.4	0.047	0.033	66.9	71.6	0.31	0.439
11	19 May 2021	Wet	25.5	55	0.5	0.083	4.873	66.2	91.7	0.44	13.471
12	24 May 2021	Wet	5.2	7	0.7	0.026	0.020	65.8	70.9	0.30	0.897
13	8 June 2021	Dry	17.5	13	1.3	0.033	0.262	57.9	75.4	0.27	0.950
14	13 July 2021	Dry	27.3	4	6.5	0.240	0.595	41.9	69.2	0.23	0.689
15	1 August 2021	Dry	8.9	3	3.0	0.033	0.099	39.1	48.0	0.11	0.177
16	4 August 2021	Dry	7.4	15	0.5	0.010	0.113	39.0	46.3	0.09	0.538
17	28 August 2021	Dry	11.6	8	1.4	0.009	0.081	32.2	43.7	0.03	0.283
18	16 September 2021	Dry	15.4	32	0.5	0.012	0.201	29.6	45.0	0.07	0.843
19	18 September 2021	Dry	10.8	14	0.8	0.021	0.156	32.5	43.3	0.15	0.462
20	19 September 2021	Dry	17.3	12	1.5	0.087	0.310	42.1	59.4	0.24	0.579
21	26 September 2021	Dry	36.3	20	1.8	0.114	0.940	42.0	78.3	0.44	1.276
22	4 October 2021	Wet	11.7	9	1.3	0.012	0.106	45.1	56.8	0.07	0.283
23	5 October 2021	Wet	13.2	21	0.6	0.016	0.450	45.7	58.9	0.19	0.921
24	6 October 2021	Wet	72.0	99	0.7	0.040	8.198	52.7	124.7	0.32	10.615
25	1 November 2021	Wet	19.7	12	1.6	0.078	1.012	47.4	67.1	0.23	1.417
26	3 November 2021	Wet	22.9	25	0.9	0.081	3.878	53.6	76.5	0.13	6.257
27	7 November 2021	Wet	10.2	4	2.5	0.057	0.242	57.1	67.2	0.16	0.953
28	13 November 2021	Wet	1.5	4	0.3	0.091	0.383	57.3	58.8	0.17	1.048
29	27 November 2021	Wet	11.2	55	0.2	0.049	3.491	63.4	74.7	0.28	9.990
30	2 December 2021	Wet	44.8	54	0.8	0.124	12.509	64.5	109.3	0.39	20.415
31	4 December 2021	Wet	13.6	31	0.4	0.114	4.060	63.8	77.4	0.45	12.890
32	8 December 2021	Wet	13.5	25	0.6	0.043	1.437	62.9	76.4	0.31	4.479
33	23 December 2021	Wet	60.4	221	0.3	0.228	46.777	62.0	122.4	0.50	62.206
34	5 January 2021	Wet	19.2	57	0.3	0.048	3.506	64.3	83.5	0.33	11.272

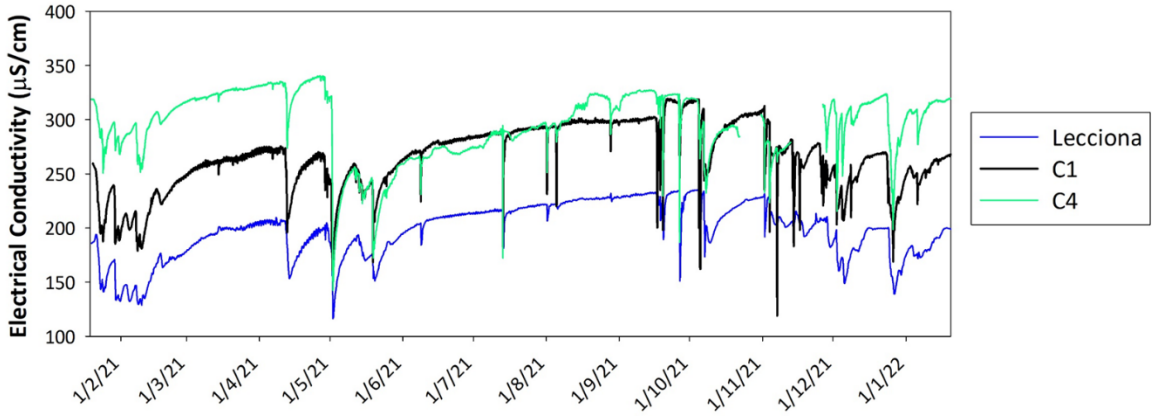

Figure S1. Time series of electrical conductivity at Lecciona, C1, and C4 stream gauges.

4. Conclusions

Hydrological processes in Mediterranean forested catchments are challenging to reproduce and model due to their complex interactions and highly variable drivers, even at small spatial scales. As a result, precise observation and monitoring of water-vegetation-soil interactions at experimental sites are essential for advancing our understanding of these systems. This PhD thesis largely relies on field data collected in the Re della Pietra experimental catchment in the Apennine Mountains (Central Italy), representative of mountain forested catchments of the Mediterranean region. The experimental results underline the pivotal roles of vegetation cover, hillslope topography, and antecedent soil moisture in shaping the hydrological response of catchments that are strongly influenced by a strong seasonality in the meteorological forcing.These works highlighted how topography (and seasonality) controls tree physiological responses, such as sap flow velocity, to rising temperatures and declining soil moisture. The relationship between vapor pressure deficit (VPD) and sap flow is shaped by both soil moisture and topographic position: for trees on the upper hillslope, soil moisture becomes a limiting factor, resulting in reduced sap flow during periods of high temperature and VPD, often accompanied by visible signs of water stress such as yellowing leaves. In contrast, trees in riparian zones maintain higher sap flow rates and do not exhibit water stress, owing to greater soil moisture availability.
This has led to the growth of larger trees with more developed crowns in the lower part of the hillslope than in the upper part. Larger trees and canopy proved to be more effective in intercepting rainfall along the hillslope giving lower throughfall amounts in the lower hillslope, compared to the upper hillslope. Higher quantity of rainfall that reach soil in upper part of the catchment could slightly mitigate effect of summer drought on trees physiology.
At the catchment scale those effects, regulating water balance, contributes to governs the timing and propagation of streamflow peaks across multiple spatial scales. In particular soil moisture and its variability, often in combination with precipitation depth, are key controls on streamflow generation and the proportion of event water delivered to the stream. These factors affect groundwater response and the formation of subsurface hydrological connectivity under wet conditions.
This thesis provided new findings and novel results on the role of how forest stand characteristics, seasonality in the meteorological forcing, and hillslope topography control interception, tree response to atmospheric demand, especially during drought conditions, and the hydrological response of a forested mountain catchment in the Mediterranean region. Given the complexity and variability of these processes, further studies in this and other Mediterranean catchments are needed to validate current findings and improve our understanding of catchment responses to climate change. Such research will also support the development of models that adequately represent small-scale variability in hydrological and ecohydrological processes.
Future studies should explore the complex interrelationships between individual hydrometeorological variables from the single tree scale to the forest stand and up to the entire catchment scale, considering the stand variability enanched by topography. This will lead to the development of accurate hydrological models for better use of water resources in a period of change such as the current one.

Publications

1. Verdone, M., Van Meerveld, I., Massari, C., & Penna, D. (2025). Variability and temporal stability of throughfall along a hillslope. Journal of Hydrology, 647, 132294. https://doi.org/10.1016/j.jhydrol.2024.132294

2. Verdone, M., Massari, C., Murgia, I., Cocozza, C., Van Meerveld, I., & Penna, D. (2025). Topography controls tree response to atmospheric demand during droughts. Ecohydrology (conditionally accepted)

3. Macchioli Grande, M., Kaffas, K., Verdone, M., Borga, M., Cocozza, C., Dani, A., Errico, A., Fabiani, G., Gourdol, L., Klaus, J., Manca di Villahermosa, F., Massari, C., Murgia, I., Pfister, L., Preti, F., Segura, C., Tailliez, C., Trucchi, P., Zuecco, G., Penna, D. (2024). Seasonal meteorological forcing controls runoff generation at multiple scales in a Mediterranean forested mountain catchment. Journal of Hydrology, 639, 131642. https://doi.org/10.1016/j.jhydrol.2024.131642

4. Kaffas, K., Murgia, I., Menapace, A., Macchioli Grande, M., Verdone, M., Dani, A., Manca di Villahermosa, F., Preti, F., Segura, C., Massari, C., Klaus, J., Borga, M., & Penna, D. (2025). Controls on preferential flow and its role on streamflow generation in a Mediterranean forested catchment. *Journal of Hydrology*, *660*, 133469. https://doi.org/10.1016/j.jhydrol.2025.133469

5. Benettin, P., Tagliavini, M., Andreotti, C., Verdone, M., Dani, A., & Penna, D. (2025). Ecohydrological Dynamics and Temporal Water Origin in a European Mediterranean Vineyard. Ecohydrology, 18(2), e2711. https://doi.org/10.1002/eco.2711

6. Lehmann, M. M., Geris, J., van Meerveld, I., Penna, D., Rothfuss, Y., Verdone, M., Ala-Aho, P., Arvai, M., Babre, A., Balandier, P., Bernhard, F., Butorac, L., Carrière, S. D., Ceperley, N. C., Chen, Z., Correa, A., Diao, H., Dubbert, D., Dubbert, M., Ercoli, F., Floriancic, M. G., Gimeno, T. E., Gounelle, D., Hagedorn, F., Hissler, C., Huneau, F., Iraheta, A., Jakovljević, T., Kazakis, N., Kern, Z., Knaebel, K., Kobler, J., Kocum, J., Koeber, C., Koren, G., Kübert, A., Kupka, D., Le Gall, S., Lehtonen, A., Leydier, T., Malagoli, P., Manca di Villahermosa, F. S., Marchina, C., Martínez-Carreras, N., Martin-StPaul, N., Marttila, H., Meyer Oliveira, A., Monvoisin, G., Orlowski, N., Palmik-Das, K., Persoiu, A., Popa, A., Prikaziuk, E., Quantin, C., Rinne-Garmston, K. T., Rohde, C., Sanda, M., Saurer, M., Schulz, D., Stockinger, M. P., Stumpp, C., Venisse, J.-S., Vlcek, L., Voudouris, S., Weeser, B., Wilkinson, M. E., Zuecco, G., and Meusburger, K.: Soil and stem xylem water isotope data from two pan-European sampling campaigns, Earth Syst. Sci. Data Discuss. [preprint], https://doi.org/10.5194/essd-2024-409, in review, 2024.

7. Verdone, M., van Meerveld I., Massari, C., Penna, D. (2024). Fattori di controllo sulla variabilità spaziotemporale dell'intercettazione in un versante forestato appenninico, Quaderni di Idronomia Montana, vol. 37/2, 277-284, ISBN 978-88-97181-89-7.

8. Macchioli Grande, M., Kaffas, K., Verdone, M., Borga, M., Cocozza, C., Dani, A., Errico, A., Fabiani, G., Gourdol, L., Klaus, J., Manca di Villahermosa, F., Massari, C., Murgia, I., Pfister, L., Preti, F., Segura, C., Tailliez, C., Trucchi, P., Zuecco, G., Penna, D. (2024). Generazione di deflusso superficiale e sottosuperficiale in un piccolo bacino appenninico, Quaderni di Idronomia Montana, vol. 37/2, 277-284, ISBN 978-88-97181-89-7.

Conference presentations and posters

Controls on throughfall spatial variability along a steep forested hillslope, Giornate dell'Idrologia 2024, Udine, 24-26 giugno 2024 (Poster)

Fattori di controllo sulla variabilità spaziotemporale dell'intercettazione in un versante forestato Appenninico, Giornate di studio in onore del Prof. Giuseppe Provenzano, Palermo, 4-5 dicembre 2023

Identifying controls on throughfall variability at the hillslope scale through field measurements and remote sensing techniques, 8th Galileo Conference, Napoli, 12-15 giugno 2023 (Poster)

Does tree size matter? Controls on throughfall variability in a mountain forested hillslope, Giornate dell'idrologia 2022, Genova, 9-11 novembre 2022

Spatio-temporal variability in throughfall at the hillslope scale in a mountain beech stand, AIIA 2022 Biennial Conference, Palermo, 19-22 settembre 2022

Throughfall spatio-temporal dynamics at the hillslope scale, ERB 18th Biennial Conference, Isola d'Elba, 7-10 giugno 2022

Throughfall variability at the hillslope scale: the role of topography and tree characteristics, EGU General Assembly, online, 22-27 maggio 2022

Abstract in conferences

EGU General Assembly 2025

Peruzzo, L., Pavoni, M., Cioffi, V., Censini, M., Manca, F., Barone, I., Verdone, M., Boaga, J., and Cassiani, G.: On the use of geophysics to support and connect soil sensors and cosmic ray neutron sensing: a case study highlighting the relevance of soil heterogeneity, EGU General Assembly 2025, Vienna, Austria, 27 Apr–2 May 2025, EGU25-12782, https://doi.org/10.5194/egusphere-egu25-12782, 2025.

Marchetti, E., Belli, G., Gheri, D., Innocenti, L., Murgia, I., Chirici, D., Verdone, M., Nicoletti, S., Solari, L., Morandi, O., and Penna, D.: Seismic analysis of bedload transport in a small mountain creek, EGU General Assembly 2025, Vienna, Austria, 27

Apr–2 May 2025, EGU25-21164, https://doi.org/10.5194/egusphere-egu25-21164, 2025.

Murgia, I., Kaffas, K., Verdone, M., Manca di Villahermosa, F. S., Dani, A., Preti, F., Segura, C., Massari, C., and Penna, D.: Revealing the interrelation among eco-hydro-meteorological variables in a forested Mediterranean catchment, EGU General Assembly 2025, Vienna, Austria, 27 Apr–2 May 2025, EGU25-1066, https://doi.org/10.5194/egusphere-egu25-1066, 2025.

Feng, M., Manco di Villahermosa, F. S., Verdone, M., Murgia, I., Fabiani, G., Zuecco, G., Brighenti, S., Klaus, J., Massari, C., Borga, M., Jiang, M., and Penna, D.: Geographical, spatial, and temporal water sources in a Mediterranean forested catchment., EGU General Assembly 2025, Vienna, Austria, 27 Apr–2 May 2025, EGU25-9957, https://doi.org/10.5194/egusphere-egu25-9957, 2025.

Chirici, D., Murgia, I., Verdone, M., Innocenti, L., Nigro, M., Manca, F., Dani, A., Preti, F., Belli, G., Gheri, D., Mao, L., Marchetti, E., Solari, L., and Penna, D.: Investigating Suspended Sediment And Large Wood Dynamics in a Mountain Forested Catchment, EGU General Assembly 2025, Vienna, Austria, 27 Apr–2 May 2025, EGU25-19543, https://doi.org/10.5194/egusphere-egu25-19543, 2025.

Verdone, M., Kaffas, K., Murgia, I., Menapace, A., Macchioli Grande, M., Dani, A., Manca di Villahermosa, F. S., Preti, F., Segura, C., Massari, C., Klaus, J., Borga, M., and Penna, D.: Soil properties, topography, and meteorological forcing control preferential flow and streamflow generation in a Mediterranean forested catchment, EGU General Assembly 2025, Vienna, Austria, 27 Apr–2 May 2025, EGU25-16458, https://doi.org/10.5194/egusphere-egu25-16458, 2025.

AISSA #40 2024

Chirici D., Murgia I., Verdone M., Innocenti L., Manca di Villahermosa F. S., Dani A., Preti F., Mao L., Solari L., Penna D., Do forest streams deliver suspended sediment? A Evidence from a forested nested catchment in the Apennine Mountains. V Convegno AISSA#under40. Firenze 26-27 giugno 2024

Giornate dell'idrologia 2024

Verdone M., Murgia I., Manca di Villahermosa F. S., Chirici D., Hildebrandt A., Massari C., van Meerveld I., Penna D., Controls on throughfall spatial variability along a steep forested hillslope, Giornate dell'Idrologia 2024, Udine, 24-26 giugno 2024.

Chirici D., Murgia I., Verdone M., Innocenti L., Manca di Villahermosa F. S., Dani A., Preti F., Belli G., Gheri D., Mao L., Marchetti E., Penna D., How do forested catchments originate and transport suspended sediments across multiple scales?, Giornate dell'Idrologia 2024, Udine, 24-26 giugno 2024.

AIIA Mid-Term conference 2024

Murgia I., Kaffas K., Verdone M., Manca di Villahermosa F.S., Dani A., Preti F., Massari C., Segura C., Penna D., Analysis of soil moisture variability during dry and wet periods using wavelet approach in the Re della Pietra catchment (Tuscan Apennines, Italy), AIIA Mid-Term Conference – Padova 17-19 June 2024

Murgia I., Chirici D., Innocenti L., Verdone M., Belli G., Nicoletti S., Dani A., Preti F., Comiti F., Mao L., Morandi O., Marchetti E., Solari L., Penna D., Drivers and sources of suspended sediment in a forested mountain catchment, AIIA Mid-Term Conference – Padova 17-19 June 2024

Kaffas K., Murgia I., Verdone M., Manca di Villahermosa F.S., Dani A., Preti F., Massari C., Penna D., Drivers of preferential flow in a mountain forested catchment, AIIA Mid-Term Conference – Padova 17-19 June 2024

Workshop "Intermittency in Headwater Streams – Challenges and Opportunities from an Interdisciplinary Perspective" 2024

Penna D., Innocenti L., Murgia I., Piemontese L., Verdone M., Belli G., Chirici D., Dani A., Gheri D., Manca di Villahermosa F. S., Nicoletti S., Nigro M., Preti F., Morandi O., Marchetti E., Solari L., Precipitation and soil moisture control stream network seasonal dynamics in a Mediterranean headwater catchment., Workshop "Intermittency in Headwater Streams – Challenges and Opportunities from an Interdisciplinary Perspective", Bonn, 4-6 June, 2024.

EGU General Assembly 2024

Murgia, I., Kaffas, K., Verdone, M., Manca di Villahermosa, F. S., Dani, A., Preti, F., Massari, C., Segura, C., and Penna, D.: Controls on soil moisture variability on two Mediterranean hillslopes during dry and wet periods using wavelet coherence analysis, EGU General Assembly 2024, Vienna, Austria, 14–19 Apr 2024, EGU24-13242, https://doi.org/10.5194/egusphere-egu24-13242, 2024.

8th Galileo Conference 2023

Verdone, M., Llorens, P., Massari, C., van Meerveld, I., and Penna, D.: Identifying controls on throughfall variability at the hillslope scale through satellite data and UAV-assisted techniques, A European vision for hydrologicalbobservations and experimentation, Naples, Italy, 12–15 Jun 2023, GC8-Hydro-69, https://doi.org/10.5194/egusphere gc8-hydro-69, 2023.

Penna, D., Brighenti, S., Borga, M., Comiti, F., Dani, A., Fabiani, G., Klaus, J., Manca di Villahermosa, F. S., Marchina, C., Pfister, L., Preti, F., Trucchi, P., Verdone, M., Zuecco, G., and Kaffas, K.: Flow pathways, transit time, and tree water sources: linking

ecohydrological processes with stable isotopes in a small forested catchment, A European vision for hydrological observations and experimentation, Naples, Italy, 12–15 Jun 2023, GC8-Hydro-81, https://doi.org/10.5194/egusphere-gc8-hydro-81, 2023.

EGU General Assembly 2023

Dionigi, M., Verdone, M., Penna, D., Barbetta, S., and Massari, C.: Throughfall variability between oak and beech trees in a mountainous Mediterranean catchment, EGU General Assembly 2023, Vienna, Austria, 24–28 Apr 2023, EGU23-2433, https://doi.org/10.5194/egusphere-egu23-2433, 2023.

Mary, B., Kaffas, K., Censini, M., Manca di Villahermosa, F. S., Dani, A., Verdone, M., Preti, F., Trucchi, P., Penna, D., and Cassiani, G.: Supporting subsurface preferential flow in a small forested catchment from geophysical data and hydrological modelling, EGU General Assembly 2023, Vienna, Austria, 24–28 Apr 2023, EGU23-5954, https://doi.org/10.5194/egusphere-egu23-5954, 2023. 3 / 613.

Benettin, P., Manca di Villahermosa, F., Dani, A., Verdone, M., Andreotti, C., Tagliavini, M., and Penna, D.: Ecohydrological dynamics and temporal water origin in European Mediterranean vineyards: a case study in Tuscany, Central Italy, EGU General Assembly 2023, Vienna, Austria, 24–28 Apr 2023, EGU23-16318, https://doi.org/10.5194/ egusphere-egu23-16318, 2023.

AIIA Biennial conference 2022

Verdone M., Borga M., Dani A., Preti F., Trucchi P., Zuecco G., Massari C., van Meerveld I., Penna D., Spatiotemporal variability in throughfall at the hillslope scale in a mountain beech stand, 12th International AIIA Conference: September 19-22, 2022 Palermo - Italy

Macchioli Grande M., Verdone M., Borga M., Cocozza C., Dani A., Fabiani G., Gourdol L., Klaus J., Manca di Villahermosa F. S., Massari C., Pfister L., Preti F., Tailliez C., Trucchi P., Zorzi I., Zuecco G., Penna D., Seasonal meteorological forcing controls runoff generation in a Mediterranean mountain catchment, 12th International AIIA Conference: September 19-22, 2022 Palermo - Italy

Giornate dell'idrologia 2022

Verdone M., Borga M., Dani A., Preti F., Trucchi P., Zuecco G., Massari C., van Meerveld I., Penna D., Does tree size matter? Controls on throughfall variability in a mountain forested hillslope, Giornate dell'idrologia 2022, Genova, 9-11 novembre 2022

Kaffas K., Verdone M., Manca di Villahermosa F. S., Dani A., Trucchi P., Preti F., Massari C., Penna D., Spatiotemporal soil moisture response and preferential flow controls in

a forested mediterranean catchment, Giornate dell'idrologia 2022, Genova, 9-11 novembre 2022

ERB 18th Biennial Conference 2022

Verdone M., Borga M., Dani A., Preti F., Trucchi P., Zuecco G., Massari C., van Meerveld I., Penna D., Throughfall spatio-temporal dynamics at the hillslope scale., 18th Biennial Conference ERB 2022, Portoferraio, Elba Island (Italy), 07-10 June 2022

EGU General Assembly 2022

Verdone, M., Borga, M., Dani, A., Preti, F., Trucchi, P., Zuecco, G., van Meerveld, I., Massari, C., and Penna, D.: Throughfall variability at the hillslope scale: the role of topography and tree characteristics, EGU General Assembly 2022, Vienna, Austria, 23–27 May 2022, EGU22-526, https://doi.org/10.5194/egusphere-egu22-526, 2022.

Penna, D., Benettin, P., Dani, A., Manca di Villahermosa, F. S., Verdone, M., Pastacaldi, G., Andreotti, C., and Tagliavini, M.: Do hillslope position and rootstock matter in root water uptake by grapevines? A case study in a Tuscany vineyard, Italy , EGU General Assembly 2022, Vienna, Austria, 23–27 May 2022, EGU22-3448, https://doi.org/10.5194/egusphere-egu22-3448, 2022.

Cassiani, G., Censini, M., Nasta, P., Allocca, C., Sica, B., Lazzaro, U., Mazzitelli, C., Verdone, M., Dani, A., Manca di Villahermosa, F., Penna, D., and Romano, N.: Time-lapse multi-frequency EMI mapping and ERT profiling for the characterization of soil water behavior in mountain catchments. , EGU General Assembly 2022, Vienna, Austria, 23–27 May 2022, EGU22-6956, https://doi.org/10.5194/egusphere-egu22-6956, 2022.

EGU General Assembly 2020

Penna, D., Borga, M., Bresci, E., Castelli, G., Castellucci, P., Cocozza, C., Errico, A., Fabiani, G., Gourdol, L., Klaus, J., Manca di Villahermosa, F. S., Pfister, L., Preti, F., Tailliez, C., Trucchi, P., Verdone, M., and Zuecco, G.: Linking hydrological response to forest dynamics in Mediterranean areas: a new experimental catchment in the Apennine Mountains, Tuscany, Italy, EGU General Assembly 2020, Online, 4–8 May 2020, EGU2020-14815, https://doi.org/10.5194/egusphere-egu2020-14815, 2020.

Ringraziamenti

Grazie a chi ha condiviso con me questo percorso, a chi mi ha sostenuto, a chi mi ha sopportato e a chi ha creduto in me.